中山大学物理与天文学院学术报告

中子星物态方程研究新进展

胡金牛

南开大学物理科学学院

hujinniu@nankai.edu.cn

- Introduction
- The inner crust of neutron star
- The properties of neutron star
- The hyperons in neutron star
- Summary

The history of neutron star

1931, L. D. Landau- anticipation:

for stars with M>1.5M⊙"density of matter becomes so great that atomic nuclei come in close contact, forming one gigantic nucleus".

L. D. Landau, "On the theory of stars," Physikalische Zs. Sowjetunion 1 (1932) 285

1932, J. Chadwick – discovery of a neutron Nature, Feb. 27, 1932

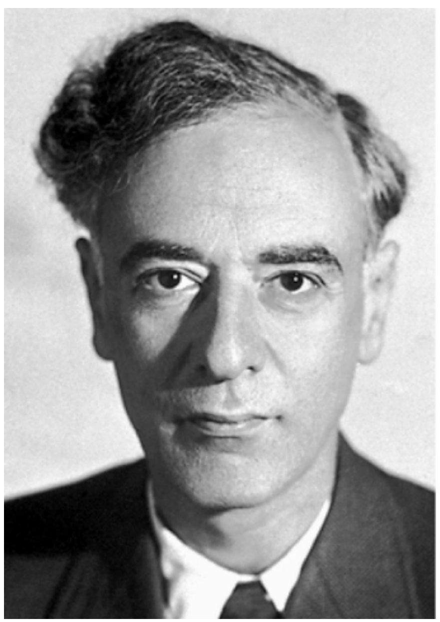

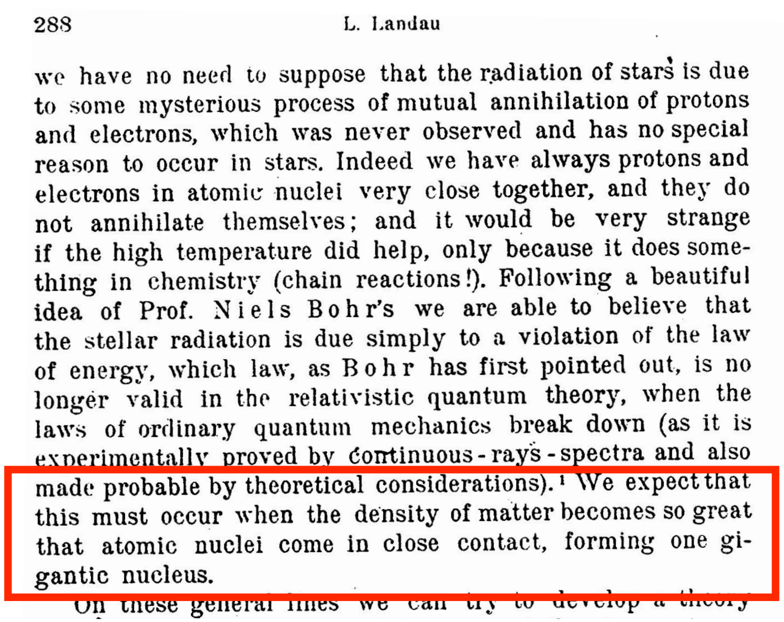

288 L. Landau

we have no need to suppose that the radiation of stars is due to some mysterious process of mutual annihilation of protons and electrons, which was never observed and has no special reason to occur in stars. Indeed we have always protons and electrons in atomic nuclei very close together, and they do not annihilate themselves; and it would be very strange if the high temperature did help, only because it does something in chemistry (chain reactions!). Following a beautiful idea of Prof. Niels Bohr's we are able to believe that the stellar radiation is due simply to a violation of the law of energy, which law, as Bohr has first pointed out, is no longer valid in the relativistic quantum theory, when the laws of ordinary quantum mechanics break down (as it is experimentally proved by continuous-rays-spectra and also made probable by theoretical considerations).[1] We expect that this must occur when the density of matter becomes so great that atomic nuclei come in close contact, forming one gigantic nucleus.

On these general lines we can try to develop a theory

The proposal of neutron star

南開大學

1933, W. Baade & F. Zwicky- prediction of neutron stars

"Supernovae and cosmic rays," Phys. Rev. 45 (1934) 138; "On super-novae," Proc. Nat. Acad. Sci. 20 (1934) 254:

"…supernovae represent the transitions from ordinary stars to neutron stars, which in their final stages consist of extremely closely packed neutrons"; "…possess a very small radius and an extremely high density."

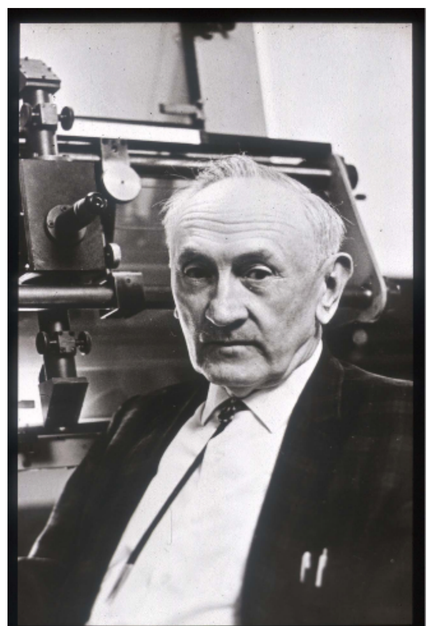

nova is about twenty days and its absolute brightness at maximum may be as high as $M_{vis} = -14^M$. The visible radiation L_ν of a supernova is about 10^8 times the radiation of our sun, that is, $L_\nu = 3.78 \times 10^{41}$ ergs/sec. Calculations indicate that the total radiation, visible and invisible, is of the order $L_\tau = 10^7 L_\nu = 3.78 \times 10^{48}$ ergs/sec. The supernova therefore emits during its life a total energy $E_\tau \geq 10^5 L_\tau = 3.78 \times 10^{53}$ ergs. If supernovae initially are quite ordinary stars of mass $M < 10^{34}$ g, E_τ/c^2 is of the same order as M itself. In the *supernova* process *mass in bulk is annihilated*. In addition the hypothesis suggests itself that *cosmic rays are produced by supernovae*. Assuming that in every nebula one supernova occurs every thousand years, the intensity of the cosmic rays to be observed on the earth should be of the order $\sigma = 2 \times 10^{-3}$ erg/cm² sec. The observational values are about $\sigma = 3 \times 10^{-3}$ erg/cm² sec. (Millikan, Regener). With all reserve we advance the view that supernovae represent the transitions from ordinary stars into *neutron stars*, which in their final stages consist of extremely closely packed neutrons.

The Chronology of neutron star

南開大學

1. February 1931, Zurich. Landau finishes his paper, in which he calculates the maximum mass of white dwarfs and predicts the existence of dense stars which look like giant atomic nuclei.

2. 25 February – 19 March, 1931. Landau in Copenhagen. He most likely discusses his paper with Bohr and Rosenfeld in the period from 28 February (when Rosenfeld arrives) to 19 March.

3. 7 January 1932. Landau submits his paper to Physikalische Zeitschrift der Sowjetunion.

4. End of January 1932. Chadwick became interested in conducting the experiment which led to the discovery of the neutron.

5. 17 February 1932. Chadwick submits his paper on the discovery of the neutron to Nature.

6. 24 February 1932. Chadwick writes a letter to Bohr informing him of the discovery of the neutron.

7. 27 February 1932. Chadwick's paper on the discovery of the neutron is published.

8. 29 February 1932. Landau's paper published.

9. 15-16 December 1933, Stanford. Baade and Zwicky give a talk at a meeting of the American Physical Society suggesting the concept of neutron stars, and their origin in supernova explosions.

10. 15 January 1934. The abstract of the talk by Baade and Zwicky is published.

D. Yakovlev, P. Haensel, G. Baym and C. J. Pethick ParXiv: 1210.0682

The theoretical descriptions

1939, R. Tolman, R. Oppenheimer and G. Volkoff– TOV equation

The equations describing static spherical stars in general relativity

Oppenheimer and Volkoff solved these equations and calculated numerically the structure of non-rotating neutron stars. Maximum mass of a neutron star (in the model of non-interacting neutrons $M_{max} = 0.71\ M_{\odot} < M_{max} = 1.44\ M_{\odot}$).

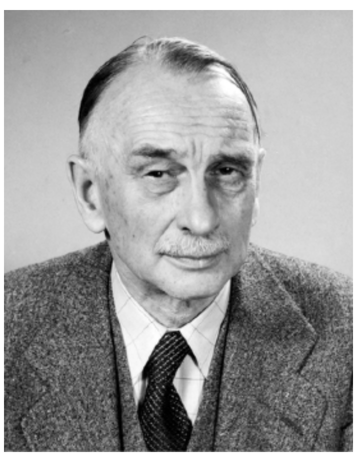

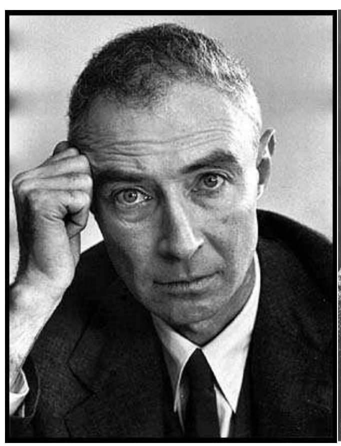

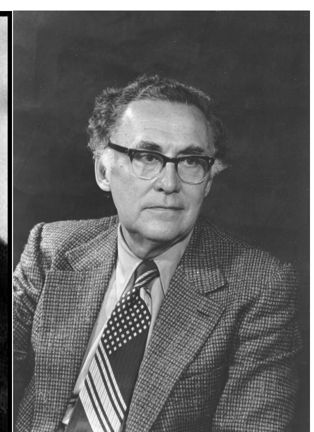

Neutron stars for undergraduates

Richard R. Silbar[a] and Sanjay Reddy[b]

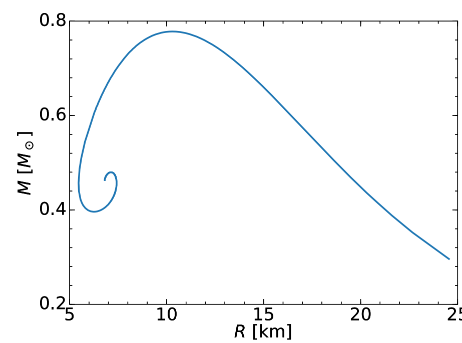

Am. J. Phys.72(2004)892

The discovery of neutron star

南開大學

1967, J. Bell - A pulsating radio source with 1 second period

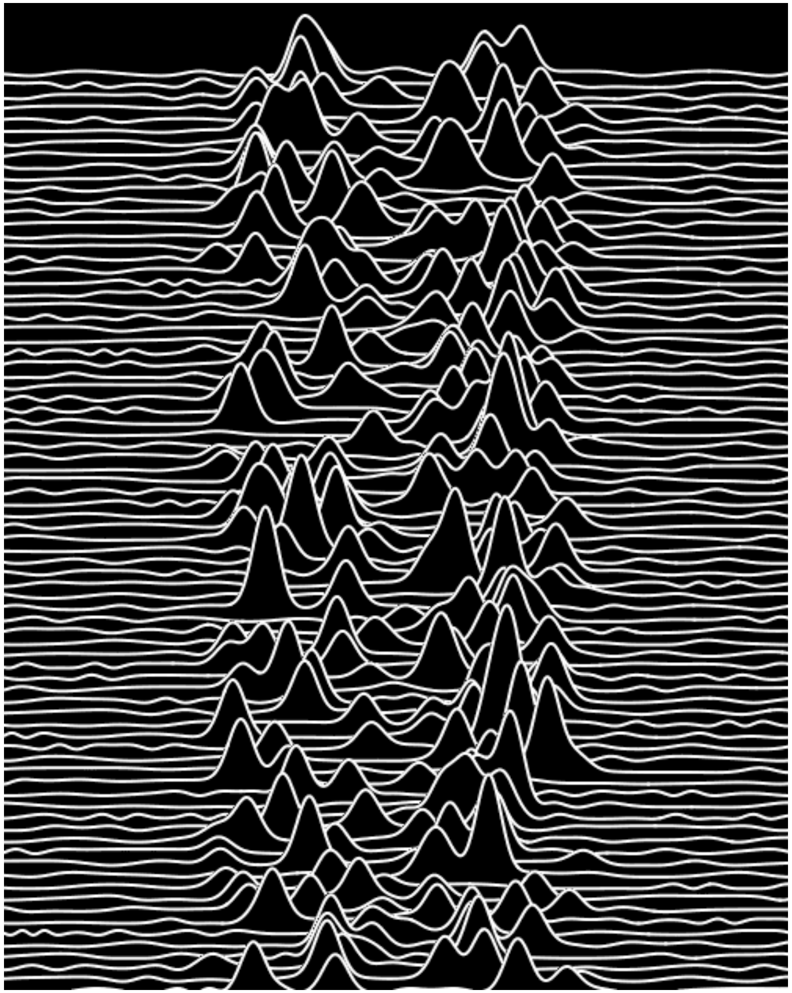

T=1.3373012 s

The binary neutron star

1974, R. Hulse and J. Taylor Jr. – The first binary pulsar

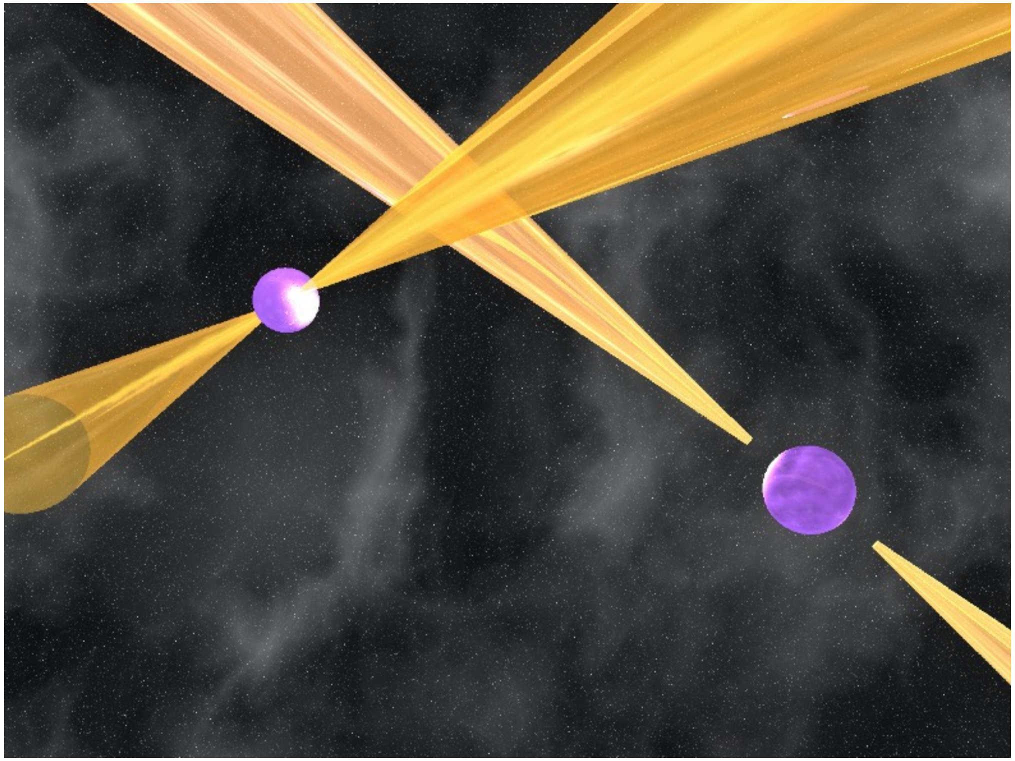

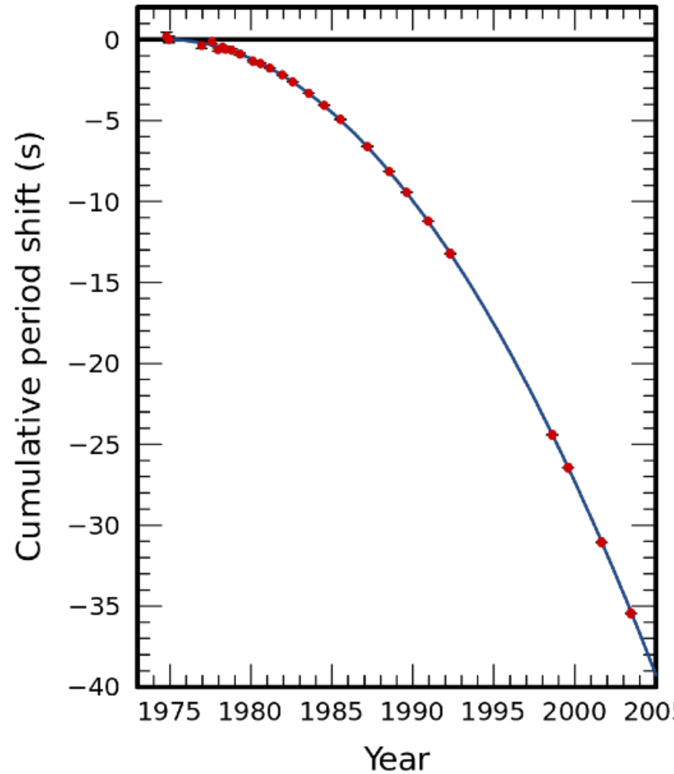

This discovery earned them the 1993 Nobel Prize in Physics "for the discovery of a new type of pulsar, a discovery that has opened up new possibilities for the study of gravitation."

The pulsars and neutron star

南開大學

Pulsars are magnetized rotating neutron stars emitting a highly focused beam of electromagnetic radiation oriented long the magnetic axis. The misalignment between the magnetic axis and the spin axis leads to a **lighthouse effect**

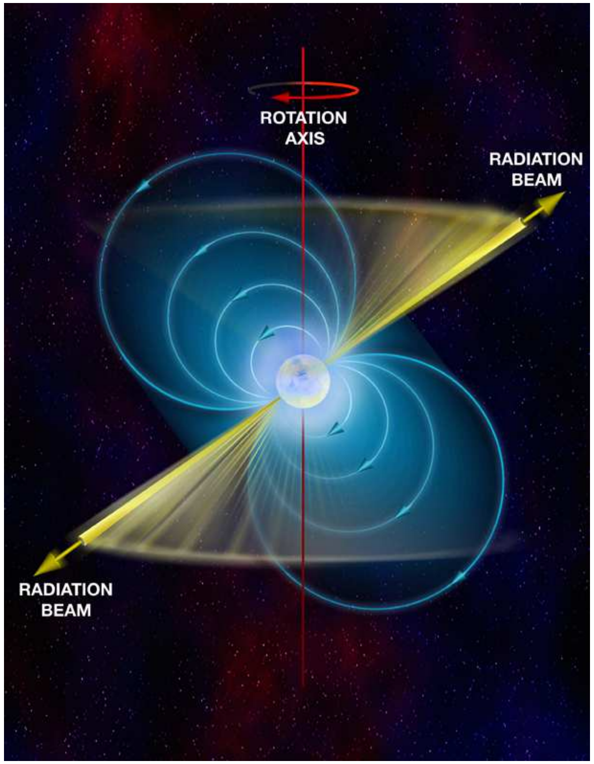

The observation equipments

The origin of neutron star

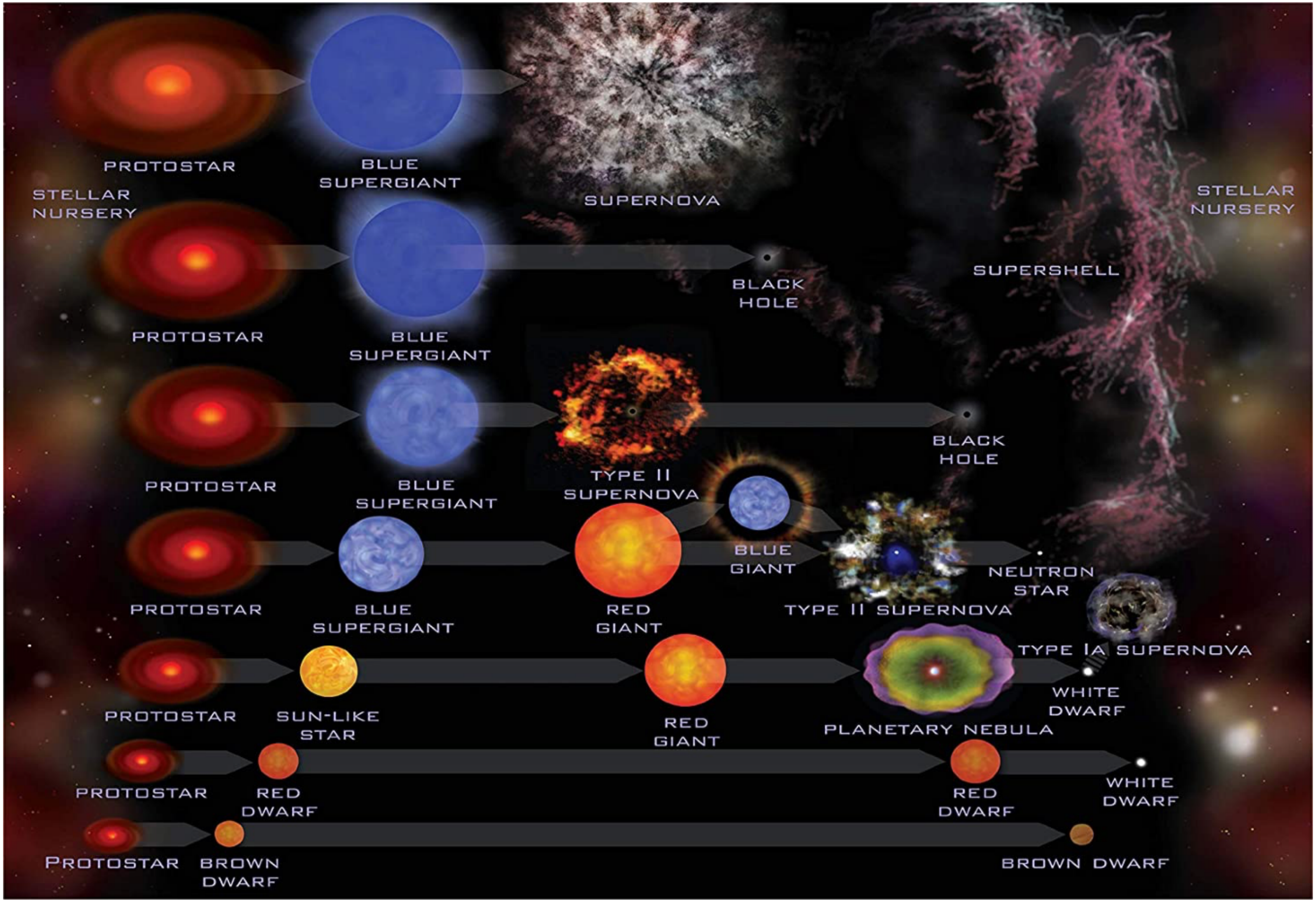

End points of stellar evolution

Starting Mass	Outcome	Final Mass	Final Size	Density
> 20 M_{Sun}	**Black Hole**	any	2.95 (M/M_{Sun}) km	N/A
8 < M < 20 M_{Sun}	**Neutron star**	< 2-3 M_{Sun}	10 &minus 20 km	10^{18} kg/m^3
0.4 < M < 8 M_{Sun}	**White Dwarfs (Carbon)**	< 1.4 M_{Sun}	7000 km	10^9 kg/m^3
0.08 < M < 0.4 M_{Sun}	**White Dwarfs (Helium)**	0.08 < M < 0.4 M_{Sun}	14000 km	
M < 0.08 M_{Sun}	**Brown Dwarfs**	M < 0.08 M_{Sun}	10^5 km	

Birth of a Neutron Star

- The death of a high-mass star (such as Betelgeuse) will leave behind a neutron star
- Initially, the neutron star will be very hot, about 1011 K.
- It will glow mainly in the X-ray part of the spectrum.
- Over its first few hundred years of life, the neutron star's surface cools down to 106 K and continues to glow in the x-ray.
- Young neutron stars are found in supernova remnants.

The observables of neutron star

南開大學

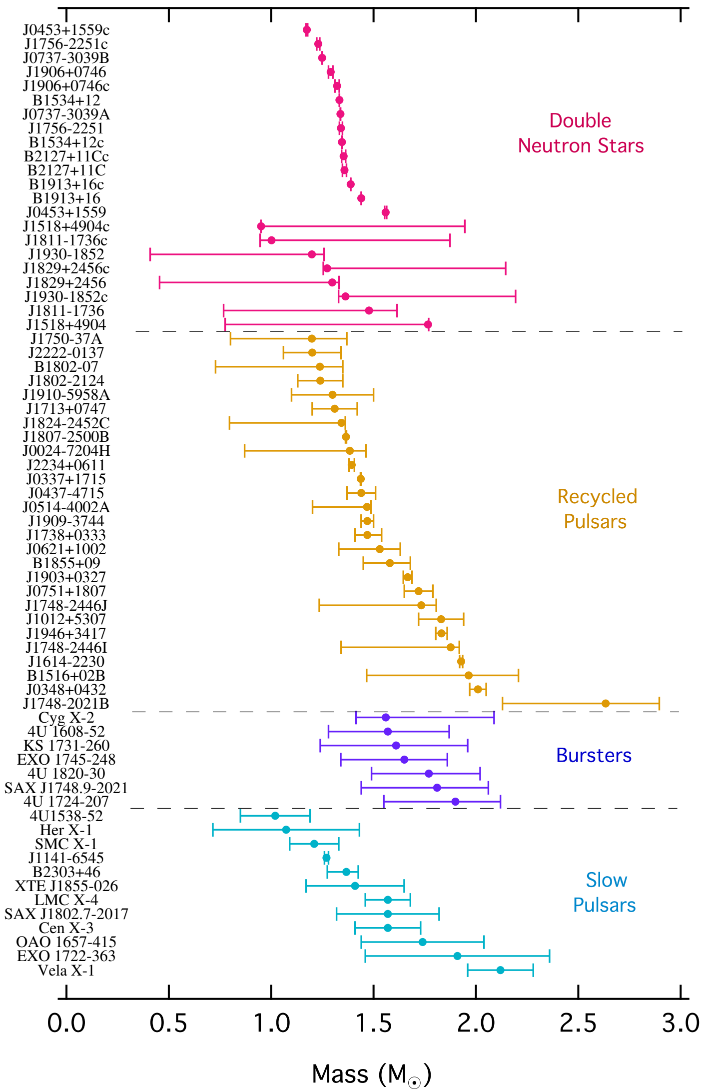

➢ **The dynamics of neutron star**

Neutron star cooling

Neutron star glitch

Superfluidity of neutron star

……

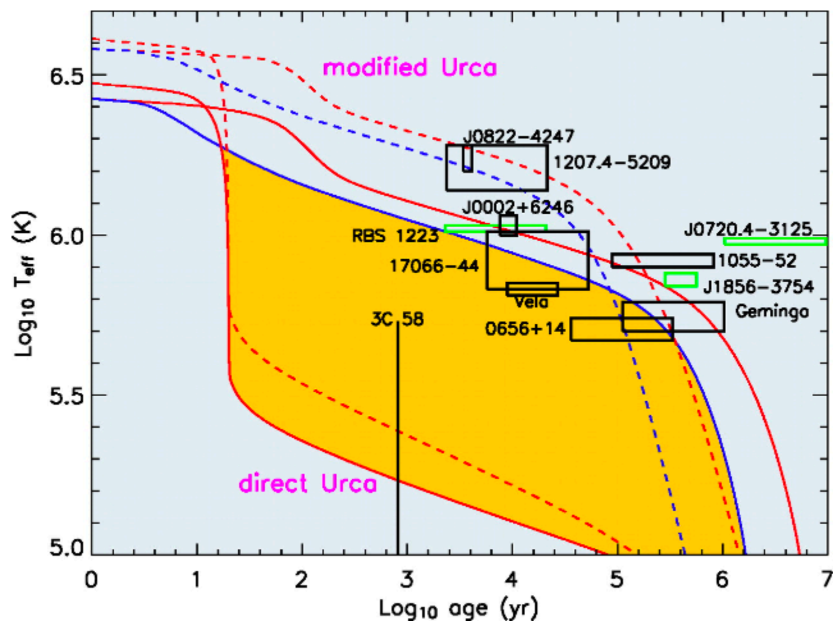

F. Oezel and P. Freire Annu. Rev. Astron. Astrophys. 54 (2016)401

The radii and masses

南開大學 NANKAI UNIVERSITY 1919

Shapiro delay measurement

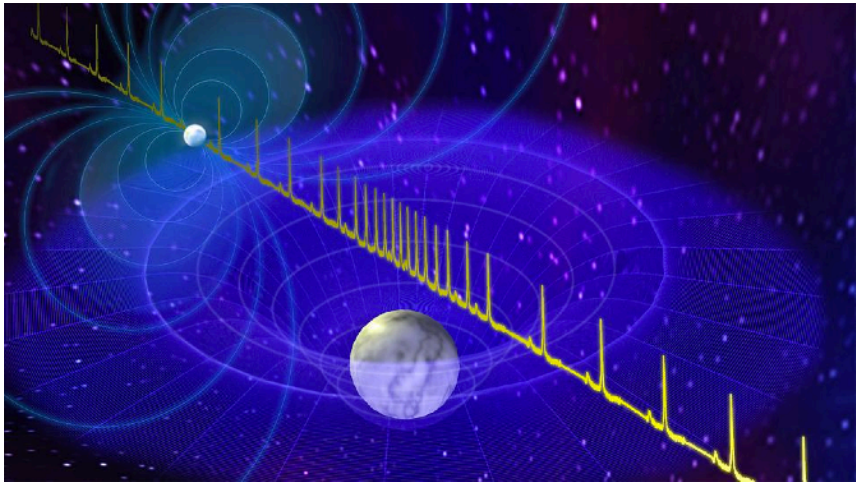

Neutron Star Interior Composition Explorer

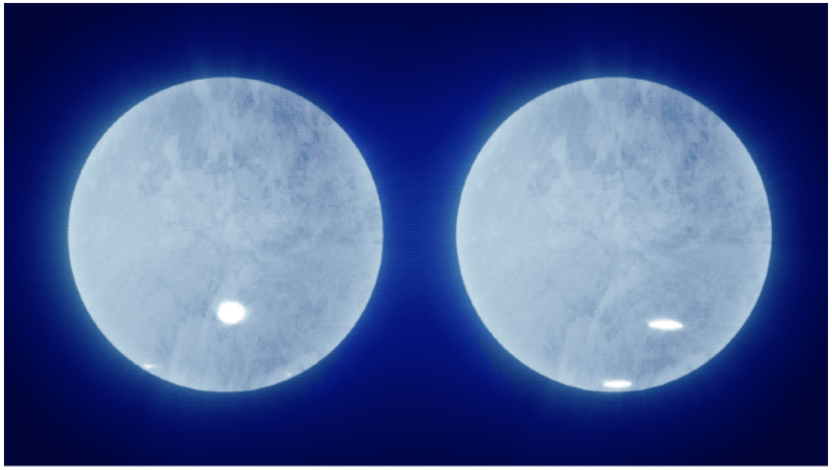

The massive neutron star

PSR J1614-2230 (1.928±0.017 M⊙),

P. B. Demorest, et al., Nature. 467(2010)108
E. Fonseca et al., Astrophys. J. 832, 167 (2016).

PSR J0348+0432 (2.01±0.04 M⊙),

P. J. Antoniadis et al., Science 340, 1233232 (2013).

PSR J0740+6620 (2.08±0.07 M⊙)

H. T. Cromartie et al., Nat. Astron. 4, 72 (2020)
M. C. Miller et al. Astrophys. J. Lett. 918(2021)L28

The NICER Measurement

PSR J0740+6620 (2.08±0.07 M⊙, 12.35±0.75 km)

H. T. Cromartie et al., Nat. Astron. 4, 72 (2020)
M. C. Miller et al. Astrophys. J. Lett. 918(2021)L28

PSR J0030+0451 (1.44±0.15M⊙, 13.02±1.24 km)

M. C. Miller et al. Astrophys. J. Lett. 887(2019)L42

Neutron star merger

Neutron star merger

南開大學

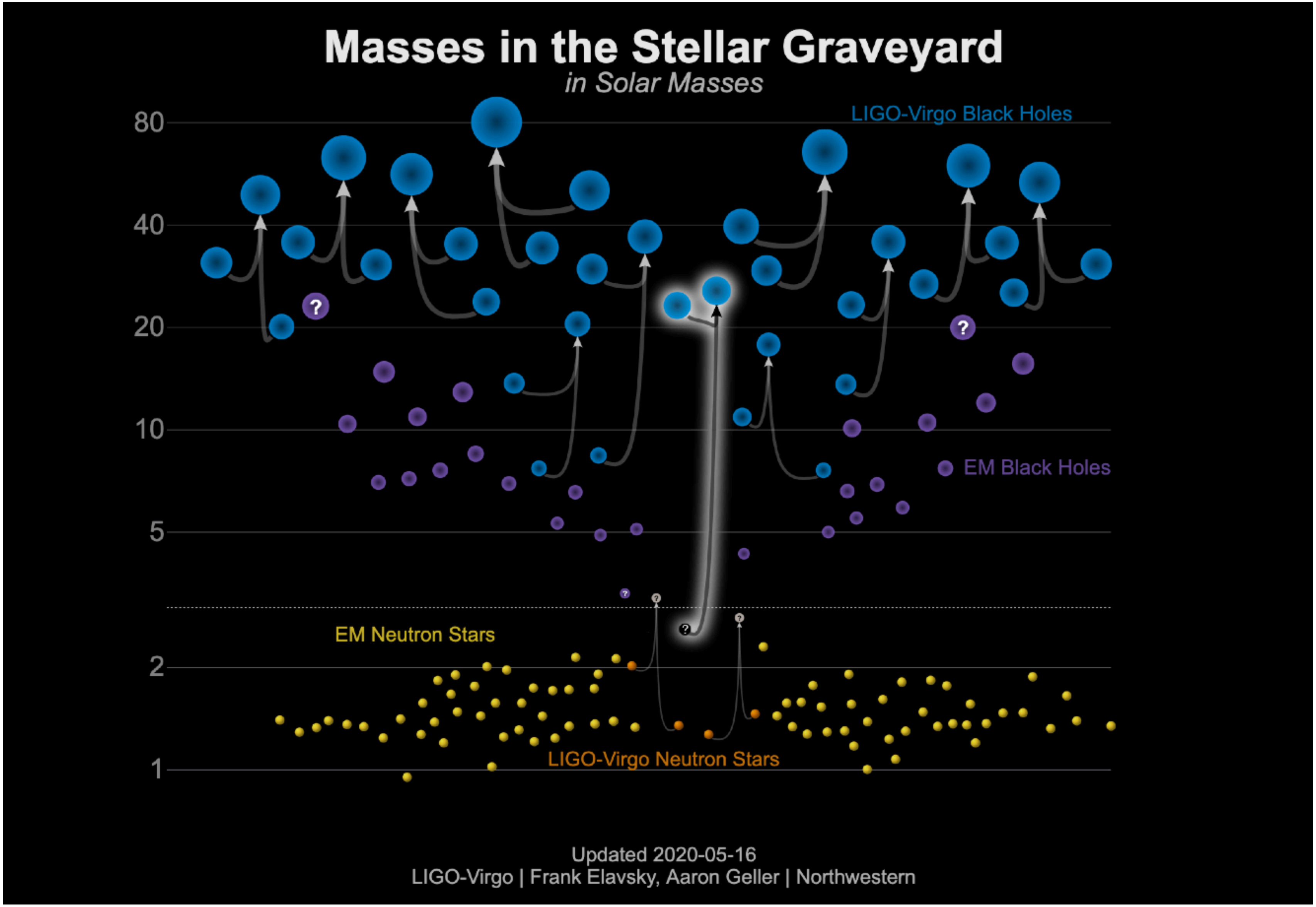

Neutron star structure

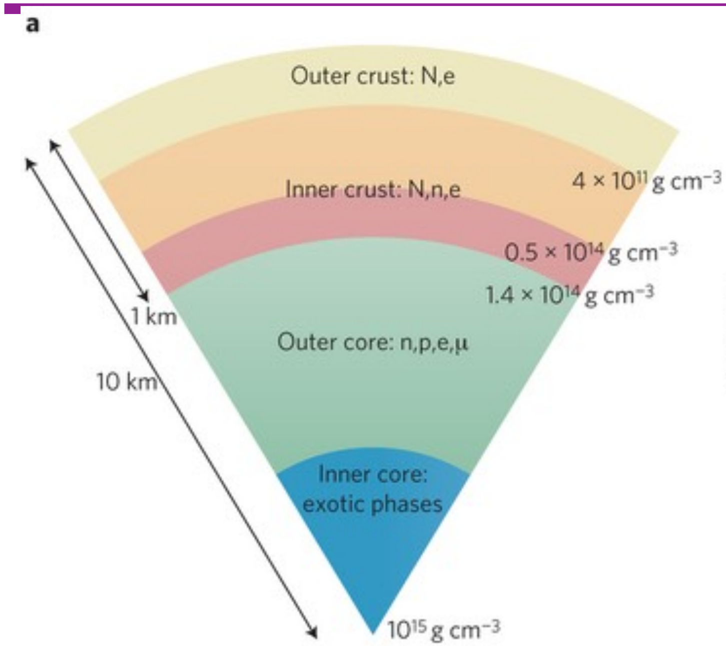

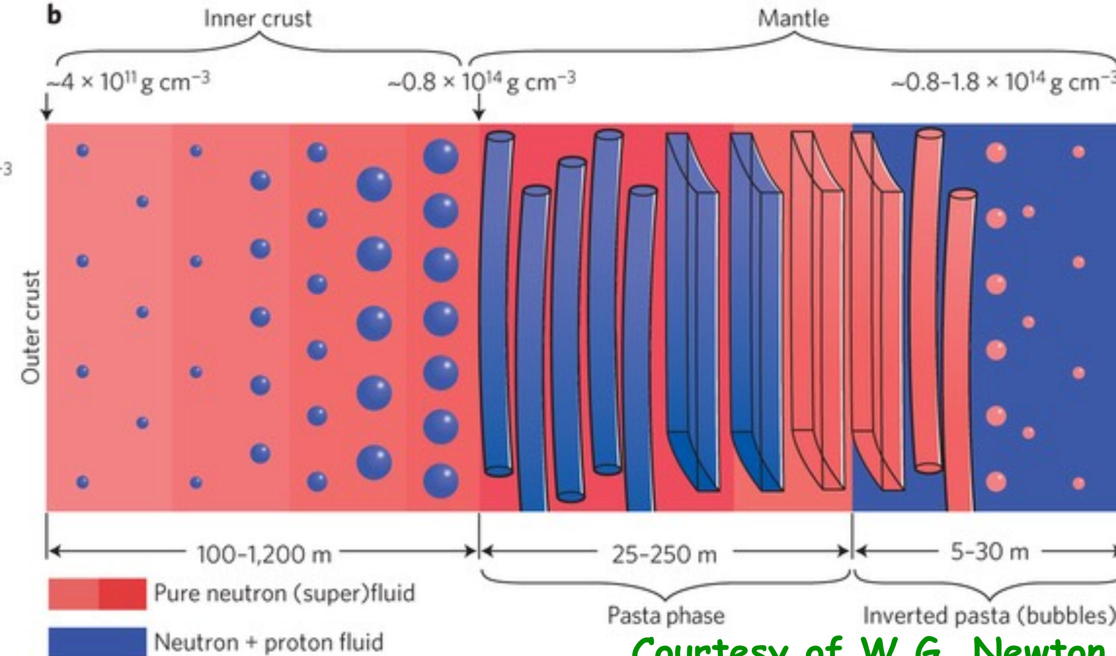

Courtesy of W.G. Newton

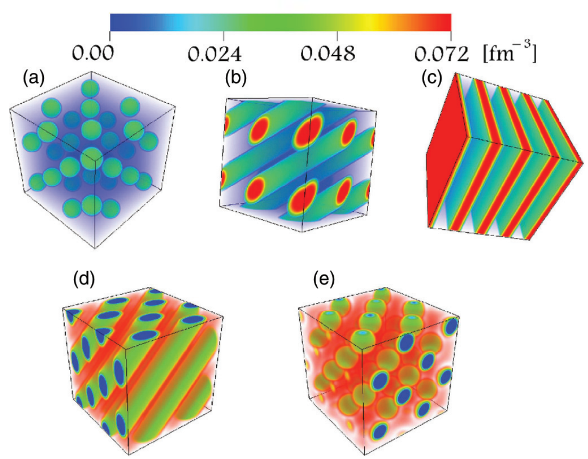

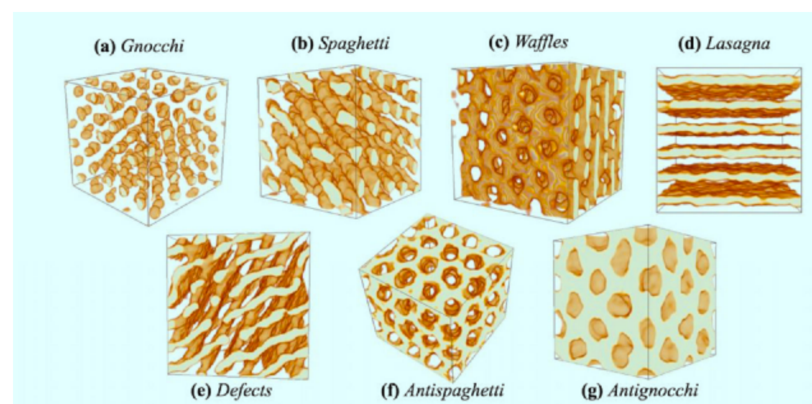

M.Okamoto, T.Maruyama, K.Yabana, T.Tatsumi, Phys. Rev. C 88 (2013) 025801

M. E. Caplan and C. J. Horowitz, Rev. Mod. Phys. 89(2017)041002

南開大學

Tolman-Oppenheimer-Volkoff equation

$$\frac{dP}{dr} = -\frac{G\rho M(r)}{r^2}\left(1+\frac{P}{\rho c^2}\right)\left(1+\frac{4\pi P r^3}{M(r)c^2}\right)\left(1-\frac{2GM(r)}{c^2 r}\right)^{-1}$$

$$M(r) = 4\pi\int_0^r \xi^2\rho(\xi)\mathrm{d}\xi$$

$$\rho(r) = \varepsilon(r)/c^2$$

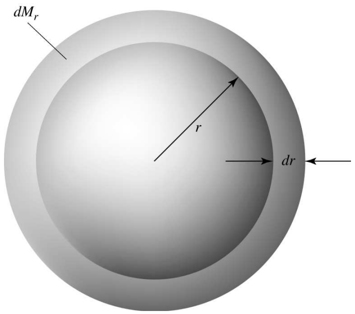

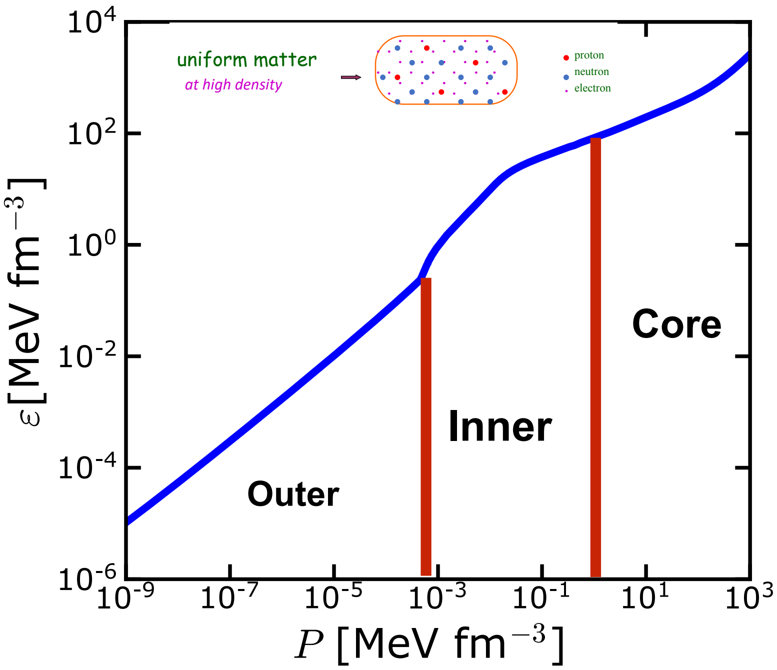

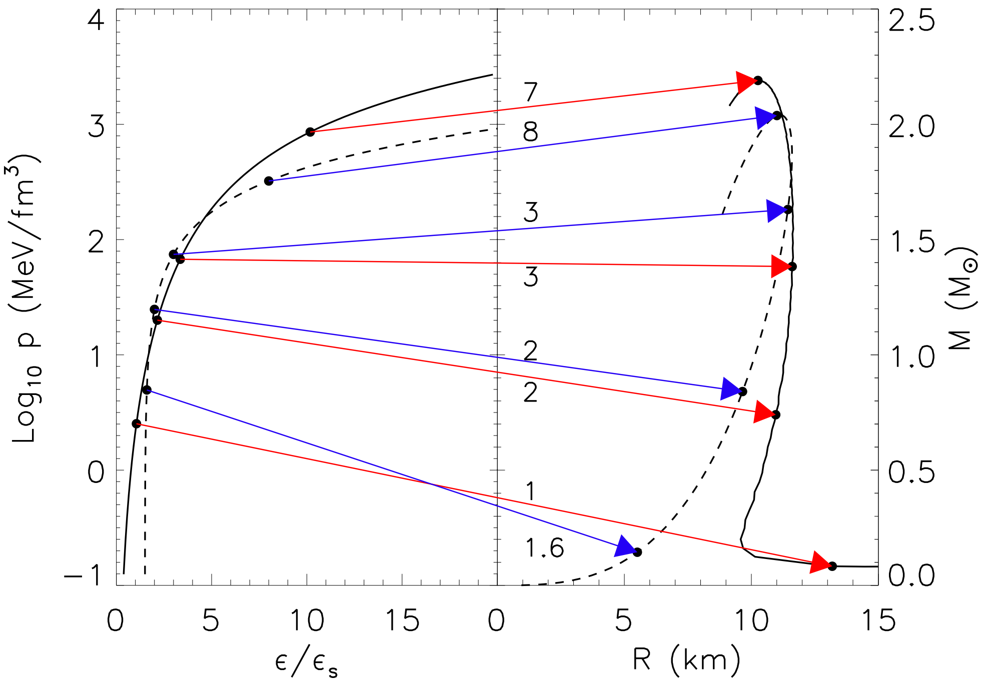

The equations of state

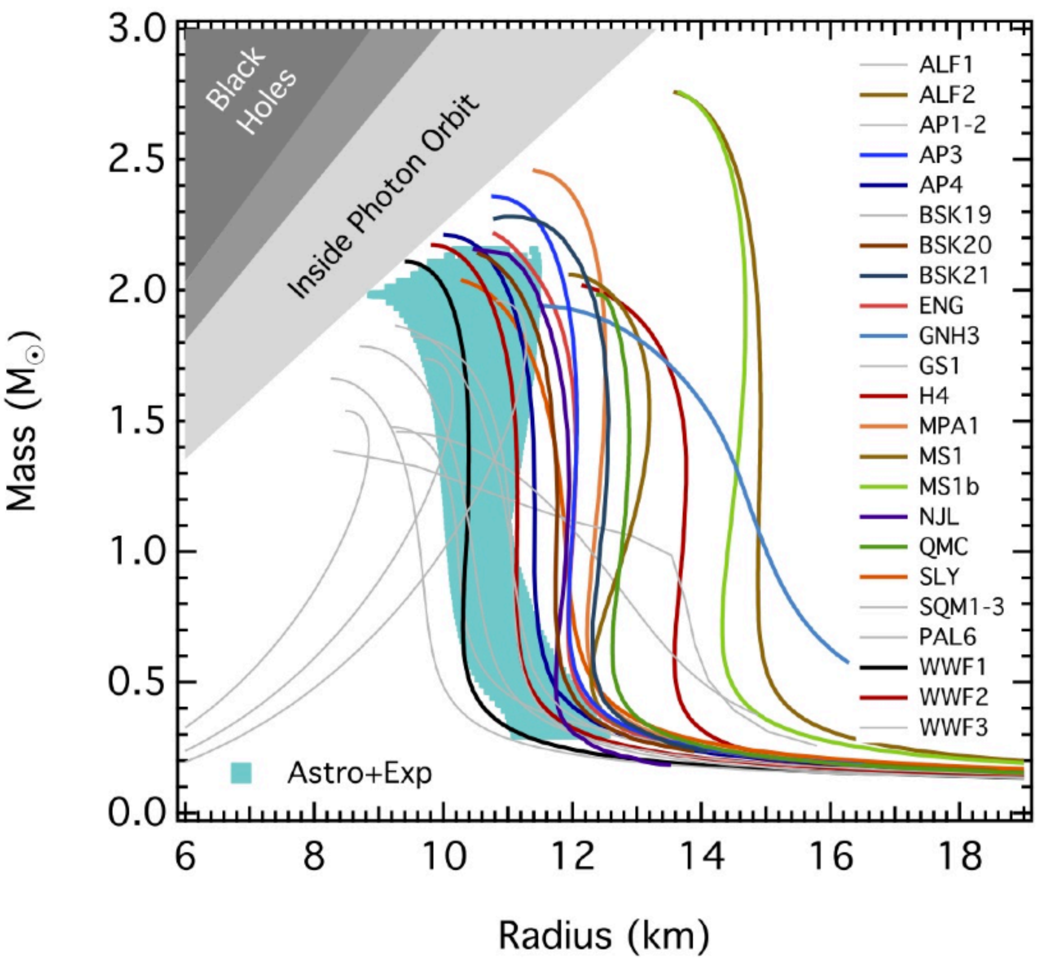

F. Oezel and P. Freire Annu. Rev. Astron. Astrophys. 54 (2016)401

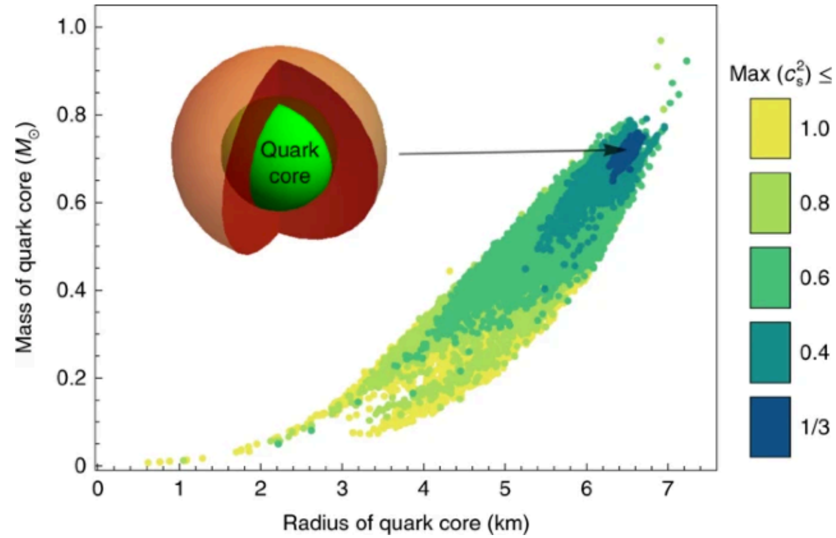

E. Annala et al. Nat. Phys. (2020)

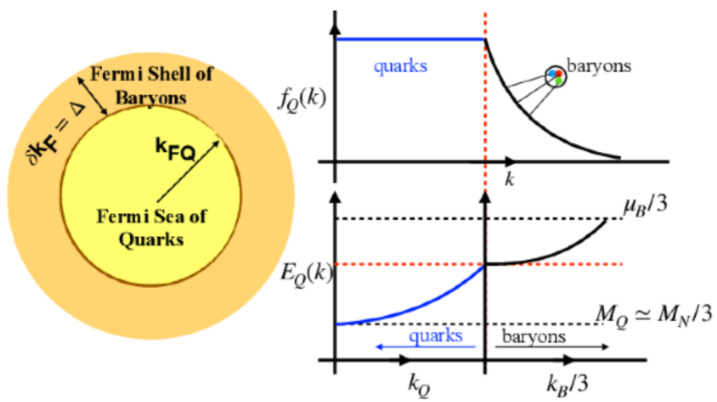

L. McLerran and S. Reddy Phys. Rev. Lett.122 (2019)122701

Unified framework in nuclear physics

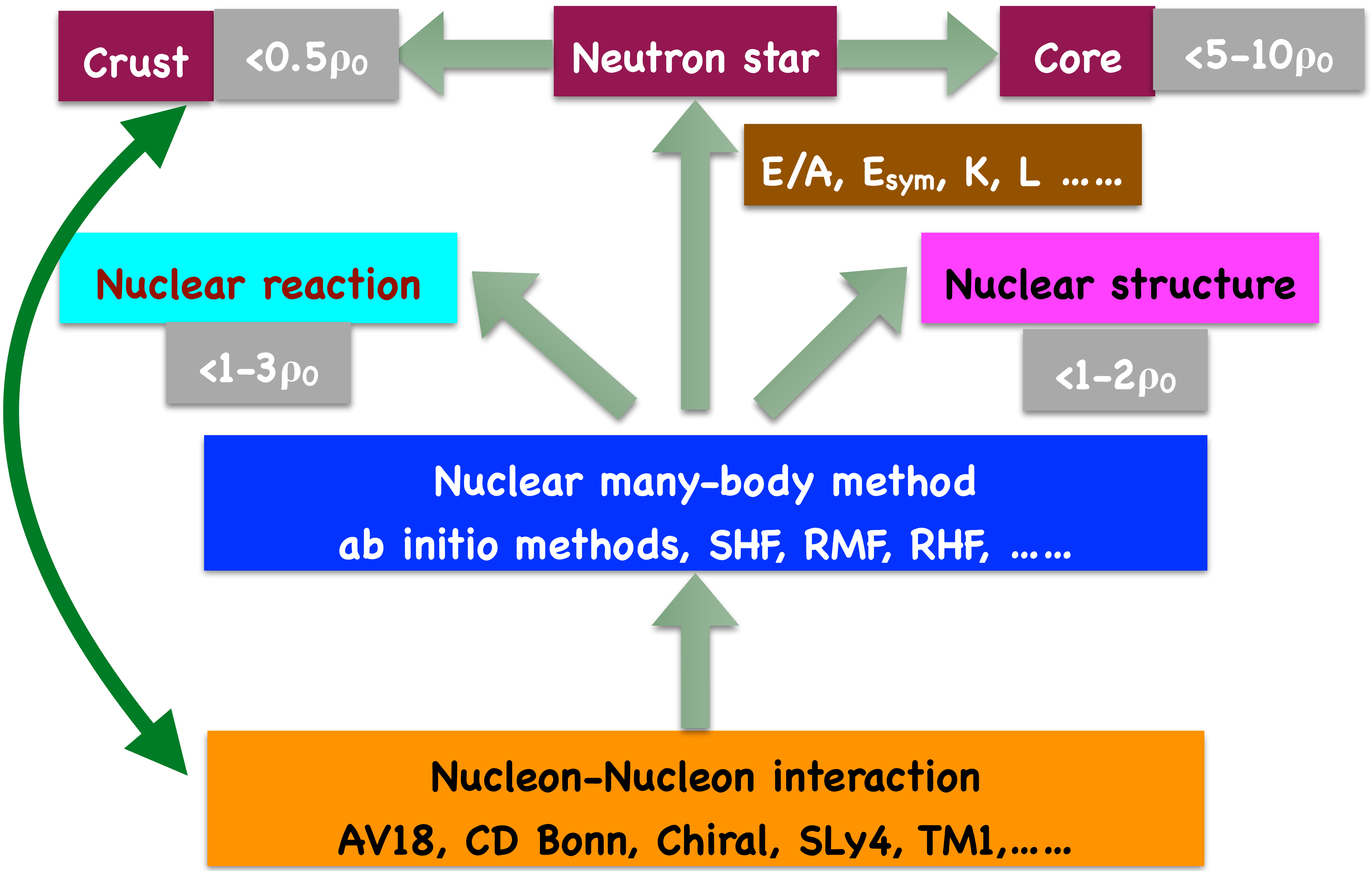

- Introduction
- The inner crust of neutron star
- The properties of neutron star
- The hyperons in neutron star
- Summary

Neutron star crust

non-uniform matter →

at low density

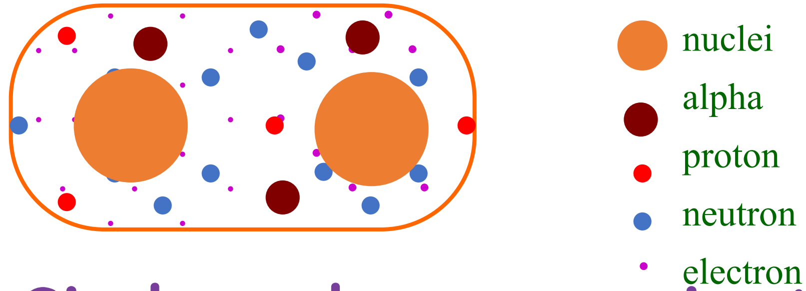

Single nucleon approximation

Nuclear statistical equilibrium

- **Liquid drop model**
  D. G. Ravenhall,, C. J. Pethick, and J. R. Wilson, Phys. Rev. Lett. 50(1983)2066

- **Thomas-Fermi approximation**
  K. Oyamatsu, Nucl. Phys. A 561(1993)431
  H. Shen, H. Toki, K. Oyamatsu, K. Sumiyoshi, Nucl. Phys. A, 637 (1998) 435
  H. Togashi, K. Nakazato, Y. Takehara, S. Yamamuro, H. Suzuki, M. Takano, Nucl. Phys. A961 (2017) 78

- **Time-dependent Hartree-Fock method**
  P. Magierski and P. H. Heenen, Phys. Rev. C 65(2002)045804

- **Molecular dynamics (MD) simulations**
  M. E. Caplan and C. J. Horowitz, Rev. Mod. Phys. 89(2017)041002

...

non-uniform matter

at low density

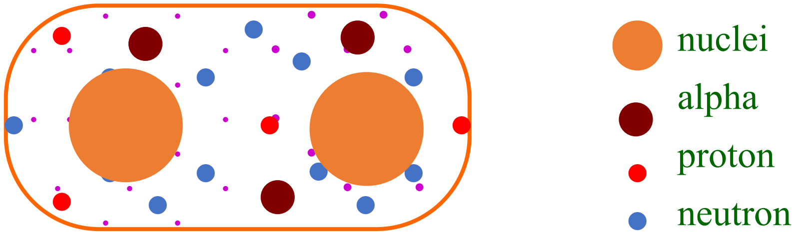

Wigner-Seitz cell

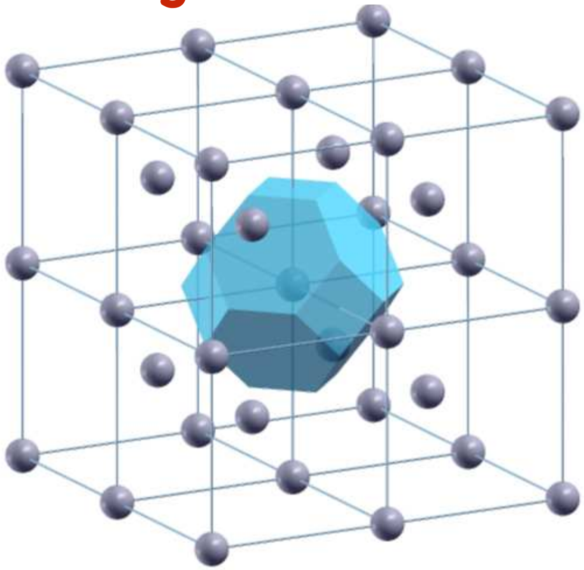

- Body-centered cubic lattice
- Parameterized nucleon distribution
- Energy

$$E = E_{bulk} + E_{surface} + E_{Coulomb} + E_{Lattice} + E_{electron}$$

Minimization!

Semi-empirical mass formula

C. Weizsaecker, Z. Phys. 96(1935)431

$$B(Z,A) = a_V A - a_S A^{2/3} - a_C Z(Z-1)A^{-1/3} - a_{sym}\frac{(A-2Z)^2}{A} + a_p \frac{(-1)^Z[1+(-1)^A]}{2}A^{-3/4}$$

Symmetry energy in nuclear matter

$$E_{sym}(\rho) = S_0 + L\left(\frac{\rho-\rho_0}{3\rho_0}\right) + \frac{K_{sym}}{2}\left(\frac{\rho-\rho_0}{3\rho_0}\right)^2 + \cdots$$

The slope of symmetry energy

$$L = 3\rho_0 \frac{\partial E_{sym}(\rho)}{\partial \rho}\Big|_{\rho=\rho_0}$$

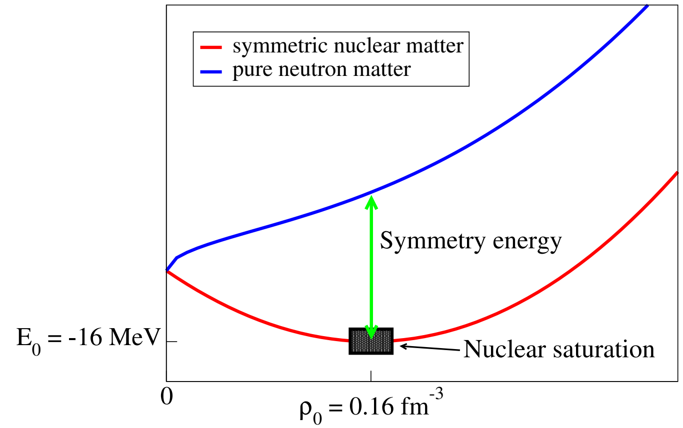

Relativistic mean-field model

南開大學

The Lagrangian

$$\begin{aligned}\mathcal{L} \;=\; & \bar{\psi}(i\gamma_\mu\partial^\mu - M_N - g_\sigma\sigma - g_\omega\gamma_\mu\omega^\mu - \frac{g_\rho}{2}\tau^a\gamma_\mu\rho^{a\mu})\psi \\ & + \frac{1}{2}\partial_\mu\sigma\partial^\mu\sigma - \frac{1}{2}{m_\sigma}^2\sigma^2 - \frac{1}{3}g_2\sigma^3 - \frac{1}{4}g_3\sigma^4 \\ & - \frac{1}{4}W_{\mu\nu}W^{\mu\nu} + \frac{1}{2}{m_\omega}^2\omega_\mu\omega^\mu + \frac{1}{4}c_3(\omega_\mu\omega^\mu)^2 \\ & - \frac{1}{4}R^a_{\mu\nu}R^{a\mu\nu} + \frac{1}{2}{m_\rho}^2\rho^a_\mu\rho^{a\mu} + \Lambda_V(g_\omega^2\omega_\mu\omega^\mu)(g_\rho^2\rho^a_\mu\rho^{a\mu}),\end{aligned}$$

Equation of motion

$$\left[i\gamma_\mu\partial^\mu - (M_N + g_\sigma\sigma) - g_\omega\gamma^\mu\omega_\mu - \frac{g_\rho}{2}\tau^a\gamma_\mu\rho^{a\mu}\right]\psi = 0,$$

$$(\partial^\mu\partial_\mu + m_\sigma^2)\sigma + g_2\sigma^2 + g_3\sigma^3 = -g_\sigma\bar{\psi}\psi,$$

$$\partial^\mu W_{\mu\nu} + m_\omega^2\omega_\nu + c_3(\omega_\mu\omega^\mu)\omega_\nu + 2\Lambda_V g_\omega^2 g_\rho^2\rho^a_\mu\rho^{a\mu}\omega_\nu = g_\omega\bar{\psi}\gamma_\nu\psi,$$

$$\partial^\mu R^a_{\mu\nu} + m_\rho^2\rho^a_\nu + 2\Lambda_V g_\omega^2 g_\rho^2\omega_\mu\omega^\mu\rho^a_\nu = g_\rho\bar{\psi}\gamma_\nu\tau^a\psi.$$

S. S. Bao, J. N. Hu, Z. W. Zhang, H. Shen, Phys. Rev. C 90(2014)045802

Family TM1 parameter set

南開大學

The TM1 Lagrangian

S. S. Bao, J. N. Hu, Z. W. Zhang, H. Shen, Phys. Rev. C 90(2014)045802

$$\mathcal{L} = \bar{\psi}(i\gamma_\mu\partial^\mu - M_N - g_\sigma\sigma - g_\omega\gamma_\mu\omega^\mu - \frac{g_\rho}{2}\tau^a\gamma_\mu\rho^{a\mu})\psi$$
$$+\frac{1}{2}\partial_\mu\sigma\partial^\mu\sigma - \frac{1}{2}{m_\sigma}^2\sigma^2 - \frac{1}{3}g_2\sigma^3 - \frac{1}{4}g_3\sigma^4$$
$$-\frac{1}{4}W_{\mu\nu}W^{\mu\nu} + \frac{1}{2}{m_\omega}^2\omega_\mu\omega^\mu + \frac{1}{4}c_3(\omega_\mu\omega^\mu)^2$$
$$-\frac{1}{4}R^a_{\mu\nu}R^{a\mu\nu} + \frac{1}{2}{m_\rho}^2\rho^a_\mu\rho^{a\mu} + \Lambda_V(g_\omega^2\omega_\mu\omega^\mu)(g_\rho^2\rho^a_\mu\rho^{a\mu}),$$

The family TM1 parameter set with different L

L (MeV)	40.0	50.0	60.0	70.0	80.0	90.0	100.0	110.8
g_ρ	13.9714	12.2413	11.2610	10.6142	10.1484	9.7933	9.5114	9.2644
Λ_v	0.0429	0.0327	0.0248	0.0182	0.0128	0.0080	0.0039	0.0000
$E_{sym}(n_0)$ (MeV)	31.38	32.39	33.29	34.11	34.86	35.56	36.22	36.89
Δr_{np} (fm)	0.1574	0.1886	0.2103	0.2268	0.2402	0.2514	0.2609	0.2699

$$E_{\text{sym}} = 28.05 \text{ MeV}, \quad n = 0.11 \text{ fm}^{-3}$$

Family TM1 parameter set

南開大學

The binding energies of Pb

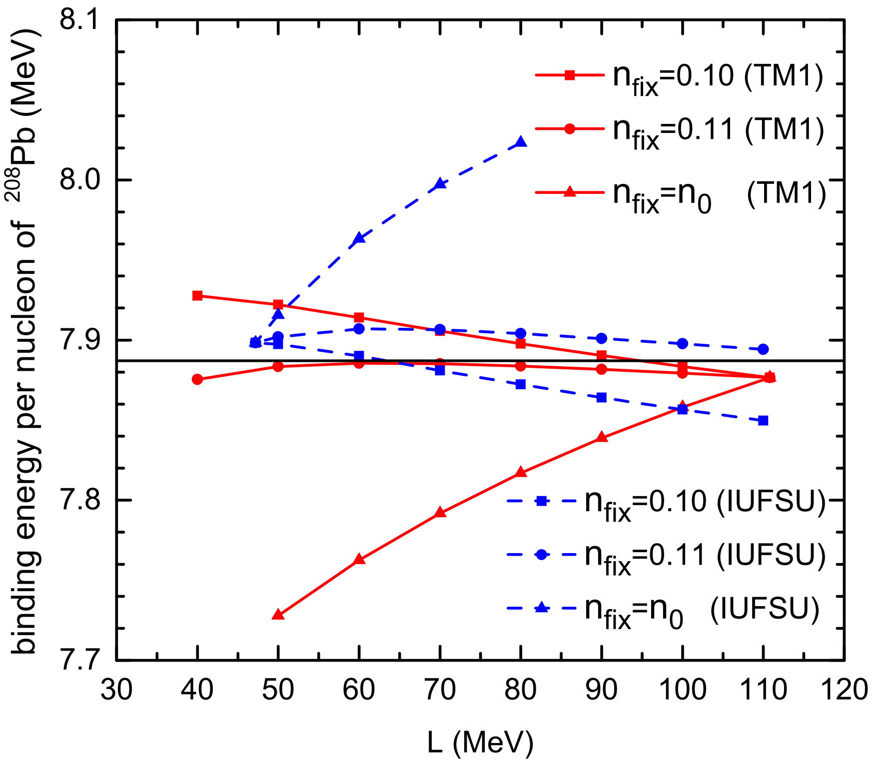

The symmetry energy

$$E_{sym}(\rho) = S_0 + L\left(\frac{\rho-\rho_0}{3\rho_0}\right) + \frac{K_{sym}}{2}\left(\frac{\rho-\rho_0}{3\rho_0}\right)^2 + \cdots$$

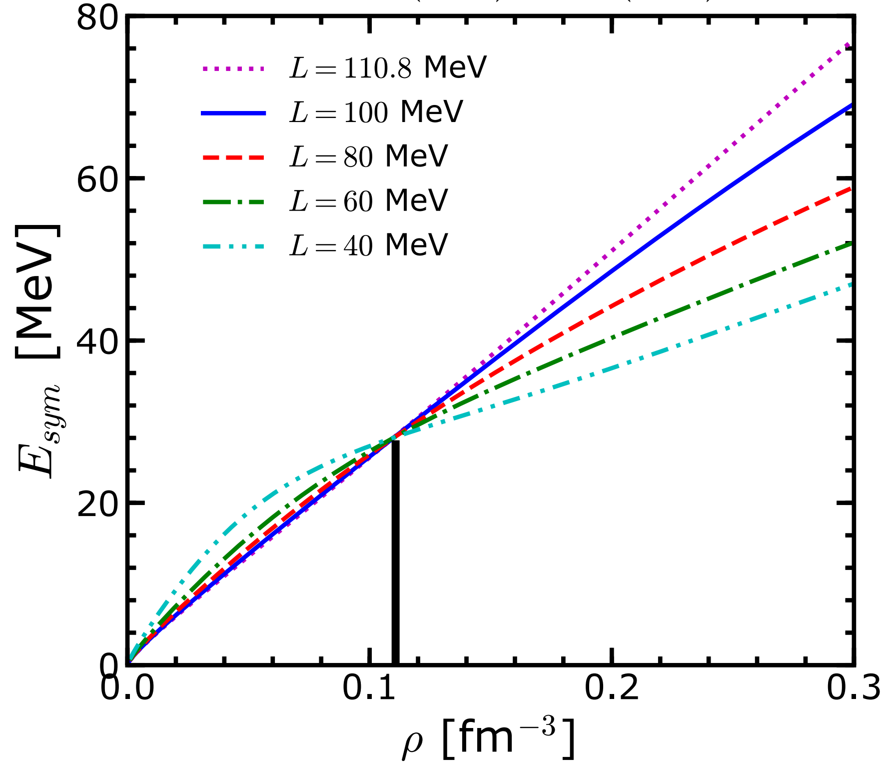

S. S. Bao, J. N. Hu, Z. W. Zhang, H. Shen, Phys. Rev. C 90(2014)045802

The symmetry energy fixed at 0.11 fm^{-3} influences the bind energy of Pb least.

Thomas-Fermi Approximation

南開大學

S. S. Bao, J. N. Hu, Z. W. Zhang, H. Shen, Phys. Rev. C 90(2014)045802

The total energy of Wigner-Seitz cell

$$E_{\text{cell}} = \int_{\text{cell}} \varepsilon_{\text{rmf}}(r)\, d^3r + \varepsilon_e V_{\text{cell}} + \Delta E_{\text{bcc}},$$

where, ε_e denotes the electron kinetic energy density

Nucleon local energy density of RMF model

$$\begin{aligned}
\varepsilon_{\text{rmf}} = & \sum_{i=p,n} \frac{1}{\pi^2} \int_0^{k_F^i} dk\, k^2 \sqrt{k^2 + M^{*2}} \\
& + \frac{1}{2}(\nabla\sigma)^2 + \frac{1}{2}m_\sigma^2\sigma^2 + \frac{1}{3}g_2\sigma^3 + \frac{1}{4}g_3\sigma^4 \\
& - \frac{1}{2}(\nabla\omega)^2 - \frac{1}{2}m_\omega^2\omega^2 - \frac{1}{4}c_3\omega^4 + g_\omega\omega(n_p + n_n) \\
& - \frac{1}{2}(\nabla\rho)^2 - \frac{1}{2}m_\rho^2\rho^2 - \Lambda_{\text{v}} g_\omega^2 g_\rho^2 \omega^2\rho^2 + \frac{g_\rho}{2}\rho(n_p - n_n) \\
& - \frac{1}{2}(\nabla A)^2 + eA(n_p - n_e),
\end{aligned}$$

The energy contribution from the different pasta configuration

$$V_{\mathrm{cell}} = \begin{cases} \frac{4}{3}\pi r_{\mathrm{ws}}^3 & \text{(droplet and bubble)}, \\ l\pi r_{\mathrm{ws}}^2 & \text{(rod and tube)}, \\ 2r_{\mathrm{ws}}l^2 & \text{(slab)}, \end{cases}$$

The equations of motion for mean fields

$$-\nabla^2\sigma + m_\sigma^2\sigma + g_2\sigma^2 + g_3\sigma^3 = -g_\sigma\left(n_p^s + n_n^s\right),$$

$$-\nabla^2\omega + m_\omega^2\omega + c_3\omega^3 + 2\Lambda_{\mathrm{v}}g_\omega^2 g_\rho^2\rho^2\omega = g_\omega(n_p + n_n),$$

$$-\nabla^2\rho + m_\rho^2\rho + 2\Lambda_{\mathrm{v}}g_\omega^2 g_\rho^2\omega^2\rho = \frac{g_\rho}{2}(n_p - n_n),$$

$$-\nabla^2 A = e(n_p - n_e),$$

Chemical potentials

$$\mu_p = \sqrt{\left(k_F^p\right)^2 + M^{*2}} + g_\omega \omega + \frac{g_\rho}{2}\rho + eA,$$

$$\mu_n = \sqrt{\left(k_F^n\right)^2 + M^{*2}} + g_\omega \omega - \frac{g_\rho}{2}\rho.$$

Beta equilibrium and charge neutrality

$$\mu_n = \mu_p + \mu_e,$$

$$N_e = N_p = \int_{\text{cell}} n_p(r)\, d^3 r.$$

Minimize the total energy density

$$\frac{\partial E_{\text{cell}}}{\partial r_{\text{WS}}} = 0$$

The neutron drip

The neutron drip density

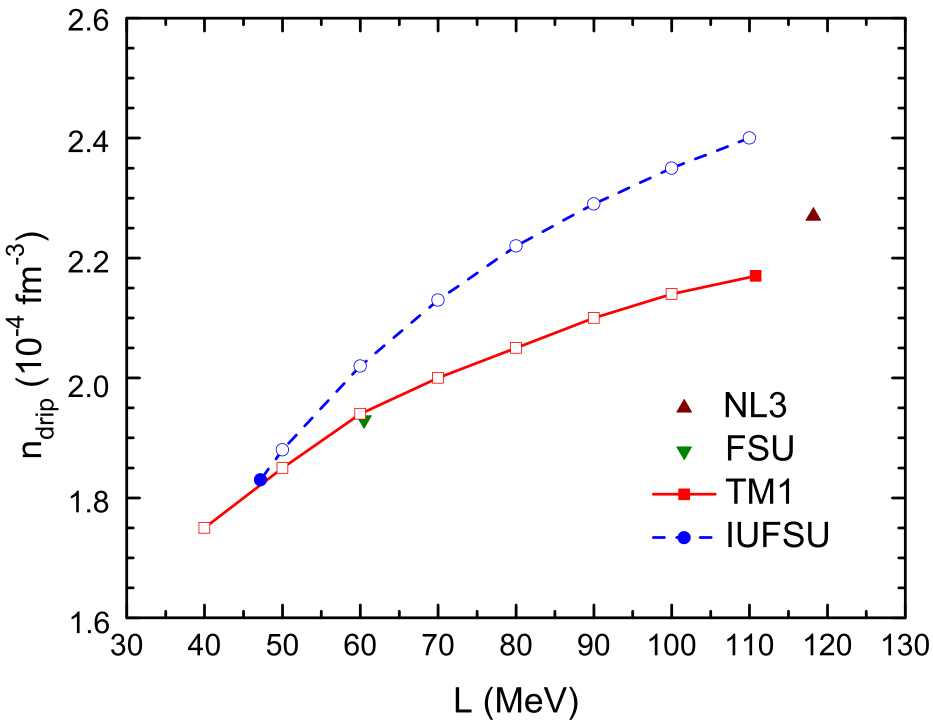

The Wigner-Seitz cell radius

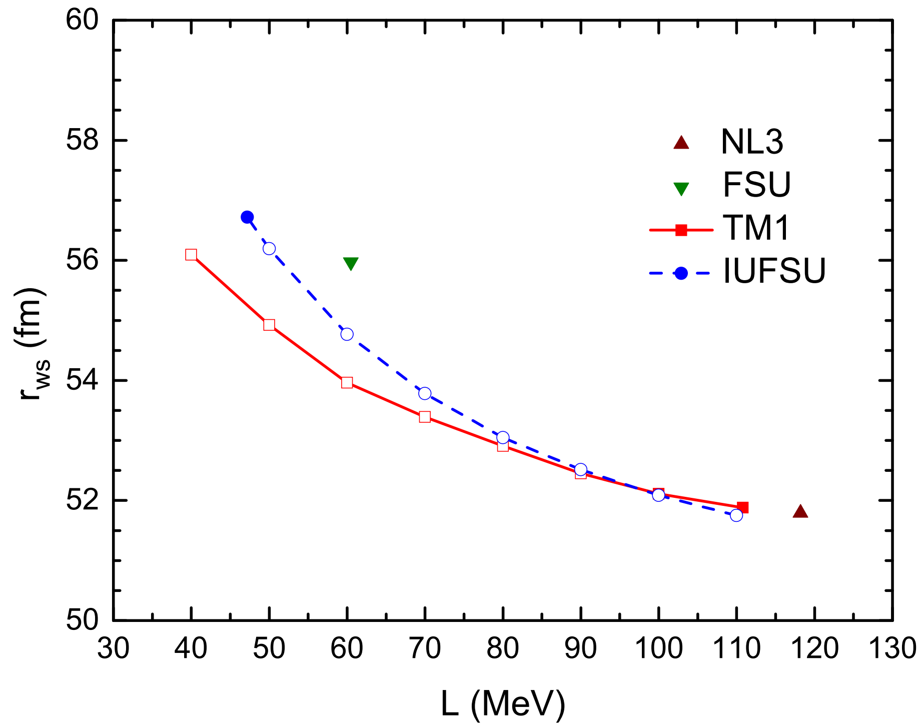

S. S. Bao, J. N. Hu, Z. W. Zhang, H. Shen, Phys. Rev. C 90(2014)045802

A larger slope L generates a higher neutron drip density.

A larger slope L corresponds to a smaller cell radius

K. Oyamatsu, K. Iida, Phys. Rev. C 75(2007)015801

The nucleon density

南開大學

The densities at neutron drip density

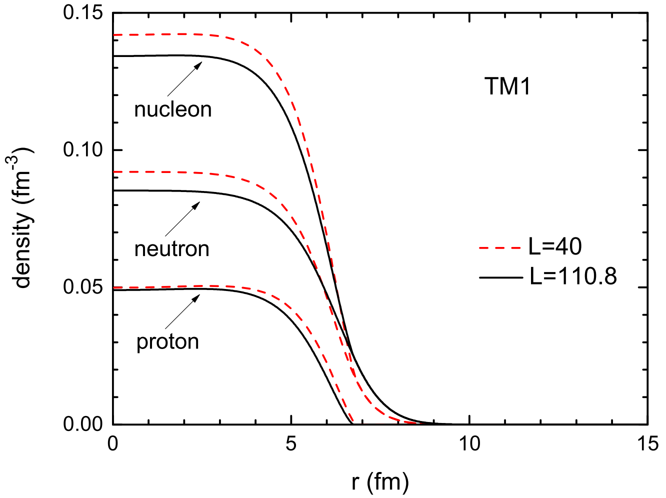

The densities of Pb208

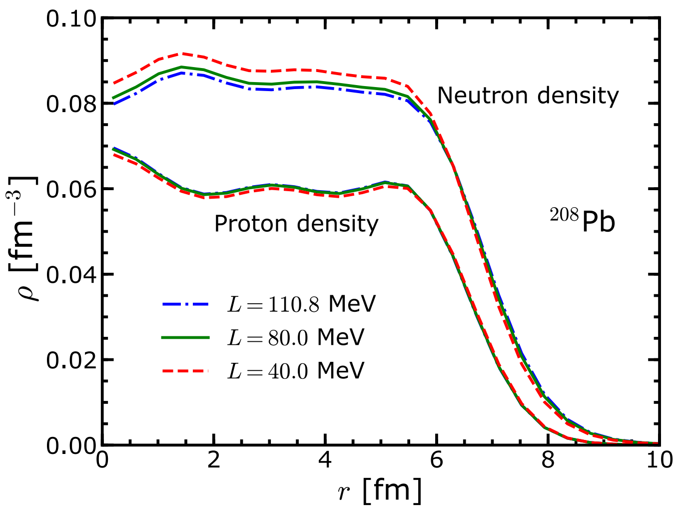

The densities at fix baryon densities

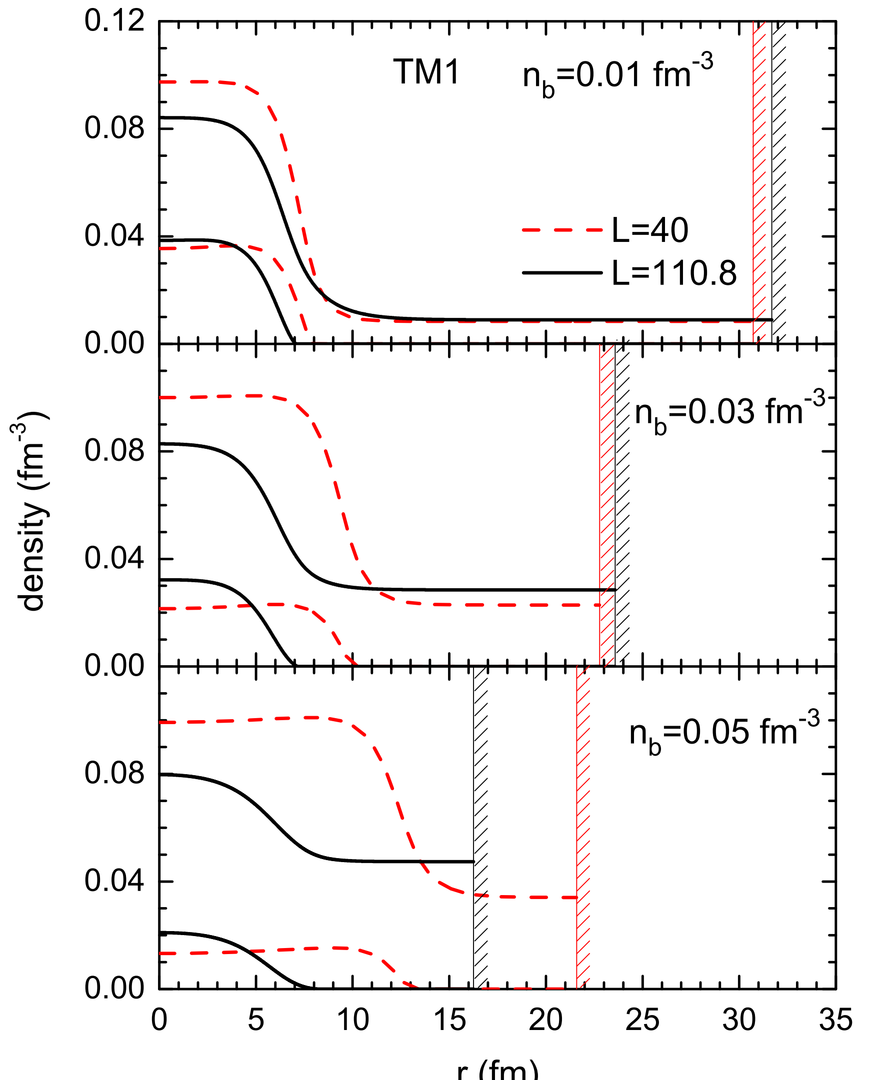

S. S. Bao, J. N. Hu, Z. W. Zhang, H. Shen, Phys. Rev. C 90(2014)045802

NANKAI UNIVERSITY 1919 南開大學

The phase diagram

S. S. Bao and H. Shen, Phys. Rev. C 91(2015)015807

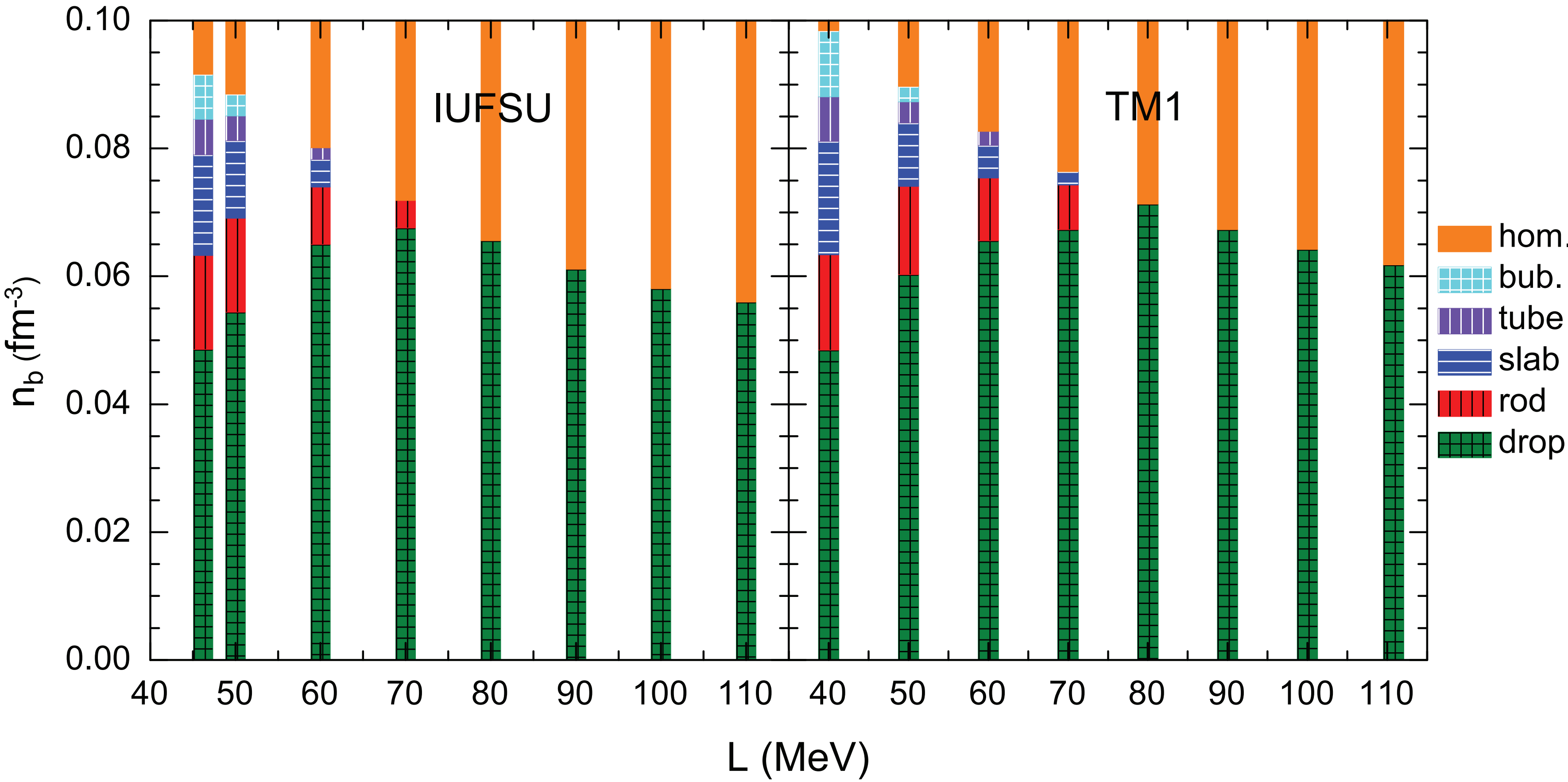

Smaller L corresponds to more pasta phases

Smaller L corresponds to larger crust-core transition density

南開大學

The periodic boundary condition

$$\varphi^{(q)}_{\boldsymbol{k}+\boldsymbol{G}}(\boldsymbol{r}) = \varphi^{(q)}_{\boldsymbol{k}}(\boldsymbol{r}) \,,$$

$$E_{\rm cell} = \int_{\rm cell} \varepsilon_{\rm rmf}(r)\, d^3 r + \cancel{\varepsilon_e V_{\rm cell}} + \Delta E_{\rm bcc} \,,$$

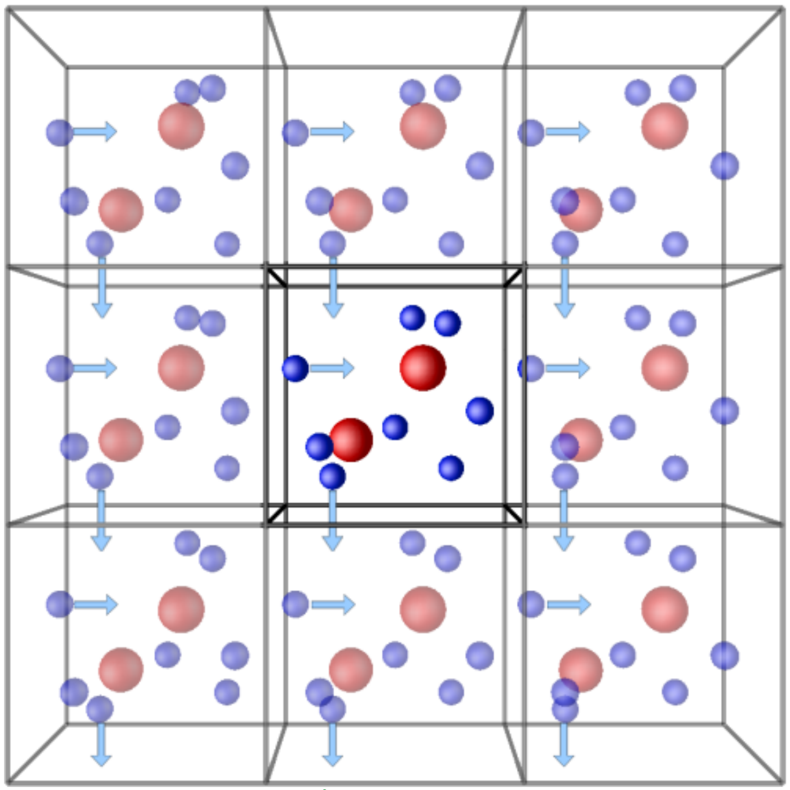

F. Ji, J. N. Hu, H. Shen, Phys. Rev. C 103(2021)055802

Three dimensional calculations

F. Ji, J. N. Hu, H. Shen, Phys. Rev. C 103(2021)055802

The density distribution

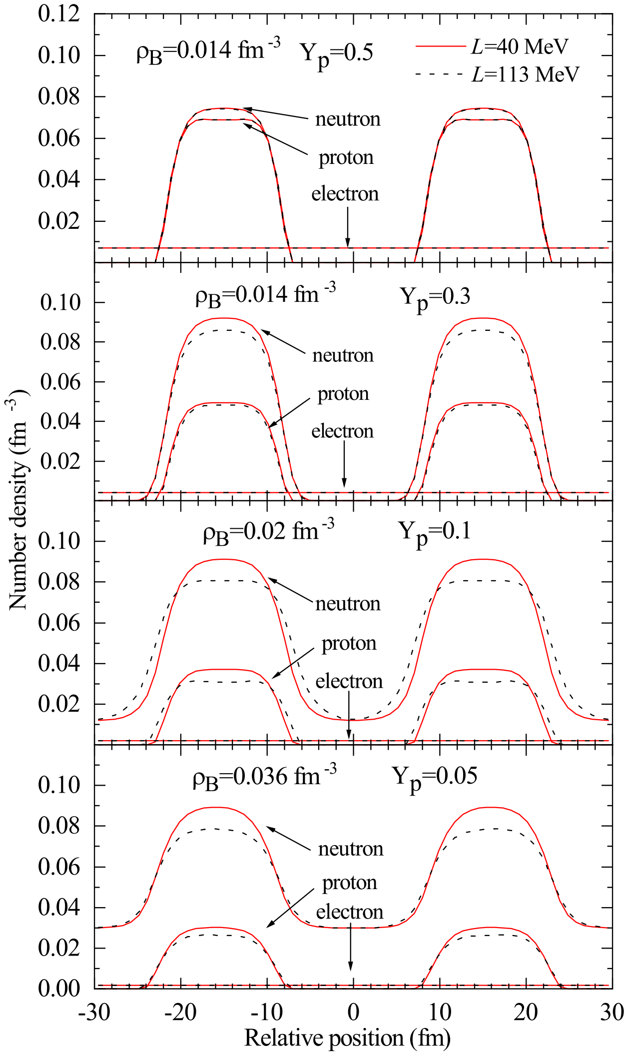

The energy per nucleon

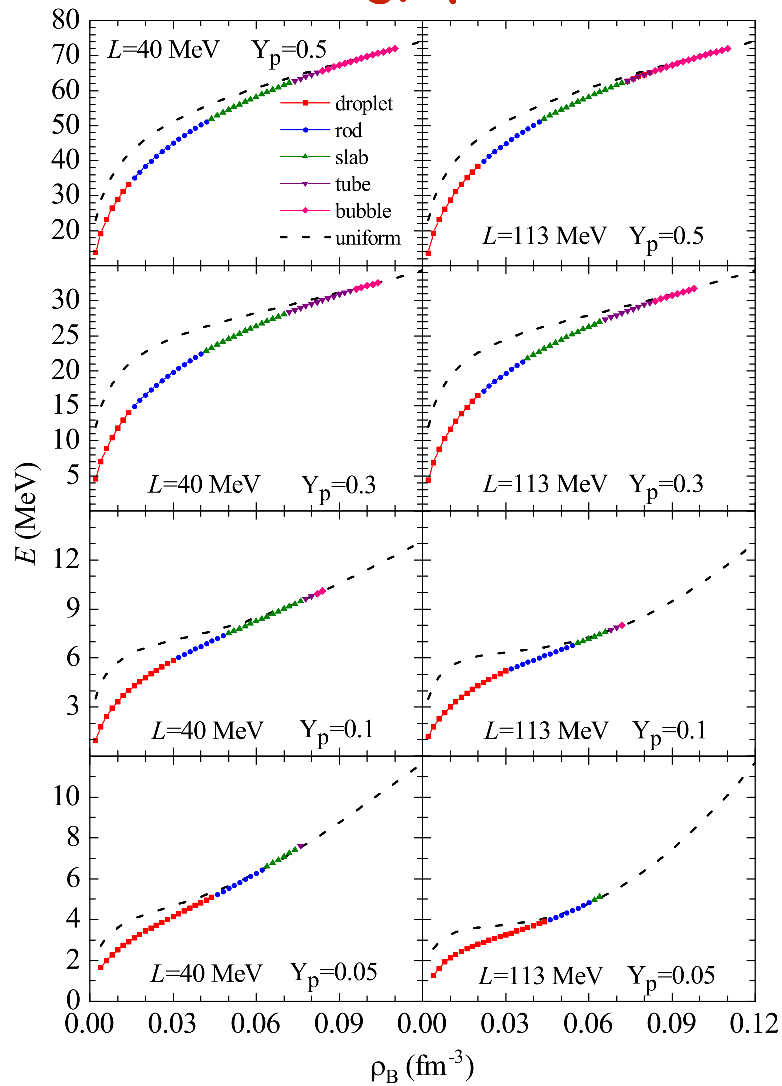

Three dimensional calculations

南開大學

The evaluations of pasta phase with density

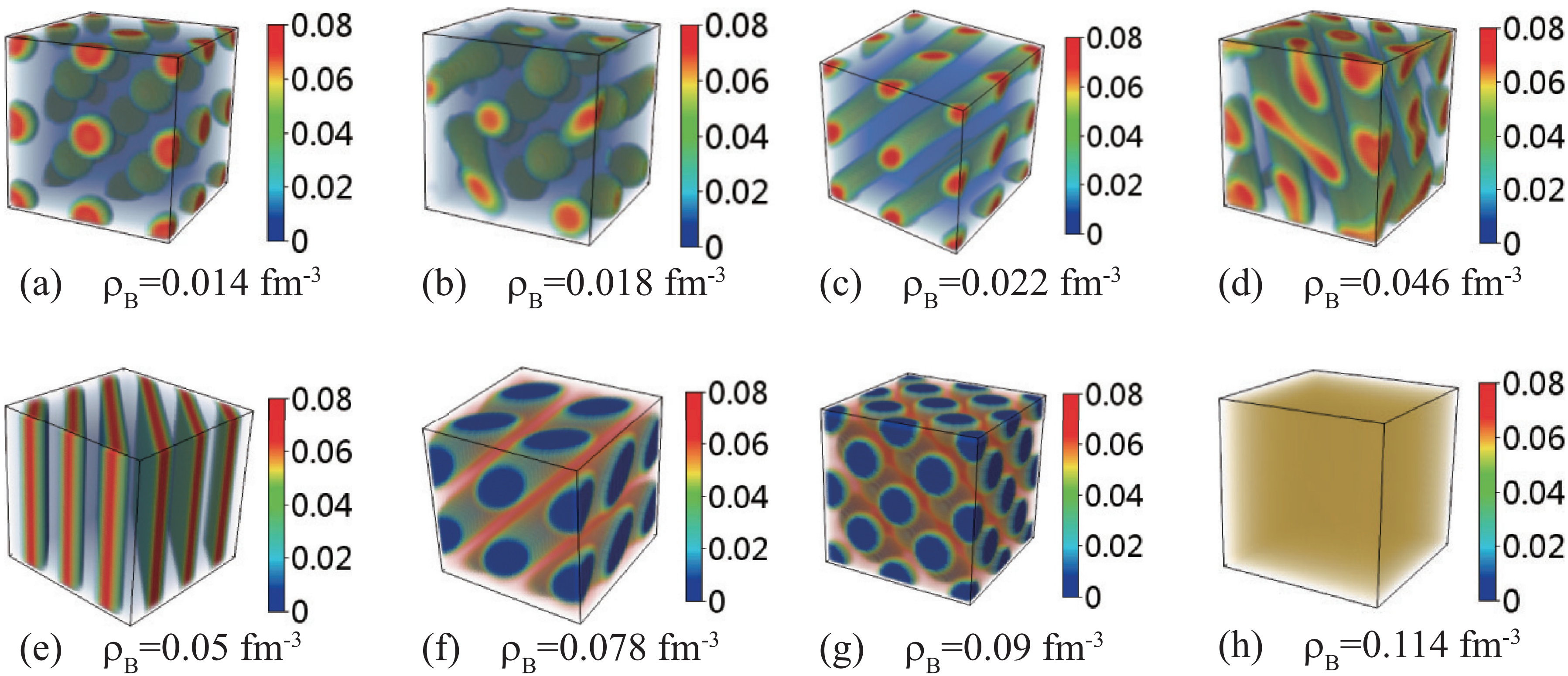

Y_p=0.5, L=40 MeV

F. Ji, J. N. Hu, H. Shen, Phys. Rev. C 103(2021)055802

Three dimensional calculations

The symmetry energy effect

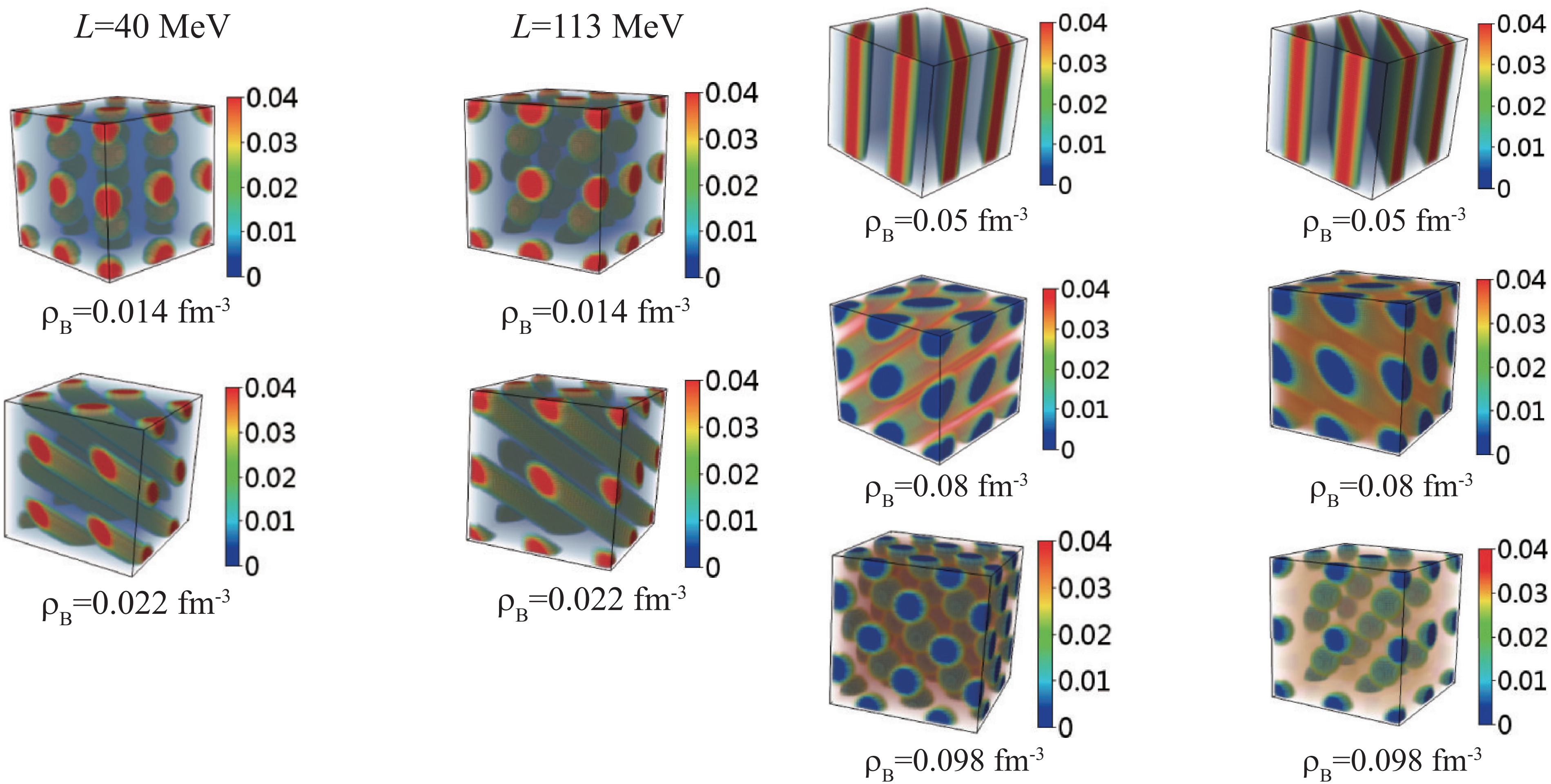

Smaller L generates more pasta structures

Y_p=0.3

F. Ji, J. N. Hu, H. Shen, Phys. Rev. C 103(2021)055802

南開大學

Magnetic effects in total energy

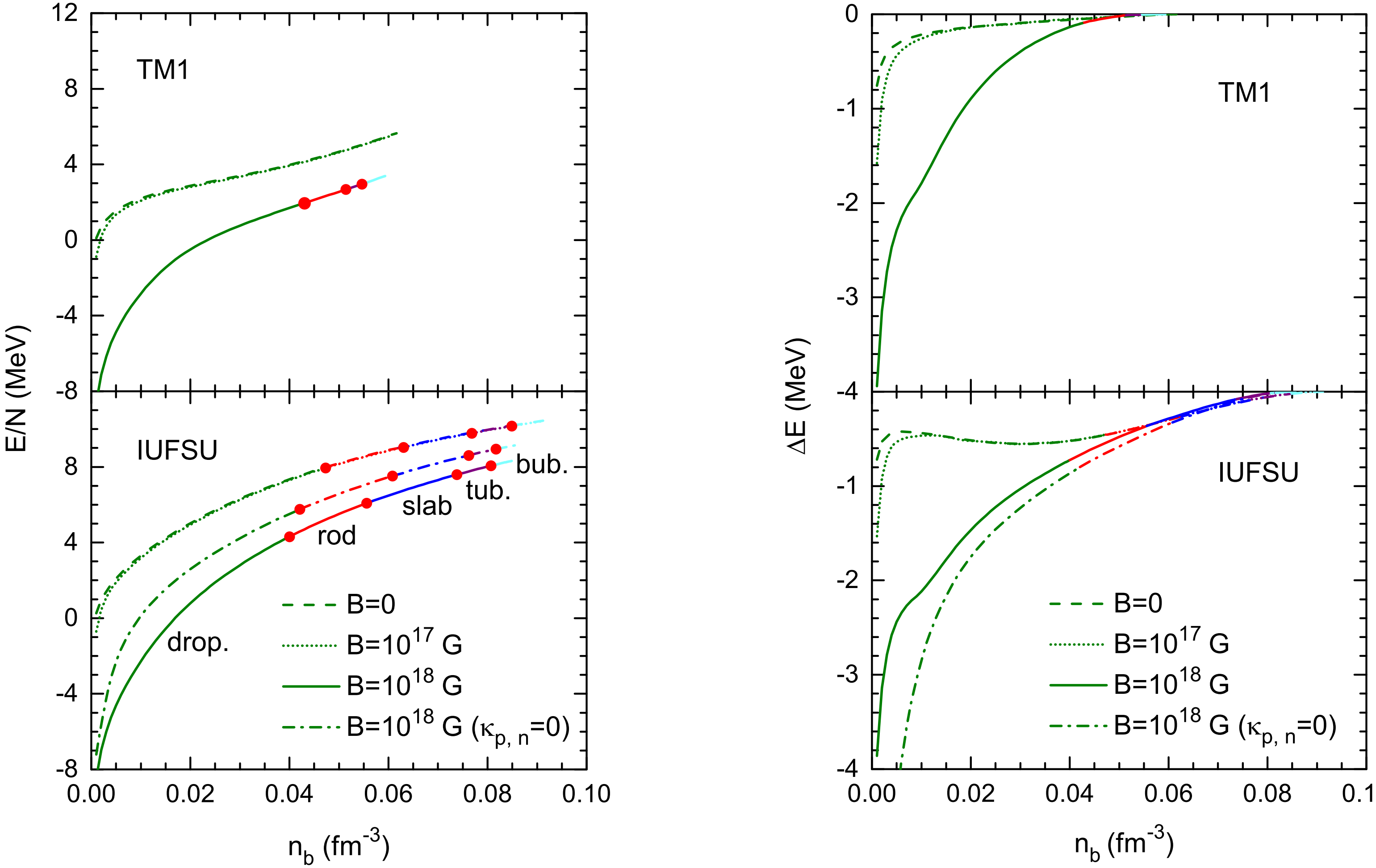

The magnetic field reduces the total energy

S. S. Bao, J. N. Hu, H. Shen, Phys. Rev. C 103(2021)015804

Magnetic field effect

南開大學

S. S. Bao, J. N. Hu, H. Shen, Phys. Rev. C 103(2021)015804

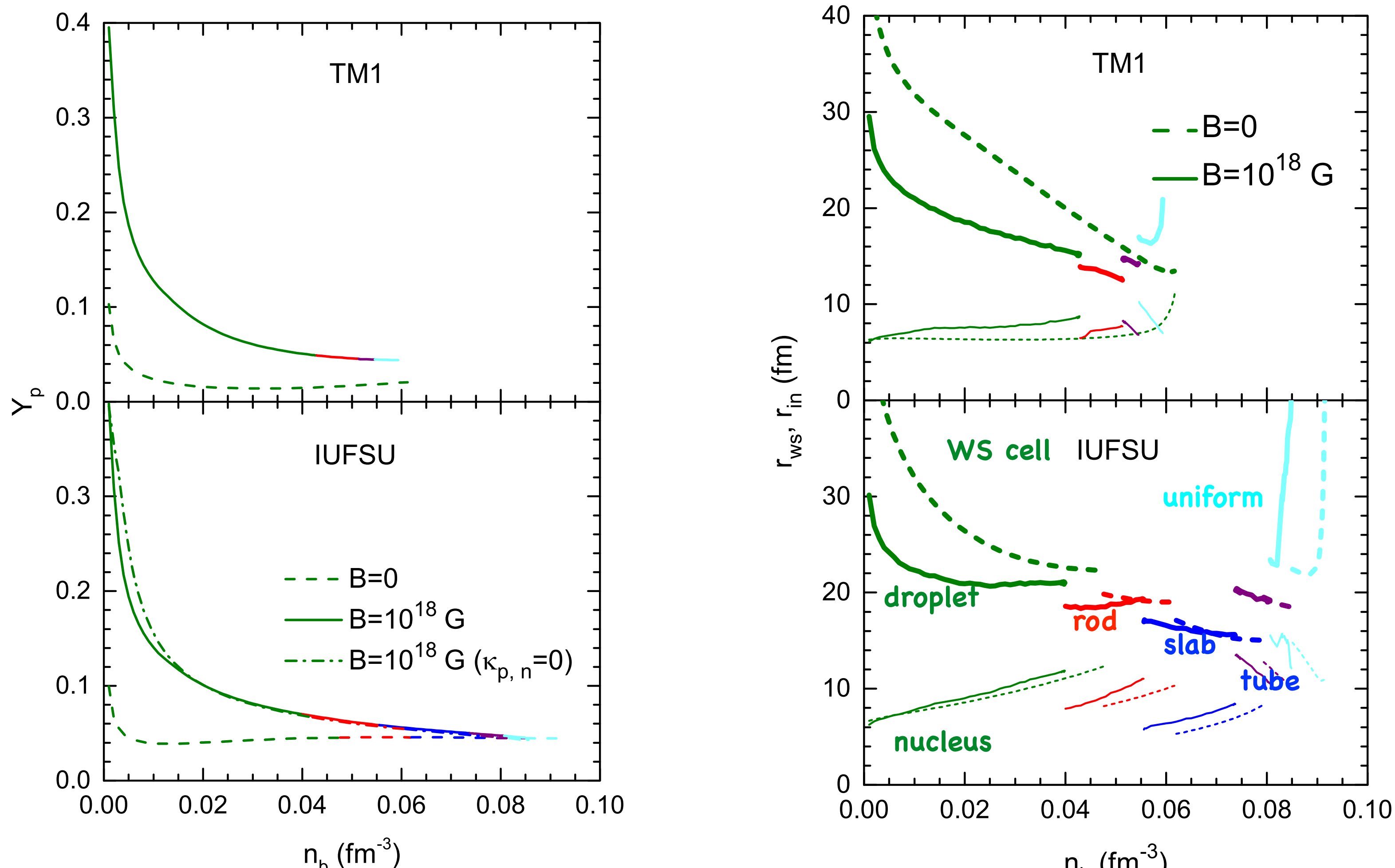

The crust-core transition density decrease significantly with strong magnetic field

Temperature effect

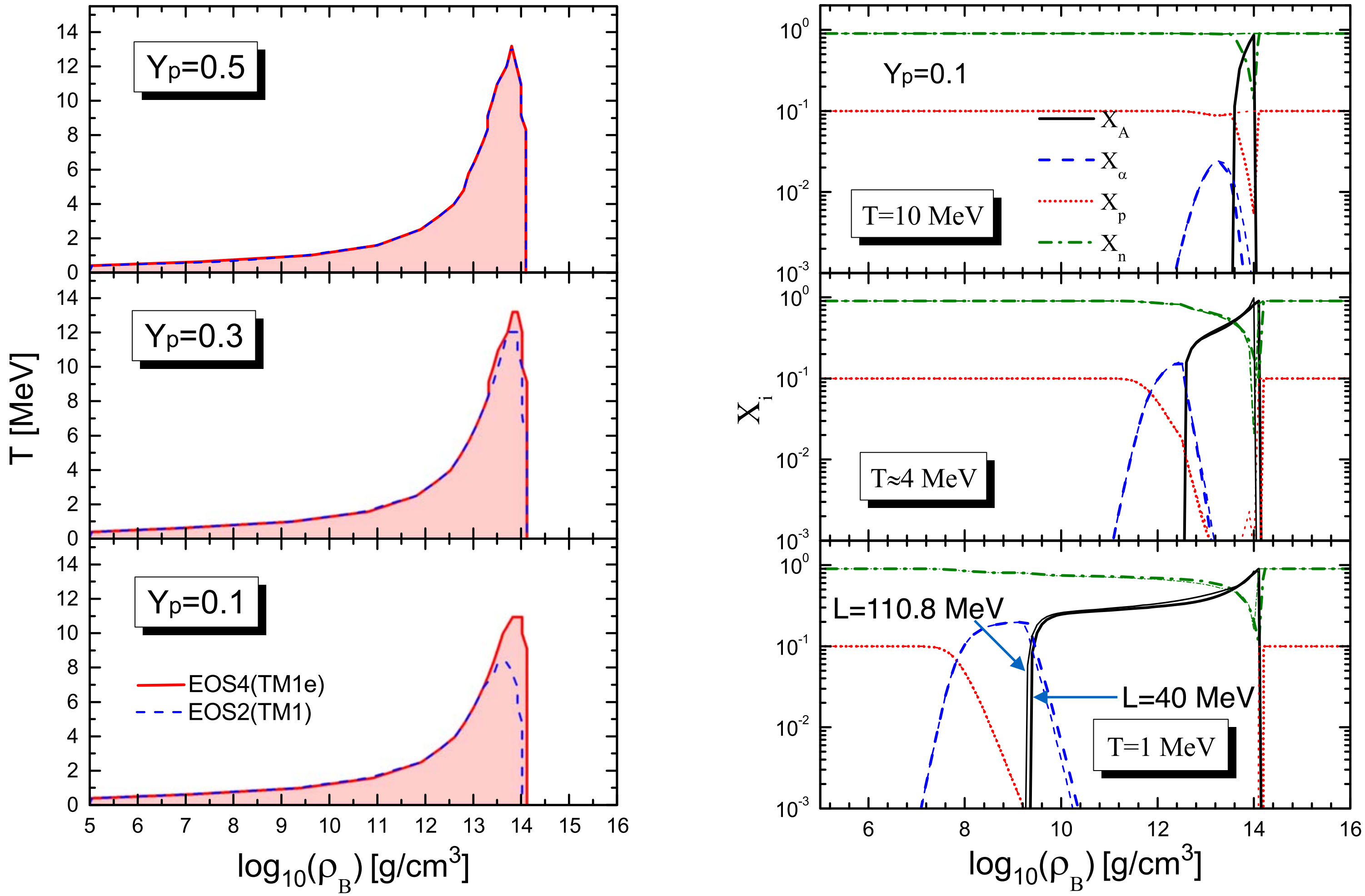

The transition density to uniform matter in TM1e is slightly larger than that in TM1

H. Shen, F. Ji, J. N. Hu, and K. Sumiyoshi, Astrophys. J 891(2019)148

南開大學

H. Shen, F. Ji, J. N. Hu, and K. Sumiyoshi, Astrophys. J 891(2019)148

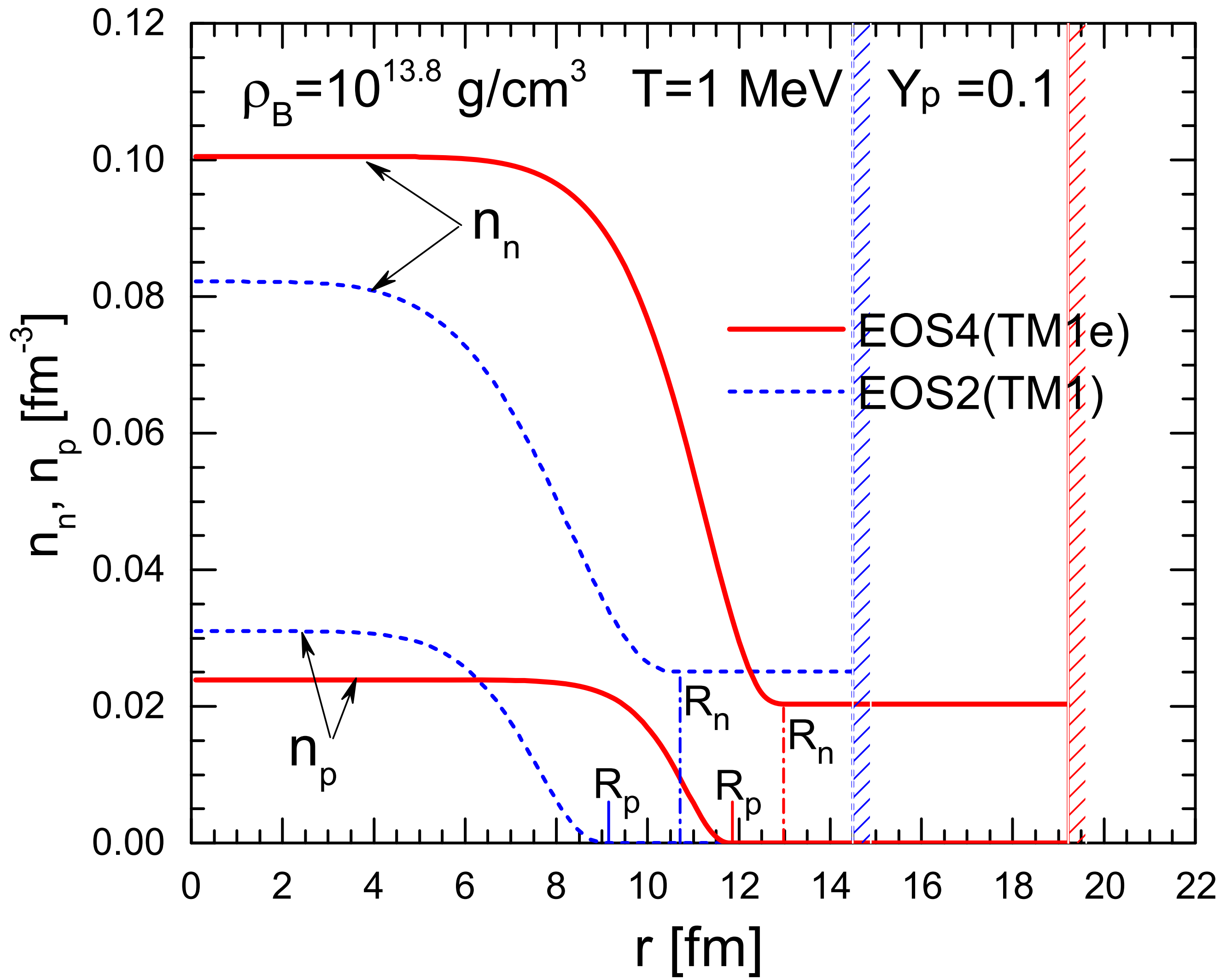

- Introduction
- The inner crust of neutron star
- The properties of neutron star
- The hyperons in neutron star
- Summary

Tolman-Oppenheimer-Volkoff equation

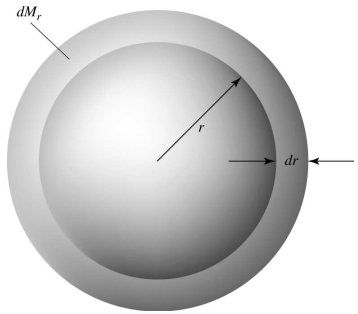

$$\frac{dP}{dr} = -\frac{G\rho M(r)}{r^2}\left(1+\frac{P}{\rho c^2}\right)\left(1+\frac{4\pi P r^3}{M(r)c^2}\right)\left(1-\frac{2GM(r)}{c^2 r}\right)^{-1}$$

$$M(r) = 4\pi\int_0^r \xi^2\rho(\xi)\mathrm{d}\xi$$

$$\rho(r) = \varepsilon(r)/c^2$$

The numerical solution of neutron star

$P(0)=P_C$ **ε-ρ** relation → R, when $P(R)=0$ → $M=M(R)$

$M(0)=0$

The pressure and mass as functions of radius

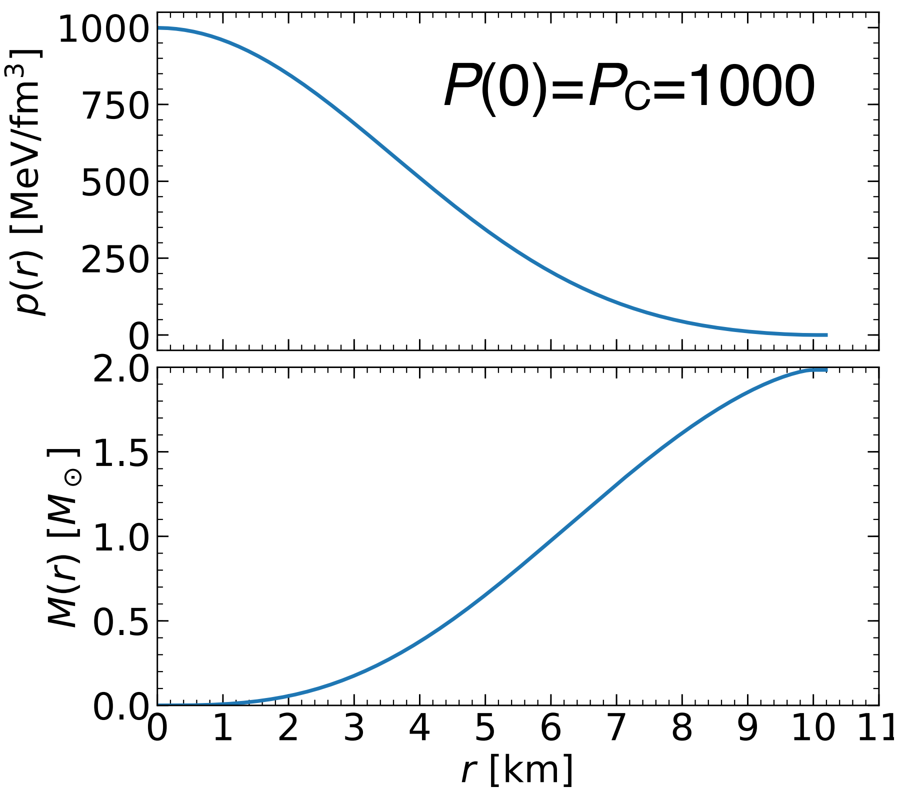

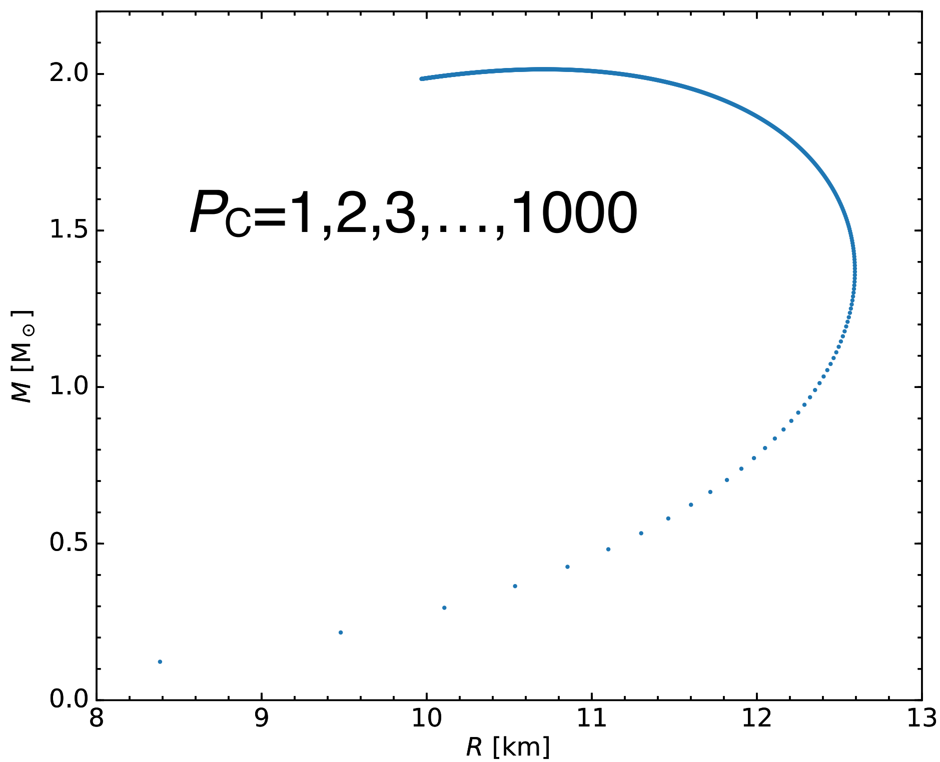

Energy density of nuclear matter

$$\varepsilon = \sum_{i=n,p} \frac{2}{(2\pi)^3} \int_{|\boldsymbol{k}|<k_F^i} d^3\boldsymbol{k} \sqrt{k^2 + M^{*2}} + g_\omega \omega \sum_{i=n,p} \rho_B^i + g_\rho \rho (\rho_B^p - \rho_B^n)$$

$$+ \frac{1}{2} m_\sigma^2 \sigma^2 + \frac{1}{3} g_2 \sigma^3 + \frac{1}{4} g_3 \sigma^4 - \frac{1}{2} m_\omega^2 \omega^2 - \frac{1}{4} c_3 \omega^4 - \frac{1}{2} m_\rho^2 \rho^2 - \Lambda_V g_\omega^2 g_\rho^2 \omega^2 \rho^2.$$

Pressure of nuclear matter

$$p = \sum_{i=n,p} \frac{2}{3(2\pi)^3} \int_{|\boldsymbol{k}|<k_F^i} d^3\boldsymbol{k} \frac{k^2}{\sqrt{k^2 + M^{*2}}} - \frac{1}{2} m_\sigma^2 \sigma^2 - \frac{1}{3} g_2 \sigma^3 - \frac{1}{4} g_3 \sigma^4$$

$$+ \frac{1}{2} m_\omega^2 \omega^2 + \frac{1}{4} c_3 \omega^4 + \frac{1}{2} m_\rho^2 \rho^2 + \Lambda_V g_\omega^2 g_\rho^2 \omega^2 \rho^2.$$

J. N. Hu, et al., Prog. Theo. Exp. Phys., 2020 (2020) 043D01

南開大學

The beta equilibrium and charge neutrality conditions

$$\mu_p = \mu_n - \mu_e,$$
$$\mu_\mu = \mu_e.$$

$$\rho_p = \rho_e + \rho_\mu.$$

Chemical potential

$$\mu_i = \sqrt{k_F^{i2} + M_N^{*2}} + g_\omega \omega + g_\rho \tau_3 \rho,$$
$$\mu_l = \sqrt{k_F^{l2} + m_l^2},$$

J. N. Hu, et al., Prog. Theo. Exp. Phys., 2020 (2020) 043D01

Tidal deformability

The tidal deformability

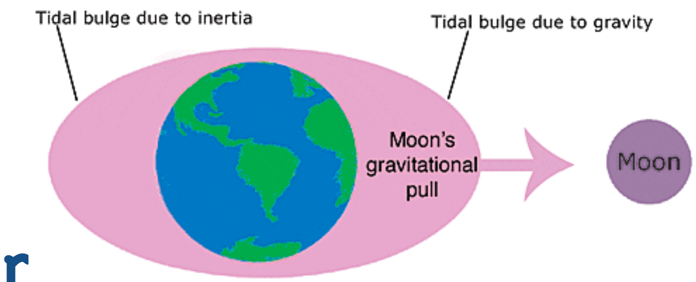

where C is the compactness parameter

$$C = GM/Rc^2$$

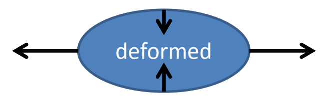

$$Q_{ij} = -\lambda \mathcal{E}_{ij}$$

and Love number

$$\begin{aligned} k_2 = \; & \frac{8C^5}{5}(1-2C)^2[2+2C(y_R-1)-y_R] \\ & \Big\{2C[6-3y_R+3C(5y_R-8)] \\ & +4C^3[13-11y_R+C(3y_R-2)+2C^2(1+y_R)] \\ & +3(1-2C)^2[2-y_R+2C(y_R-1)]\ln(1-2C)\Big\}^{-1}. \end{aligned}$$

y_R is obtained by solving the equation

$$r\frac{dy(r)}{dr} + y(r)^2 + y(r)F(r) + r^2Q(r) = 0,$$

T. Hinderer, Astrophys. J. 677 (2008) 1216

The neutron star mass as function of Radius

J. N. Hu, et al., Prog. Theo. Exp. Phys., 2020 (2020) 043D01

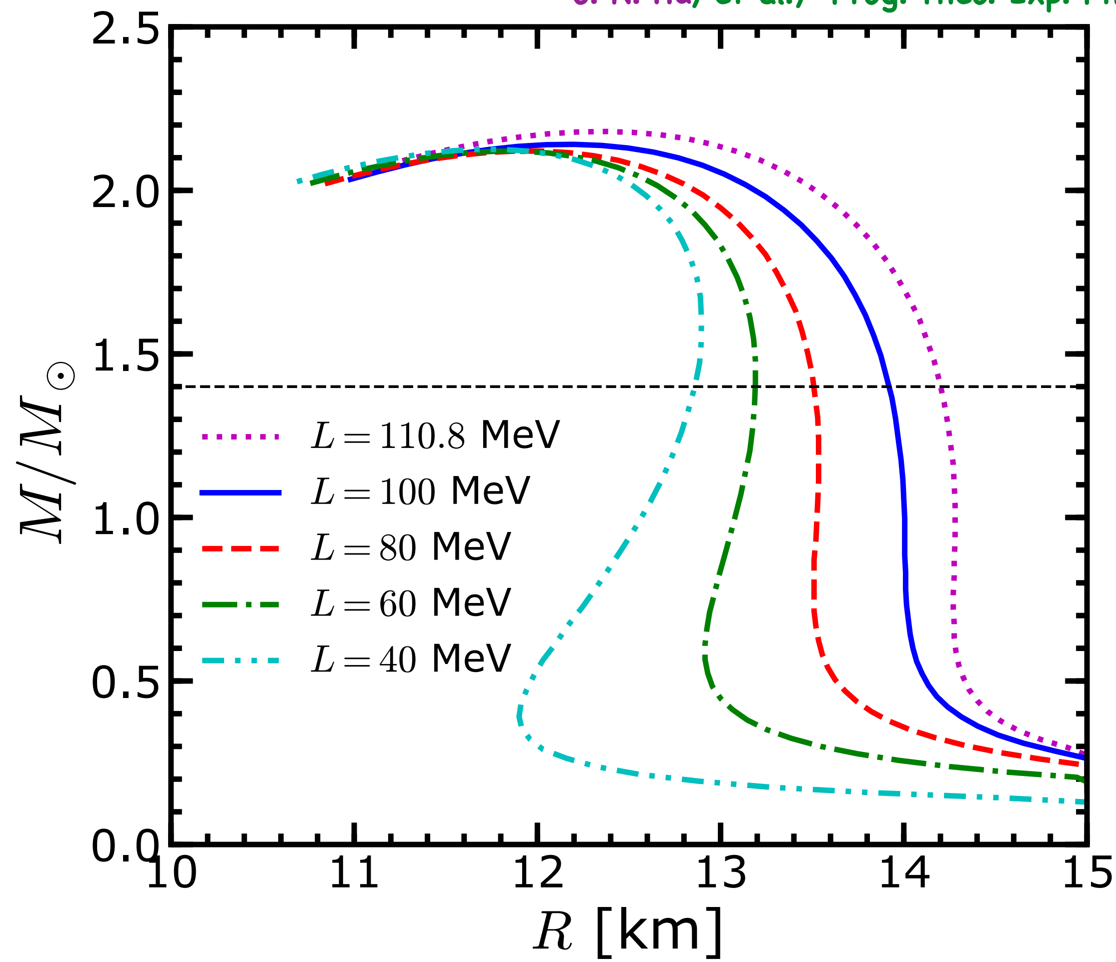

1.4M⊙

The symmetry energy affects the neutron star at small mass region

The threshold in DU process

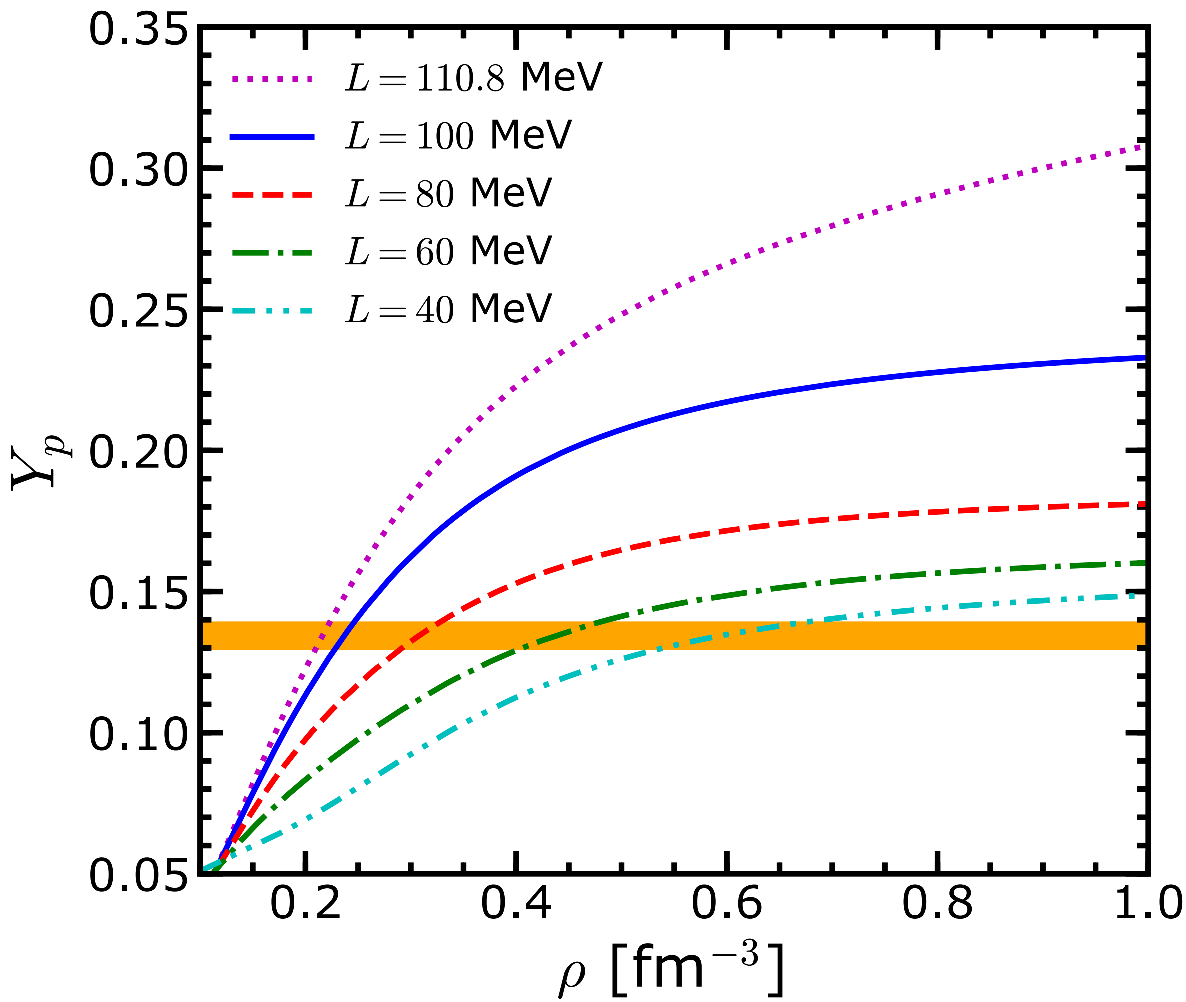

The symmetry energy affects the threshold of Yp in DU process obviously

The tidal deformability

南開大學

J. N. Hu, et al., Prog. Theo. Exp. Phys., 2020 (2020) 043D01

The tidal deformability as a function of neutron mass

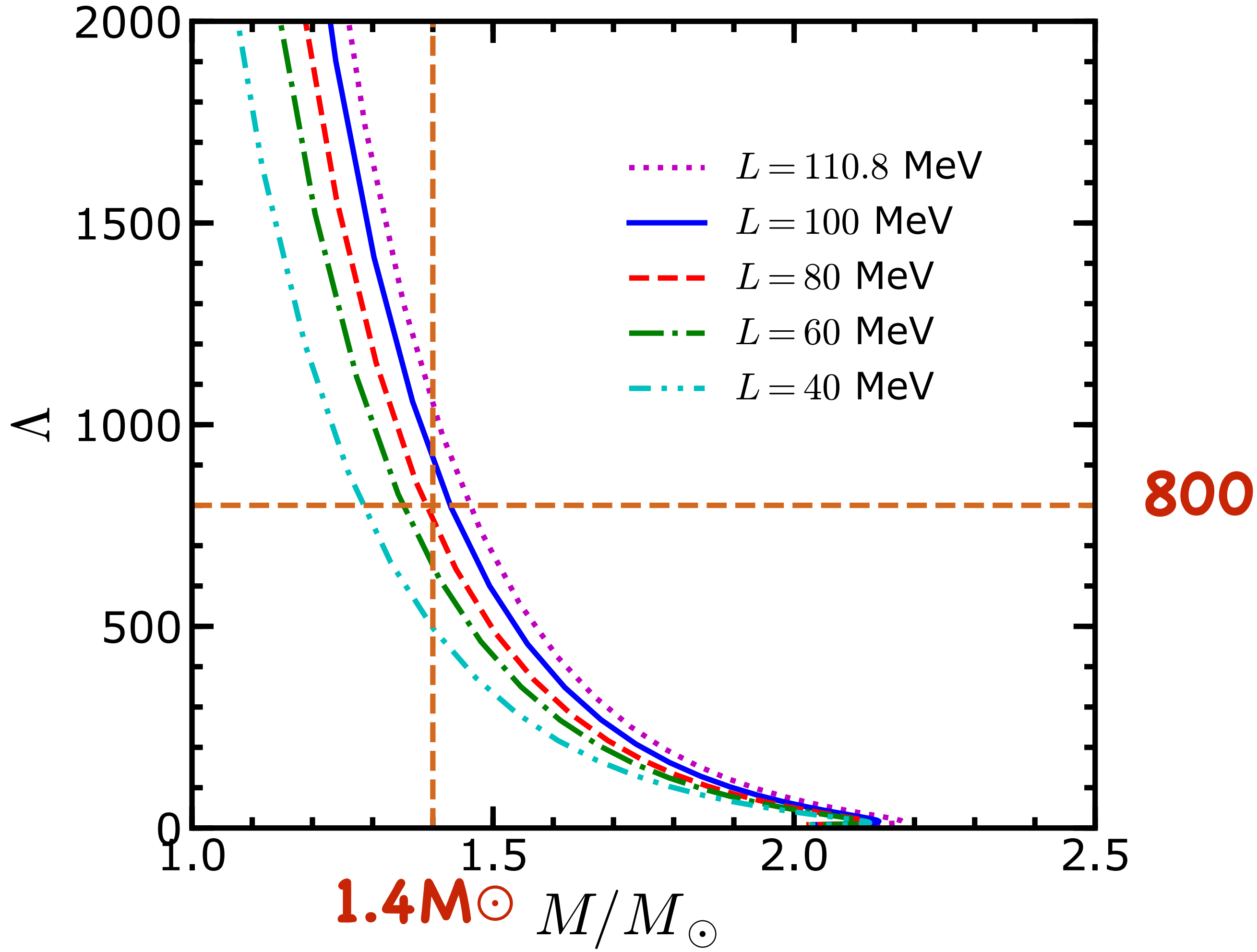

The correlations

The various correlations about neutron star and symmetry energy

J. N. Hu, et al., Prog. Theo. Exp. Phys., 2020 (2020) 043D01

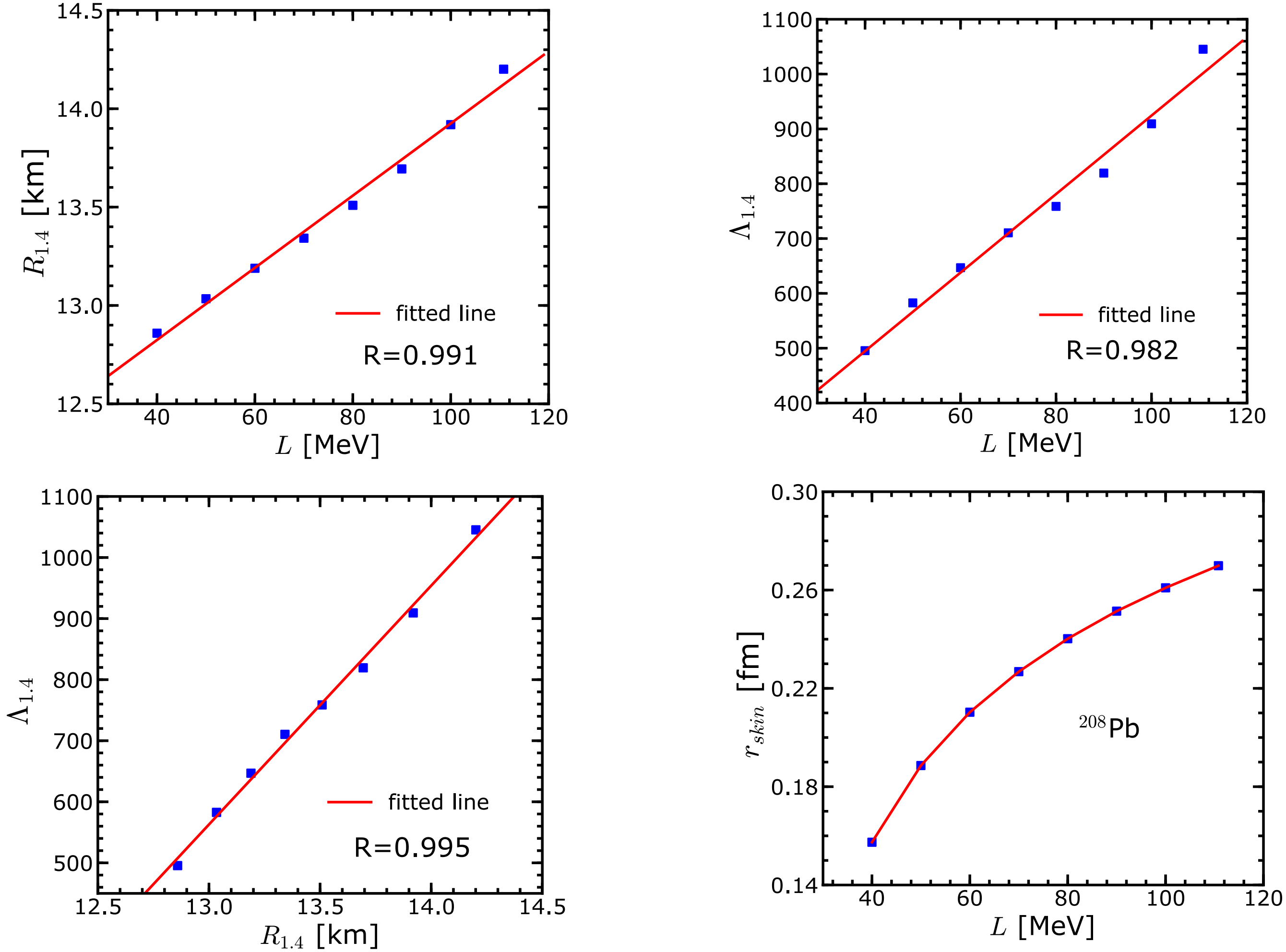

The unified equation of state

The mass-radius relation with unified EOS

F. Ji, J. N. Hu, S. Bao, and H. Shen, Phys. Rev. C, 100 (2019)045801

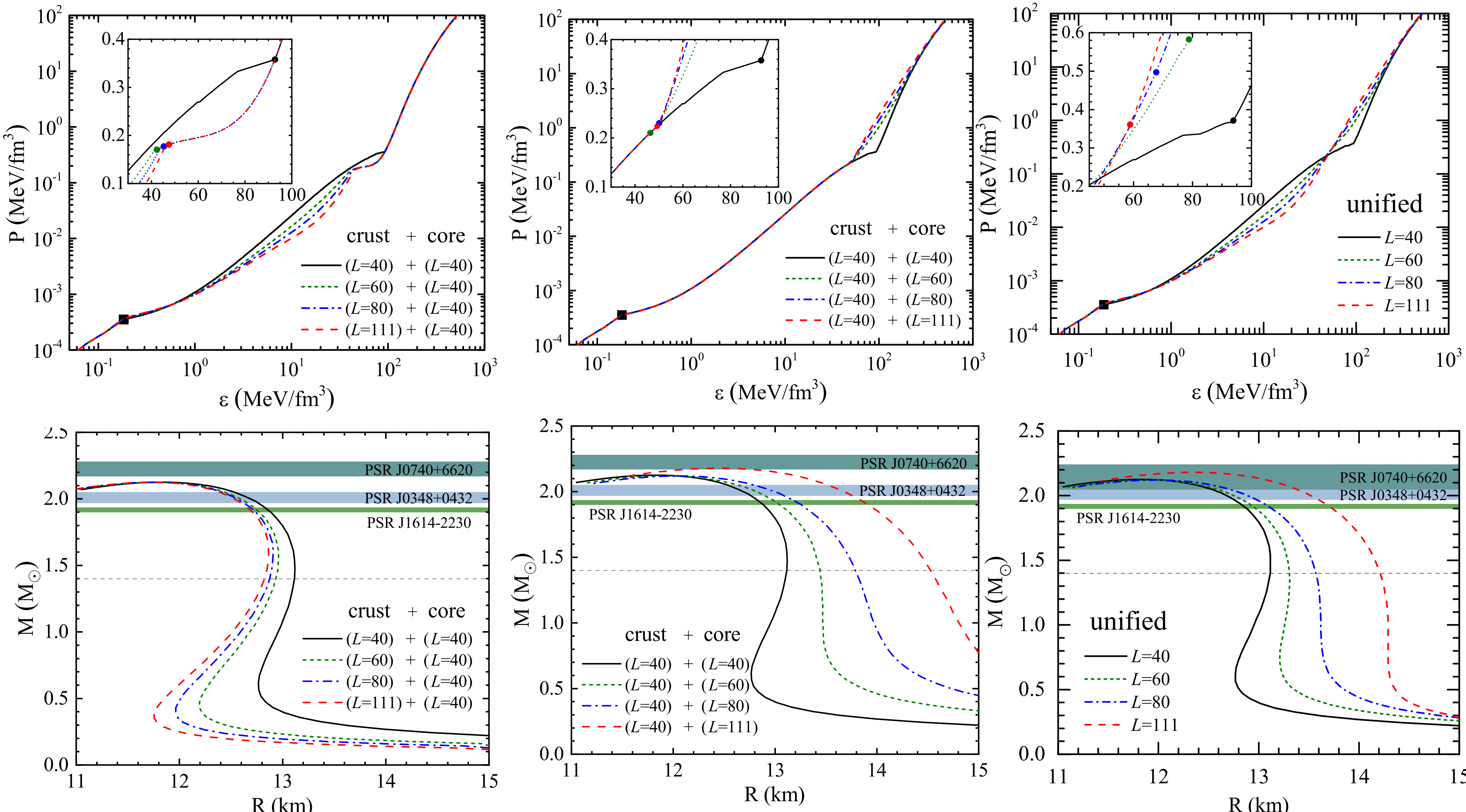

The crust effects

The EOSs with uniform EOS

F. Ji, J. N. Hu, S. Bao, and H. Shen, Phys. Rev. C, 100 (2019)045801

EOS TM1	Combination crust+core	M_{max} ($M_\odot$)	$R_{1.4}$ (km)	$\Delta R_{1.4}^{crust}$ (km)	$k_2^{1.4}$	$C_{1.4}$	$\Lambda_{1.4}$
unified	$(L=40)+(L=40)$	2.12	13.12	1.25	0.095	0.158	652
unified	$(L=111)+(L=111)$	2.18	14.21	1.27	0.103	0.145	1047
nonunified	$(L=40)+(L=111)$	2.18	14.53	1.44	0.092	0.142	1050
nonunified	$(L=111)+(L=40)$	2.12	12.82	0.84	0.110	0.161	671

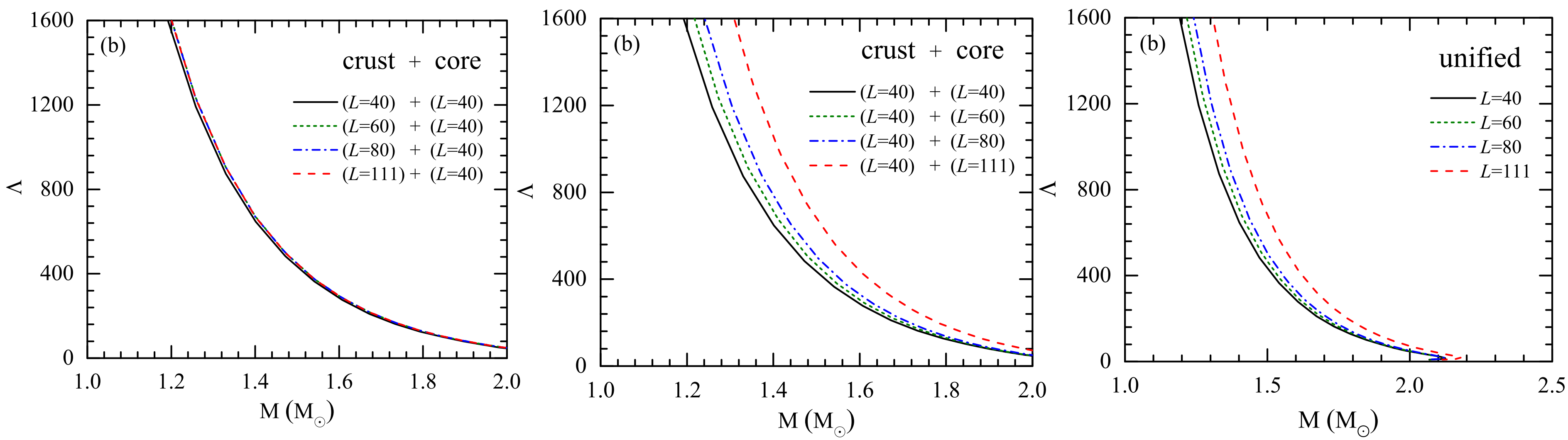

The GW190814-2.6M⊙ object

The Astrophysical Journal Letters, 896:L44 (20pp), 2020 June 20
https://doi.org/10.3847/2041-8213/ab960f

GW190814: Gravitational Waves from the Coalescence of a 23 Solar Mass Black Hole with a 2.6 Solar Mass Compact Object

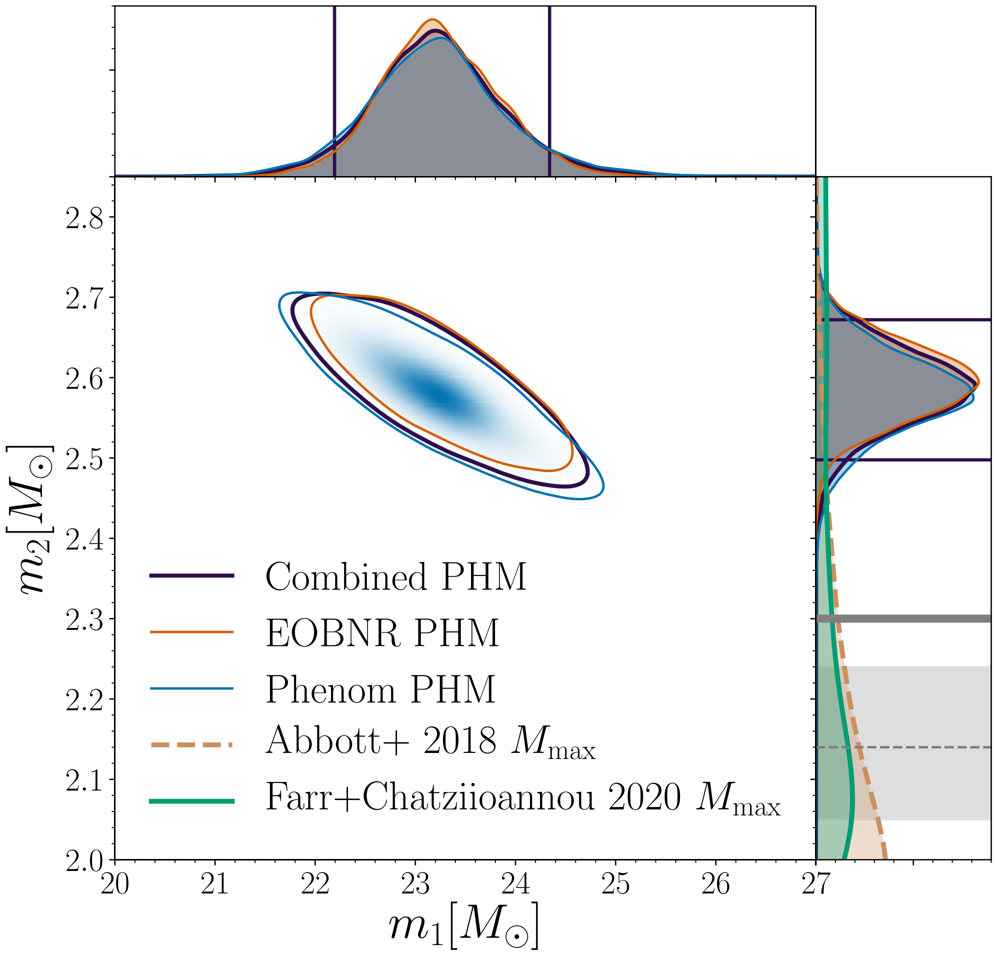

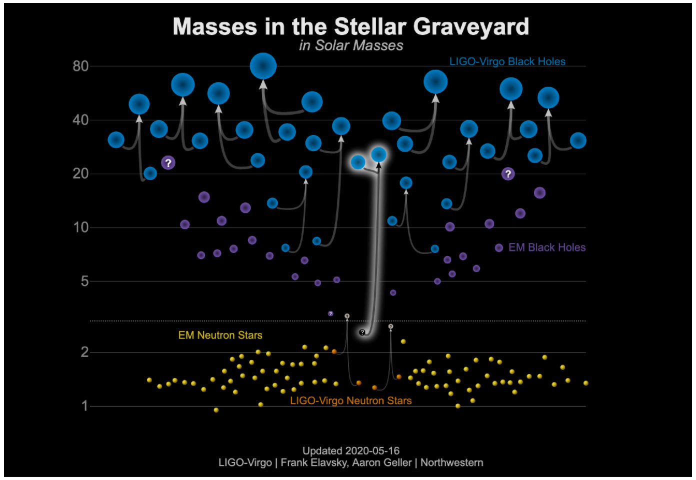

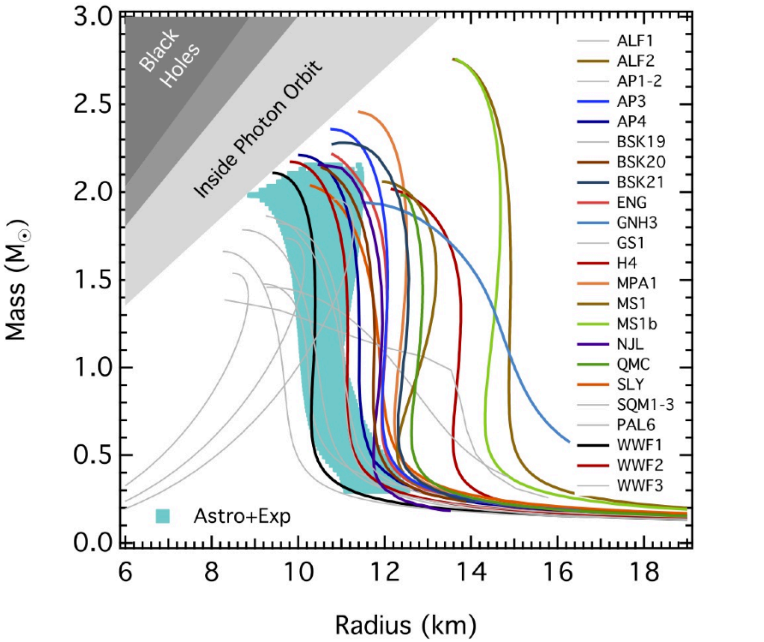

F. Oezel and P. Freire Annu. Rev. Astron. Astrophys. 54 (2016)401

The possibilities of GW190814

南開大學

A heavy neutron star including the deconfined QCD matter

H. Tan, J. Noronha-Hostler, and N. Yunes, (2020), arXiv:2006.16296

V. Dexheimer, R.O. Gomes, T. Klähn, S. Han and M. Salinas, (2020), arXiv:2007.08493

A super-fast pulsar

N. B. Zhang and B.-A. Li, (2020), arXiv:2007.02513

V. Dexheimer, R.O. Gomes, T. Klähn, S. Han and M. Salinas, (2020), arXiv:2007.08493

A normal neutron star

Y. Lim, A. Bhattacharya, J. W. Holt, and D. Pati, (2020), arXiv:2007.0652

A black hole

I. Tews, et al.,(2020), arXiv:2007.06057

F. Fattoyev, C. Horowitz, J. Piekarewicz, and B. Reed, (2020), arXiv:2007.03799

……

南開大學

	DD-LZ1	DD2	DD-ME1	DD-ME2	DD-MEX	DDV	DDVT	DDVTD
$\rho_{B0}[\mathrm{fm}^{-3}]$	0.1585	0.149	0.152	0.152	0.1518	0.1511	0.1536	0.1536
$E/A[\mathrm{MeV}]$	-16.126	-16.916	-16.668	-16.233	-16.14	-16.097	-16.924	-16.915
$K_0[\mathrm{MeV}]$	231.237	241.990	243.881	251.306	267.059	239.499	239.999	239.914
$E_{\mathrm{sym}}[\mathrm{MeV}]$	32.016	31.635	33.060	32.31	32.269	33.589	31.558	31.817
$L[\mathrm{MeV}]$	42.467	54.933	55.428	51.265	49.692	69.646	42.348	42.583
M_n^*/M	0.558	0.563	0.578	0.572	0.556	0.586	0.667	0.667
M_p^*/M	0.558	0.562	0.578	0.572	0.556	0.585	0.666	0.666

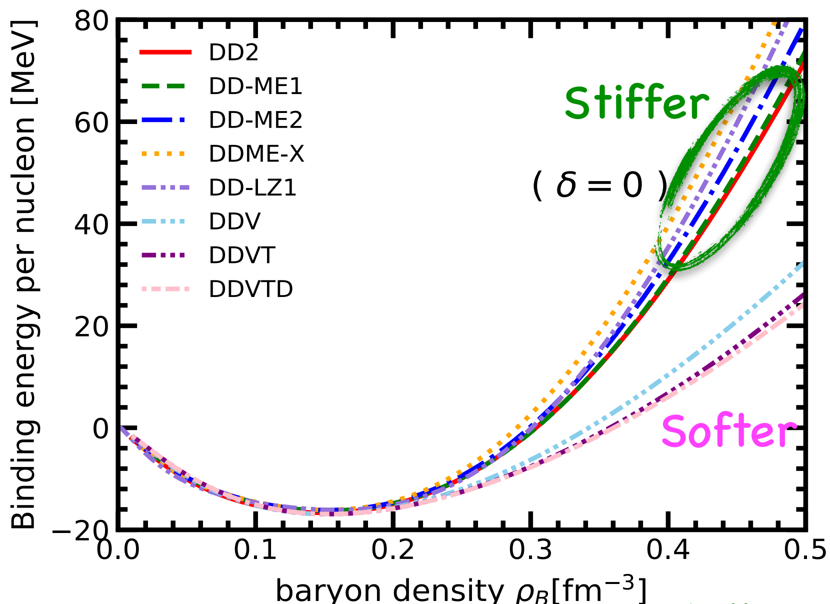

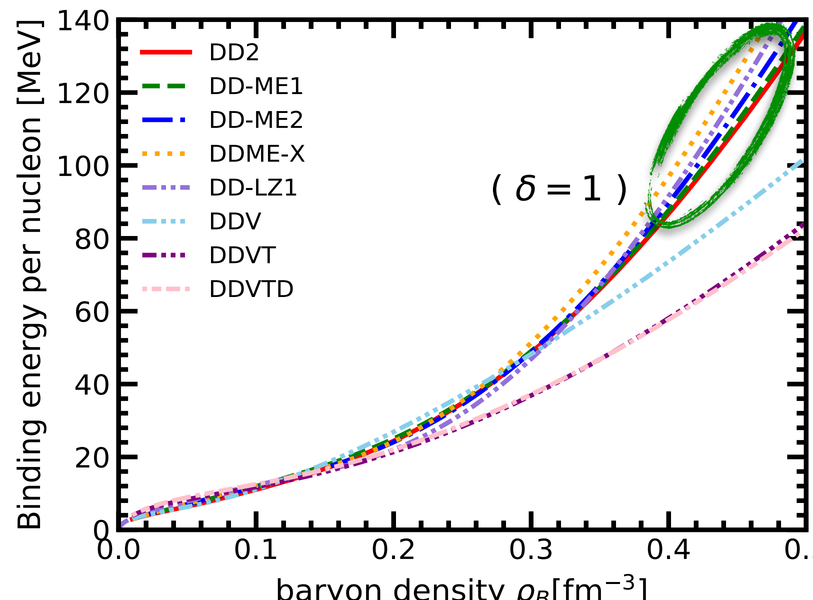

K. Huang, J. N. Hu, Y. Zhang, and H. Shen, Astrophys. J. 904(2020)39

The Strong vector potentials

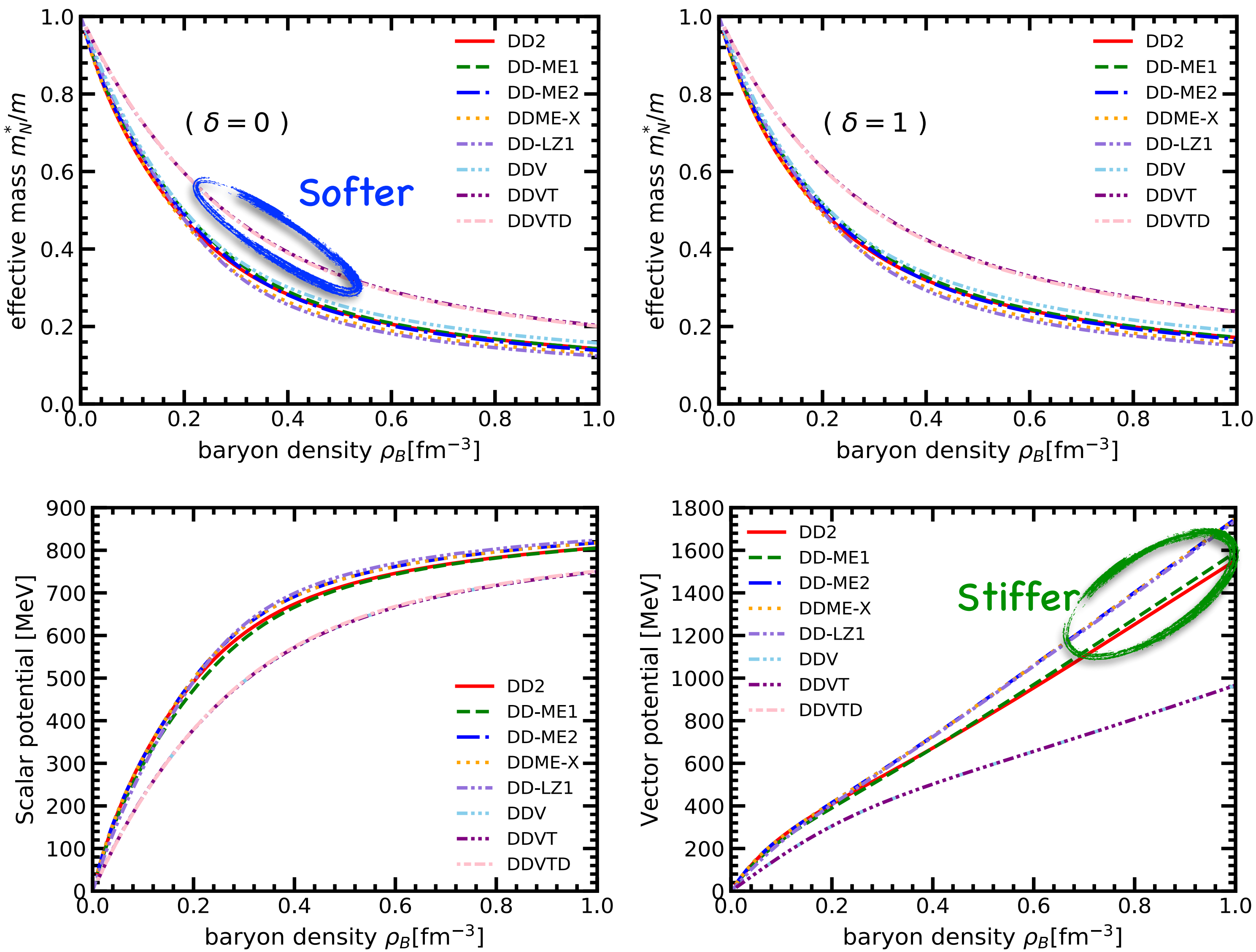

K. Huang, J. N. Hu, Y. Zhang, and H. Shen, Astrophys. J. 904(2020)39

Pressure vs. energy

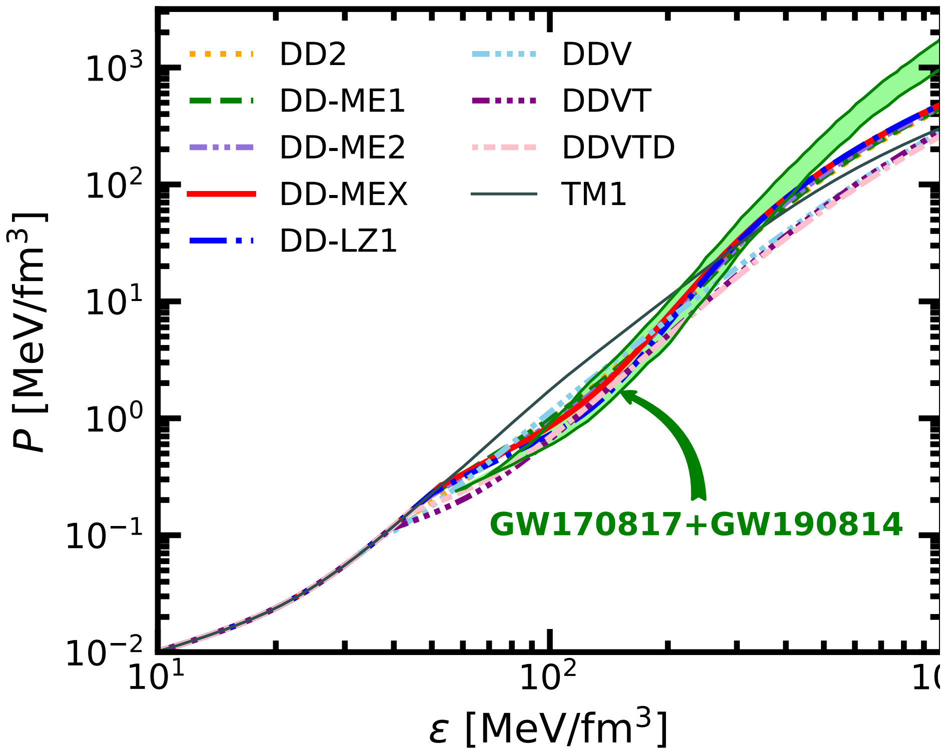

Pressure vs. density

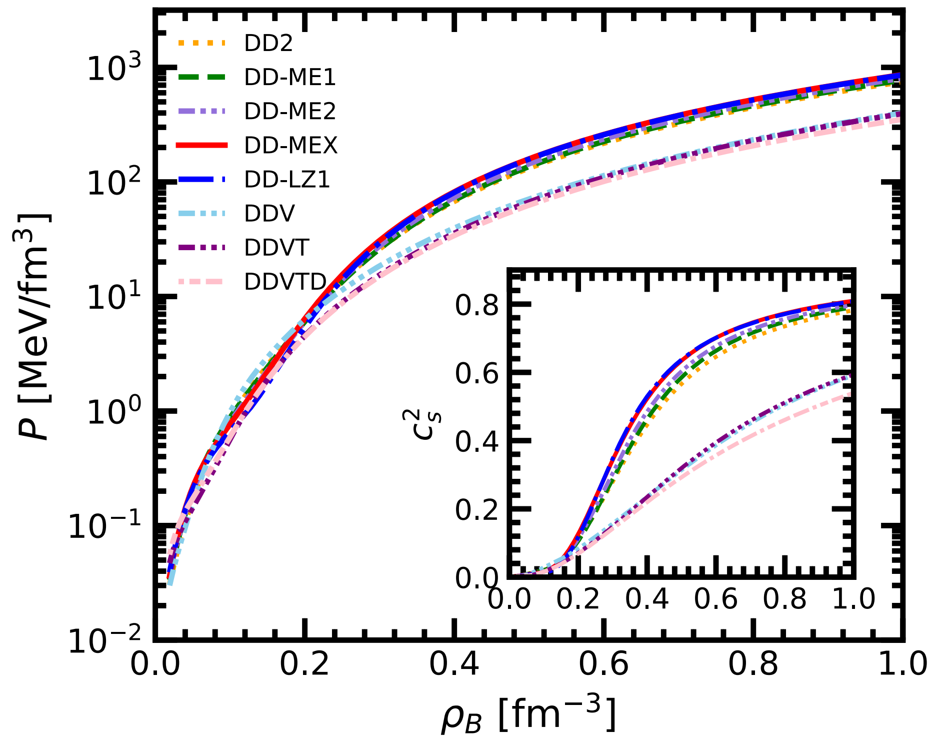

The stiffer EOSs will generate larger speeds of sound

data from: R. Abbott et al. (LIGO Scientific, Virgo), Astrophys. J. 896, L44 (2020)

The mass, radius, density relations

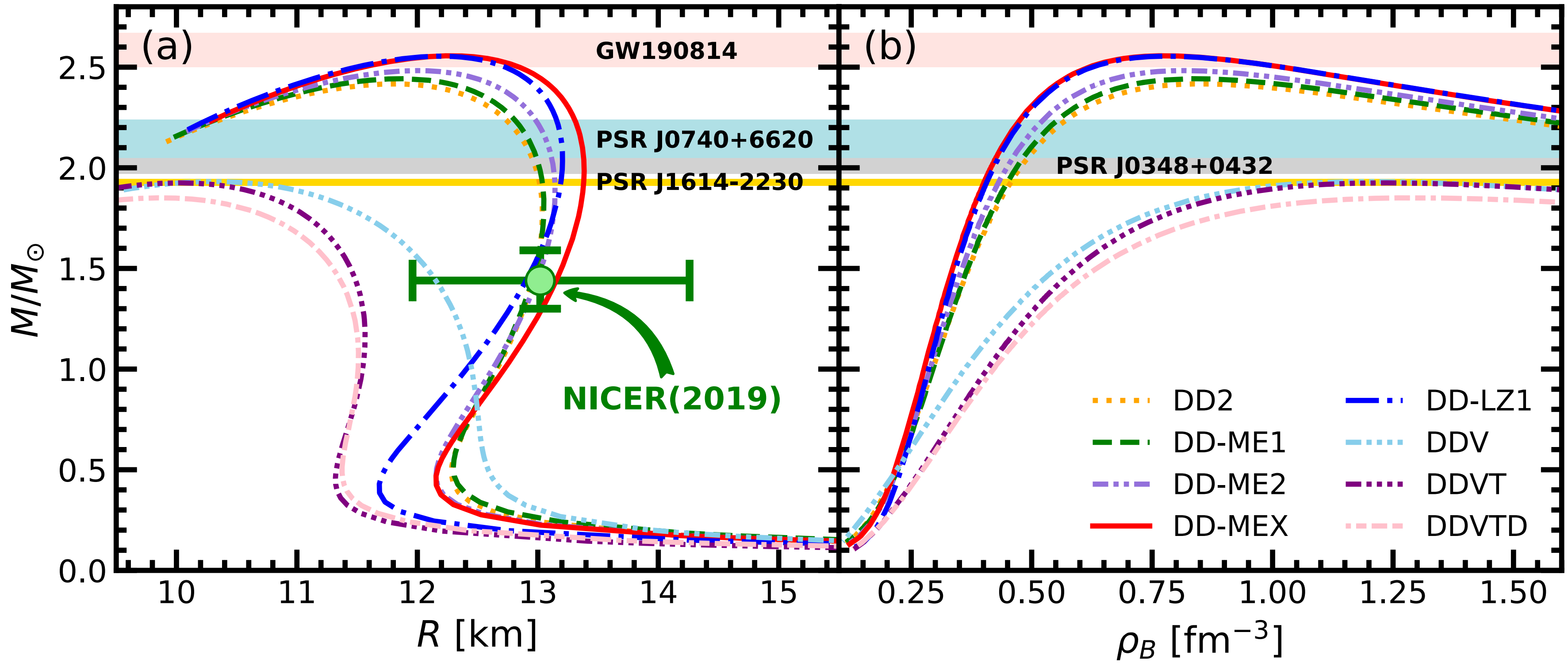

	DD-LZ1	DD2	DD-ME1	DD-ME2	DD-MEX	DDV	DDVT	DDVTD
$M_{\max}/M_{\odot}$	2.5545	2.4168	2.4426	2.4829	2.5566	1.9317	1.9251	1.8507
$R_{\max}$[km]	12.178	11.826	11.885	12.012	12.274	10.336	10.023	9.850
$\rho_{\max}$[fm^{-3}]	0.786	0.845	0.832	0.813	0.777	1.188	1.237	1.306
$R_{1.4}$[km]	12.864	12.938	12.931	12.961	13.118	12.195	11.511	11.396
$\Lambda_{1.4}$	727.071	639.032	686.786	730.737	790.051	390.005	301.388	274.908

The tidal deformabilities of neutron star

南開大學

K. Huang, J. N. Hu, Y. Zhang, and H. Shen, Astrophys. J. 904(2020)39

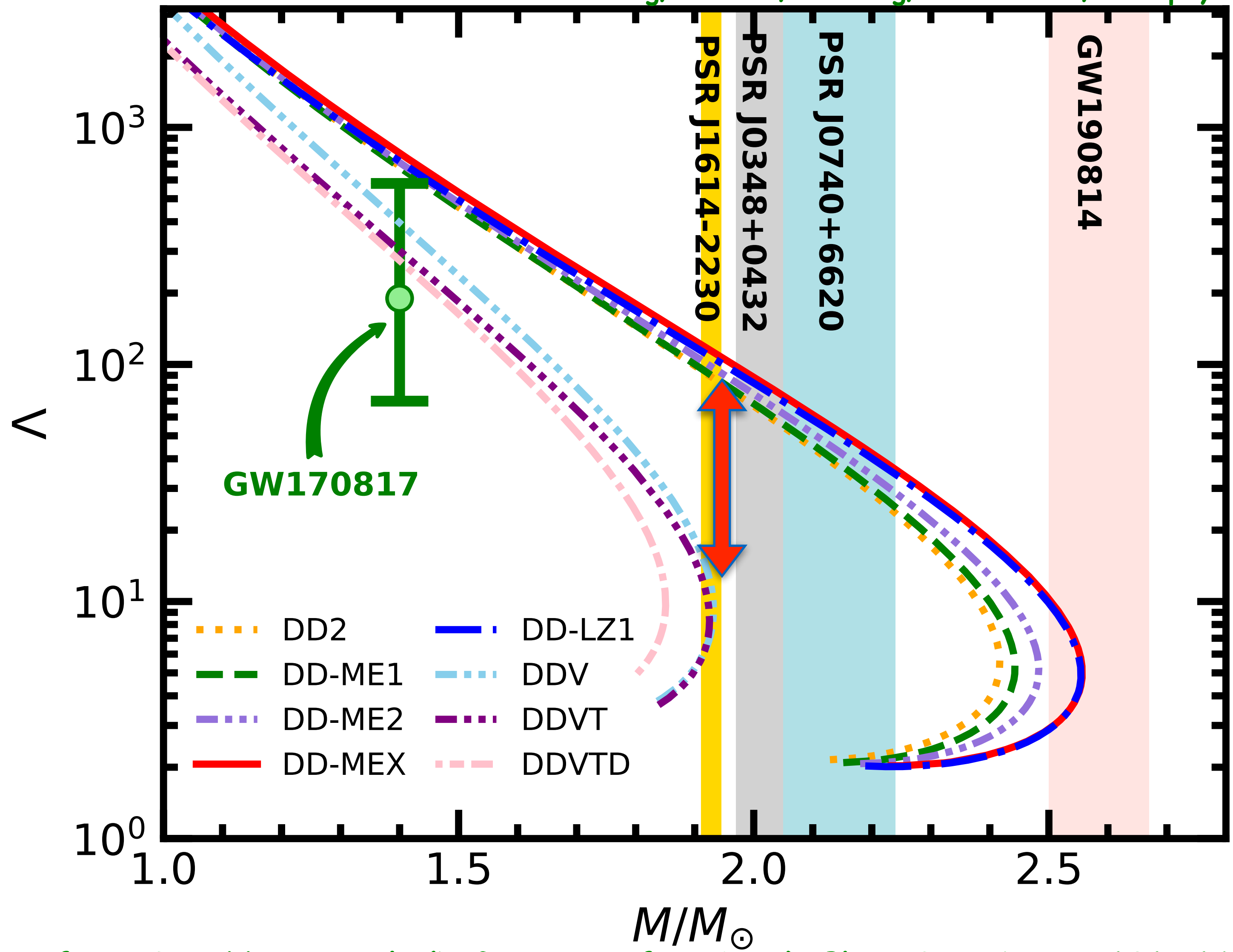

data from: R. Abbott et al. (LIGO Scientific, Virgo), Phys. Rev. Lett., 121, 161101 (2018)

- Introduction
- The inner crust of neutron star
- The properties of neutron star
- The hyperons in neutron star
- Summary

Strangeness degree of freedom

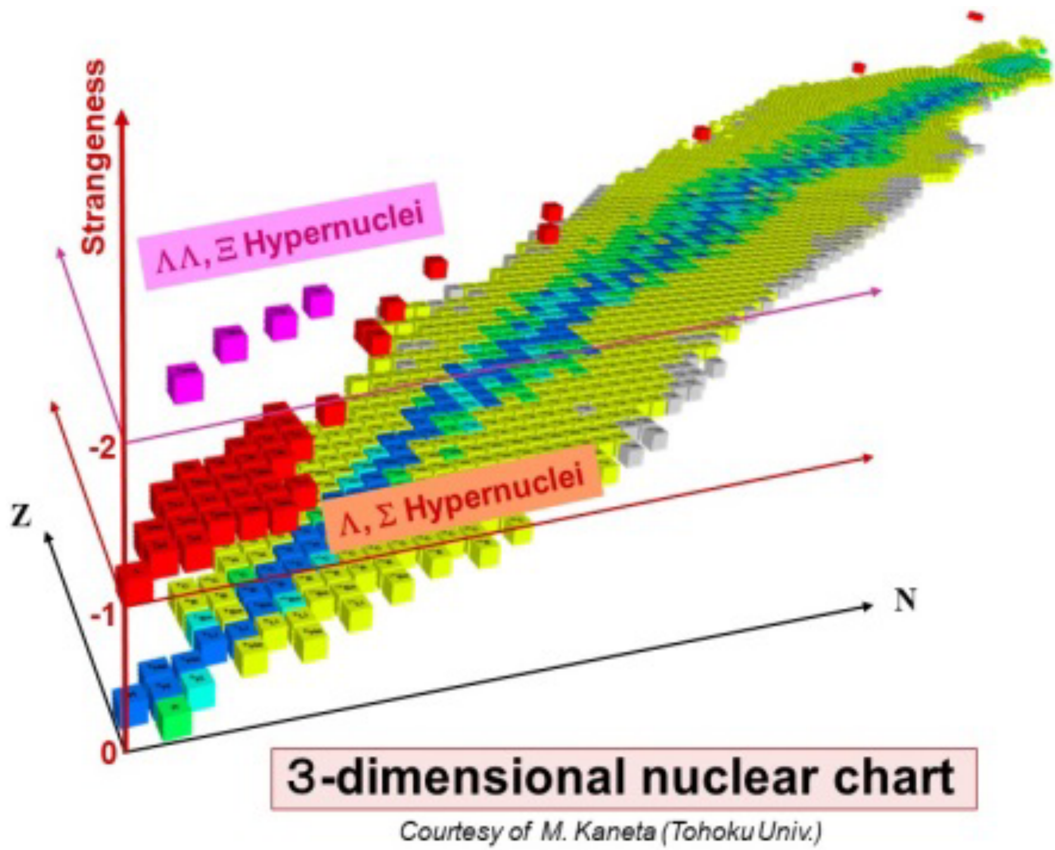

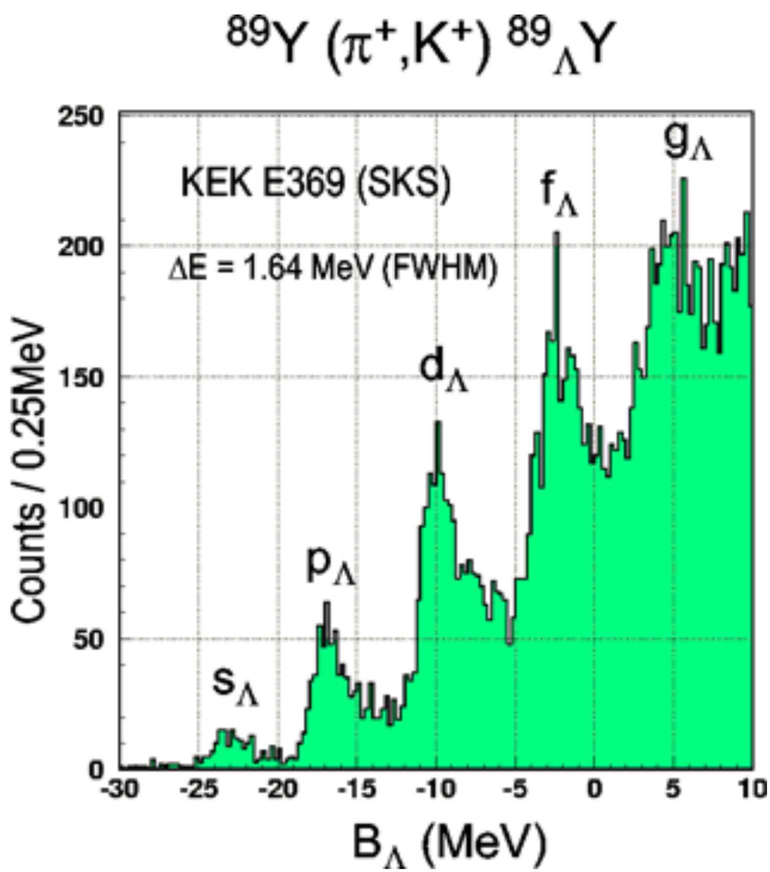

The RMF model including the hyperons

K. Huang, J. N. Hu, Y. Zhang, and H. Shen, arXiv: 2203.12357

$$
\begin{aligned}
\mathcal{L}_{\mathrm{DD}} = \sum_B \overline{\psi}_B [\gamma^\mu (i\partial_\mu - \Gamma_{\omega B}(\rho_B)\omega_\mu \\
-\Gamma_{\phi B}(\rho_B)\phi_\mu - \frac{\Gamma_{\rho B}(\rho_B)}{2}\vec{\rho}_\mu\vec{\tau}\Big) \\
- \Big(M_B - \Gamma_{\sigma B}(\rho_B)\sigma - \Gamma_{\sigma^* B}(\rho_B)\sigma^* - \Gamma_{\delta B}(\rho_B)\vec{\delta}\vec{\tau}\Big)\Big] \psi_B \\
+ \frac{1}{2}\left(\partial^\mu\sigma\partial_\mu\sigma - m_\sigma^2\sigma^2\right) + \frac{1}{2}\left(\partial^\mu\sigma^*\partial_\mu\sigma^* - m_{\sigma^*}^2\sigma^{*2}\right) \\
+ \frac{1}{2}\left(\partial^\mu\vec{\delta}\partial_\mu\vec{\delta} - m_\delta^2\vec{\delta}^2\right) - \frac{1}{4}W^{\mu\nu}W_{\mu\nu} + \frac{1}{2}m_\omega^2\omega_\mu\omega^\mu \\
- \frac{1}{4}\Phi^{\mu\nu}\Phi_{\mu\nu} + \frac{1}{2}m_\phi^2\phi_\mu\phi^\mu - \frac{1}{4}\vec{R}^{\mu\nu}\vec{R}_{\mu\nu} + \frac{1}{2}m_\rho^2\vec{\rho}_\mu\vec{\rho}^\mu,
\end{aligned}
$$

$$
\begin{aligned}
\mathcal{L}_{\mathrm{NL}} = \sum_B \overline{\psi}_B \{i\gamma^\mu\partial_\mu - (M_B - g_{\sigma B}\sigma - g_{\sigma^* B}\sigma^*) \\
-\gamma^\mu\left(g_{\omega B}\omega_\mu + g_{\phi B}\phi_\mu + \frac{1}{2}g_{\rho B}\vec{\tau}\vec{\rho}_\mu\right)\Big\} \psi_B \\
+ \frac{1}{2}\partial^\mu\sigma\partial_\mu\sigma - \frac{1}{2}m_\sigma^2\sigma^2 - \frac{1}{3}g_2\sigma^3 - \frac{1}{4}g_3\sigma^4 \\
+ \frac{1}{2}\partial^\mu\sigma^*\partial_\mu\sigma^* - \frac{1}{2}m_{\sigma^*}^2\sigma^{*2} \\
- \frac{1}{4}W^{\mu\nu}W_{\mu\nu} + \frac{1}{2}m_\omega^2\omega^\mu\omega_\mu + \frac{1}{4}c_3\left(\omega^\mu\omega_\mu\right)^2 \\
- \frac{1}{4}\Phi^{\mu\nu}\Phi_{\mu\nu} + \frac{1}{2}m_\phi^2\phi^\mu\phi_\mu \\
- \frac{1}{4}\vec{R}^{\mu\nu}\vec{R}_{\mu\nu} + \frac{1}{2}m_\rho^2\vec{\rho}^\mu\vec{\rho}_\mu \\
+ \Lambda_{\mathrm{v}}\left(g_\omega^2\omega^\mu\omega_\mu\right)\left(g_\rho^2\vec{\rho}^\mu\vec{\rho}_\mu\right),
\end{aligned}
$$

南開大學

The interaction between vector mesons and baryons

$$\Gamma_{\omega\Lambda} = \Gamma_{\omega\Sigma} = 2\Gamma_{\omega\Xi} = \frac{2}{3}\Gamma_{\omega N},$$

$$2\Gamma_{\phi\Sigma} = \Gamma_{\phi\Xi} = -\frac{2\sqrt{2}}{3}\Gamma_{\omega N},\ \ \Gamma_{\phi N} = 0,$$

$$\Gamma_{\rho\Lambda} = 0,\ \ \Gamma_{\rho\Sigma} = 2\Gamma_{\rho\Xi} = 2\Gamma_{\rho N},$$

$$\Gamma_{\delta\Lambda} = 0,\ \ \Gamma_{\delta\Sigma} = 2\Gamma_{\delta\Xi} = 2\Gamma_{\delta N}.$$

The hyperon-nucleon potentials

$$U_Y^N(\rho_{B0}) = -R_{\sigma Y}\Gamma_{\sigma N}(\rho_{B0})\sigma_0 + R_{\omega Y}\Gamma_{\omega N}(\rho_{B0})\omega_0,$$

Empirical potential values

$$U_\Lambda^N = -30\ \text{MeV}, \qquad U_\Sigma^N = +30\ \text{MeV} \qquad U_\Xi^N = -14\ \text{MeV}$$

南開大學

The hyperon-hyperon potentials

$$U_\Lambda^\Lambda(\rho_{B0}) = -R_{\sigma\Lambda}\Gamma_{\sigma N}(\rho_{B0})\sigma_0 - R_{\sigma^*\Lambda}\Gamma_{\sigma N}(\rho_{B0})\sigma_0^* + R_{\omega Y}\Gamma_{\omega N}(\rho_{B0})\omega_0 + R_{\phi\Lambda}\Gamma_{\omega N}(\rho_{B0})\phi_0,$$

$$U_\Lambda^\Lambda(\rho_{B0}) = -10 \text{ MeV},$$

	$R_{\sigma\Lambda}$	$R_{\sigma\Sigma}$	$R_{\sigma\Xi}$	$R_{\sigma^*\Lambda}$
NL3	0.618896	0.460889	0.306814	0.84695
BigApple	0.616322	0.452837	0.305436	0.86313
TM1	0.621052	0.445880	0.307606	0.83710
IUFSU	0.616218	0.453006	0.305389	0.88802
DD-LZ1	0.610426	0.465708	0.302801	0.87595
DD-MEX	0.612811	0.469159	0.304011	0.86230
DD-ME2	0.609941	0.460706	0.302483	0.85758
DD-ME1	0.608602	0.457163	0.301777	0.85828
DD2	0.612743	0.466628	0.303937	0.86420
PKDD	0.610412	0.461807	0.302729	0.84965
TW99	0.612049	0.468796	0.303632	0.85818
DDV	0.607355	0.452777	0.301101	0.87979
DDVT	0.591179	0.399269	0.292391	0.92256
DDVTD	0.591108	0.399023	0.292352	0.92246

The EoSs of neutron star and hydronic star

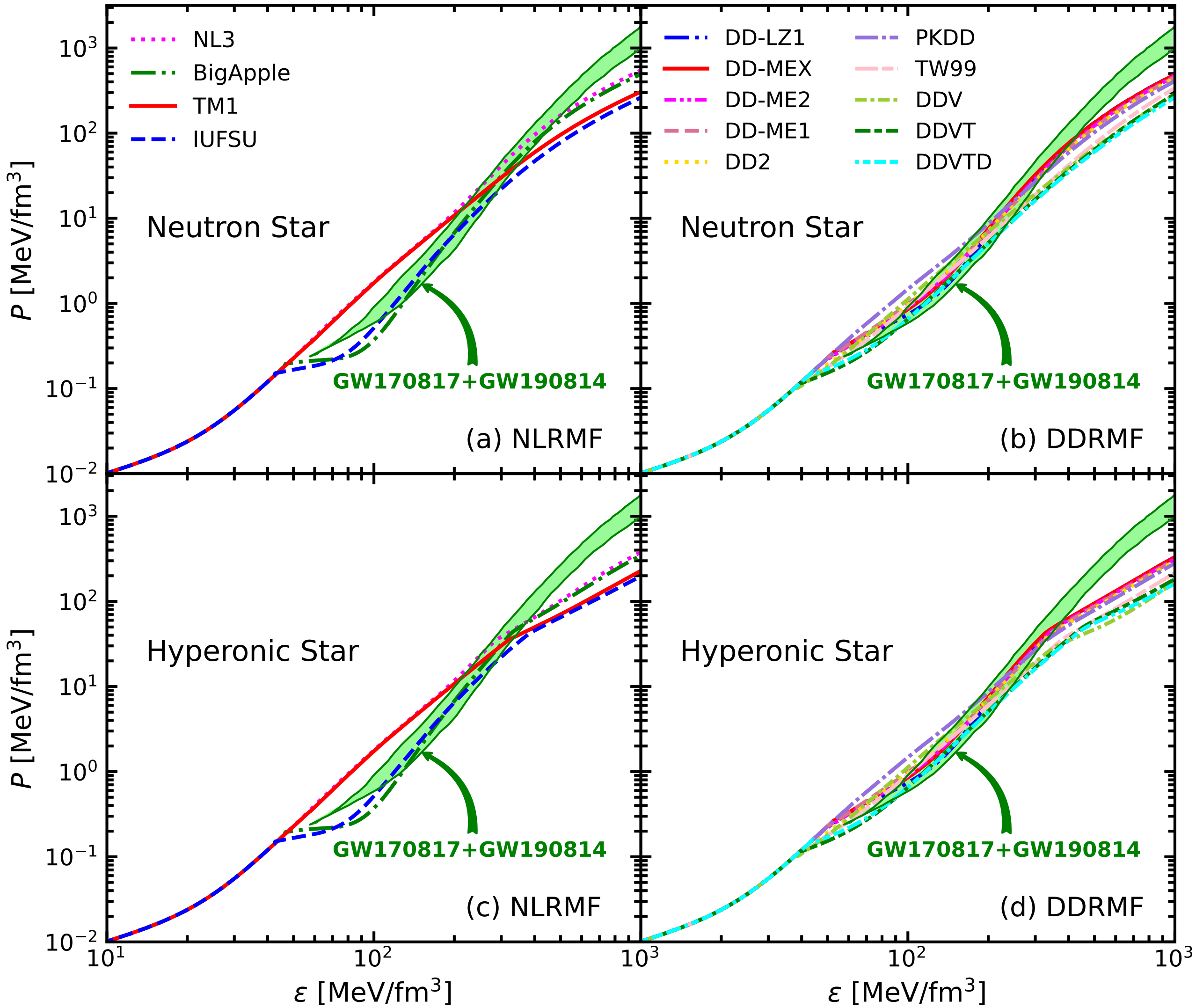

南開大學

The EoSs of neutron star and hydronic star

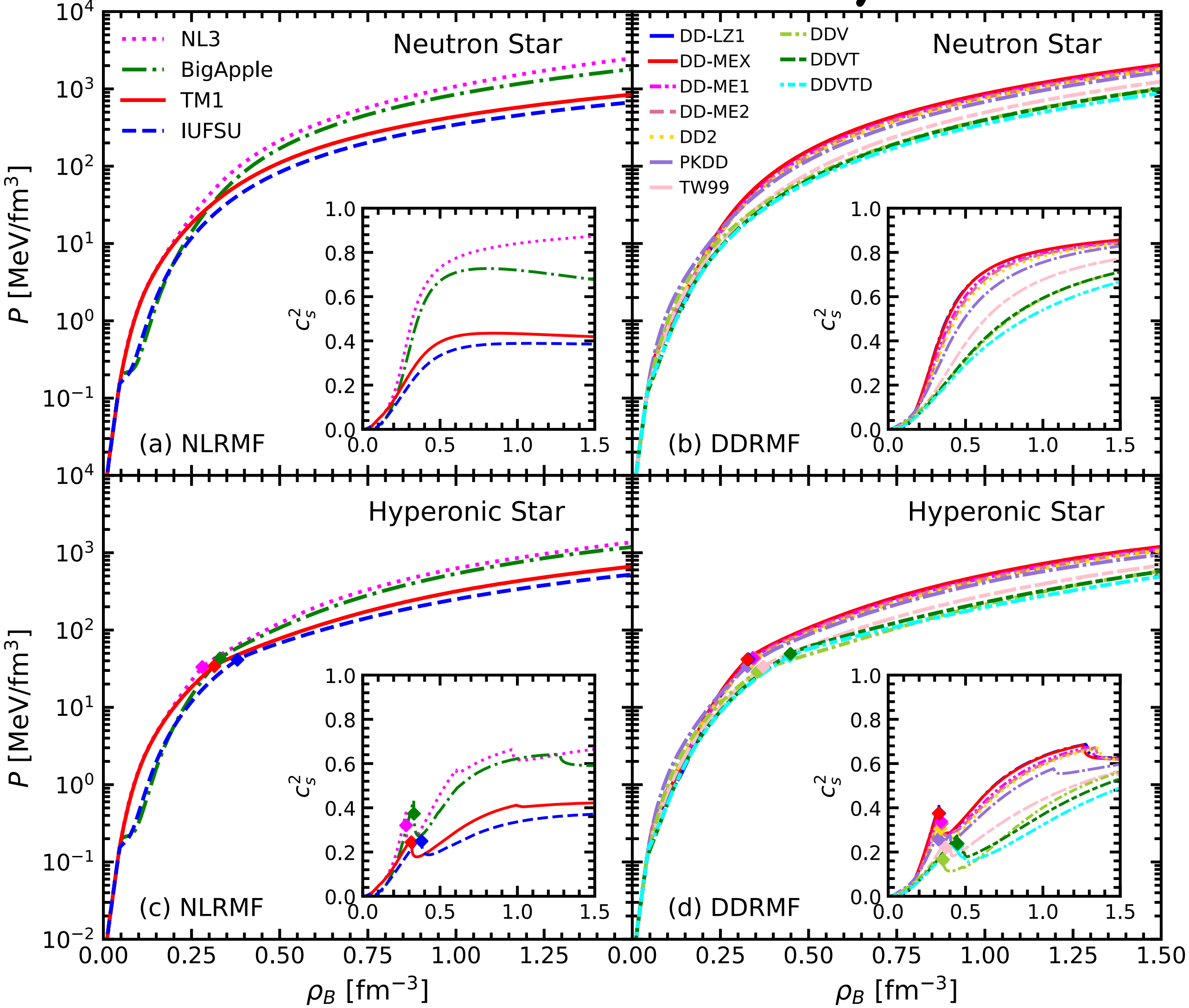

K. Huang, J. N. Hu, Y. Zhang, and H. Shen, arXiv: 2203.12357

南開大學

The radius-mass relation of neutron star and hydronic star

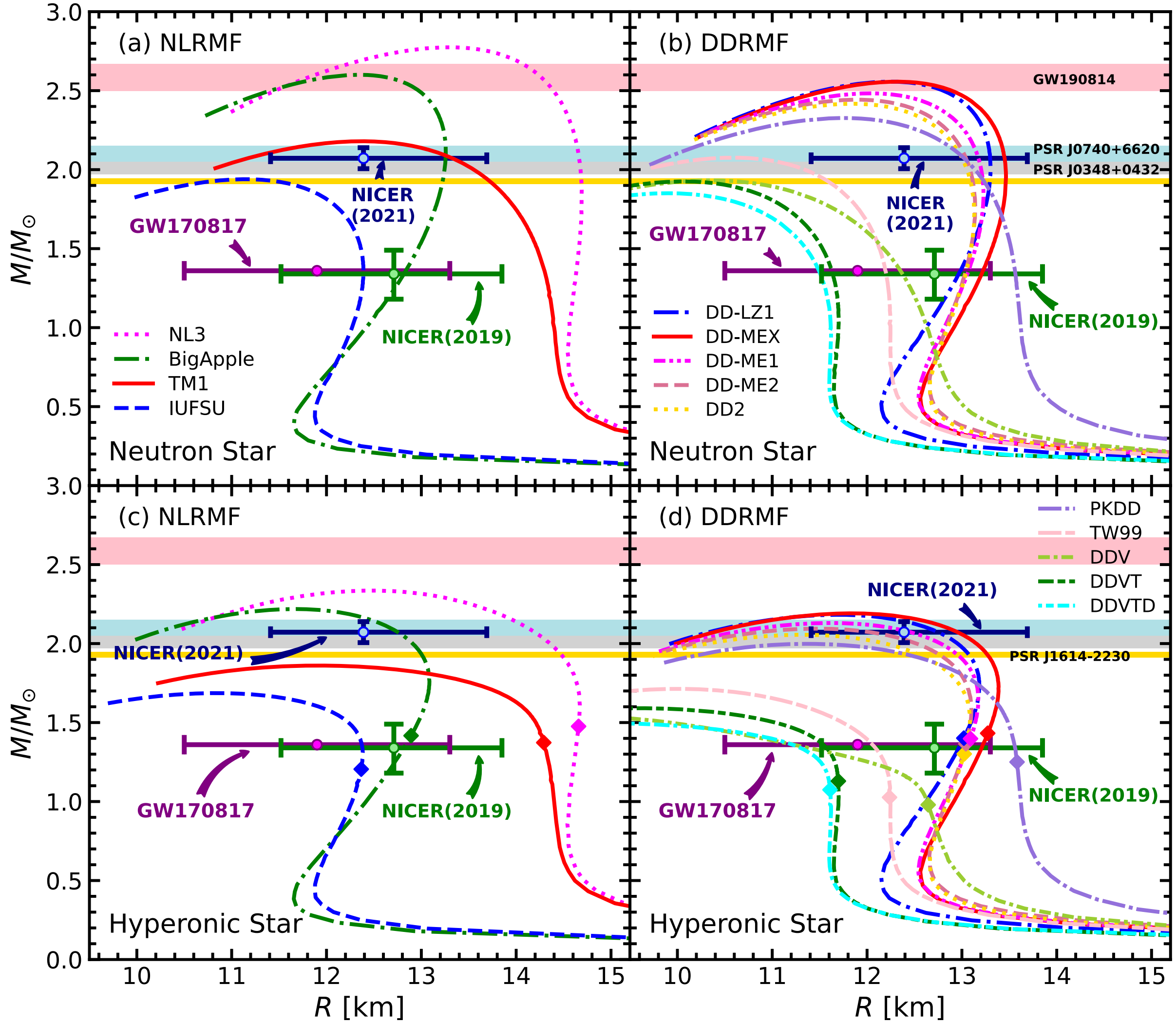

南開大學

The tidal deformabilities of neutron star and hydronic star

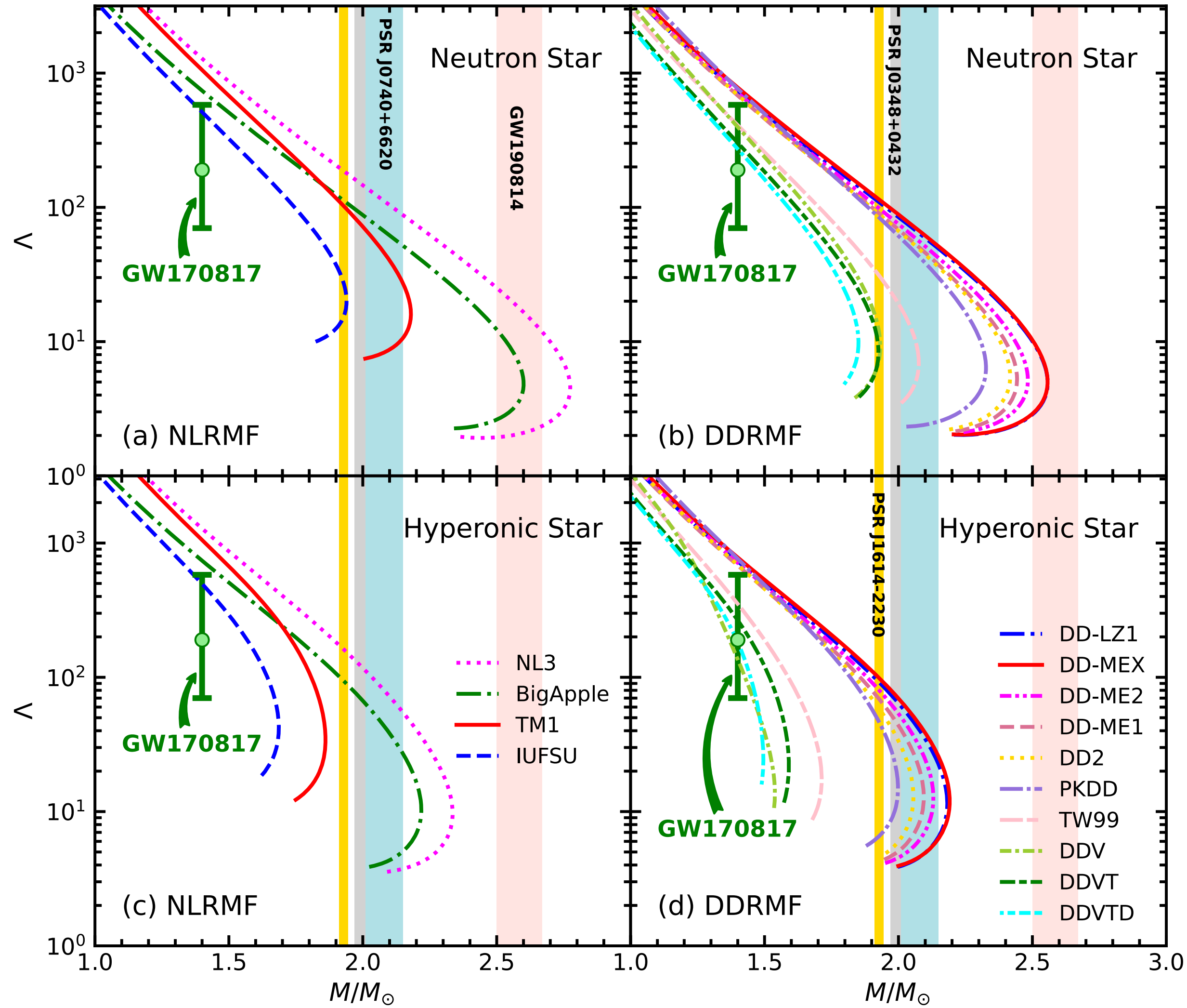

南開大學

The properties of neutron star and hydronic star

	Neutron Star						Hyperonic Star						
	$M_{max}/M_\odot$	R_{max}[km]	ρ_c[fm^{-3}]	$R_{1.4}$[km]	$\rho_{1.4}$[fm^{-3}]	$\Lambda_{1.4}$	$M_{max}/M_\odot$	R_{max}[km]	ρ_c[fm^{-3}]	$R_{1.4}$[km]	$\rho_{1.4}$[fm^{-3}]	$\Lambda_{1.4}$	1^{st} threshold [fm^{-3}]
NL3	2.7746	13.3172	0.6638	14.6433	0.2715	1280	2.3354	12.5105	0.8129	14.6426	0.2715	1280	0.2804
BigApple	2.6005	12.3611	0.7540	12.8745	0.3295	738	2.2186	11.6981	0.8946	12.8750	0.3295	738	0.3310
TM1	2.1797	12.3769	0.8510	14.2775	0.3200	1050	1.8608	11.9255	0.9736	14.2775	0.3218	1050	0.3146
IUFSU	1.9394	11.1682	1.0170	12.3865	0.4331	510	1.6865	10.8653	1.1202	12.3520	0.4705	498	0.3800
DD-LZ1	2.5572	12.2506	0.7789	13.0185	0.3294	729	2.1824	11.6999	0.9113	12.0185	0.3294	729	0.3294
DD-MEX	2.5568	12.3347	0.7706	13.2510	0.3228	785	2.1913	11.8640	0.8890	13.2510	0.3228	785	0.3264
DD-ME2	2.4832	12.0329	0.8177	13.0920	0.3410	716	2.1303	11.6399	0.9296	13.0920	0.3410	716	0.3402
DD-ME1	2.4429	11.9085	0.8358	13.0580	0.3512	682	2.0945	11.5089	0.9560	13.0578	0.3526	681	0.3466
DD2	2.4171	11.8520	0.8481	13.0638	0.3528	686	2.0558	11.3446	0.9922	13.0630	0.3585	685	0.3387
PKDD	2.3268	11.7754	0.8823	13.5493	0.3546	758	1.9983	11.3789	1.0188	13.5400	0.3642	756	0.3264
TW99	2.0760	10.6117	1.0917	12.1805	0.4720	409	1.7135	10.0044	1.3466	11.9880	0.5710	352	0.3696
DDV	1.9319	10.3759	1.1879	12.3060	0.5035	395	1.5387	9.0109	1.7317	10.8990	0.9538	136	0.3547
DDVT	1.9253	10.0846	1.2245	11.6058	0.5458	302	1.5909	9.6244	1.4675	11.4515	0.6660	266	0.4465
DDVTD	1.8507	9.9294	1.2789	11.4615	0.5790	275	1.4956	9.3019	1.6071	10.9880	0.8570	182	0.4465

K. Huang, J. N. Hu, Y. Zhang, and H. Shen, arXiv: 2203.12357

The correlations between the coupling strengths

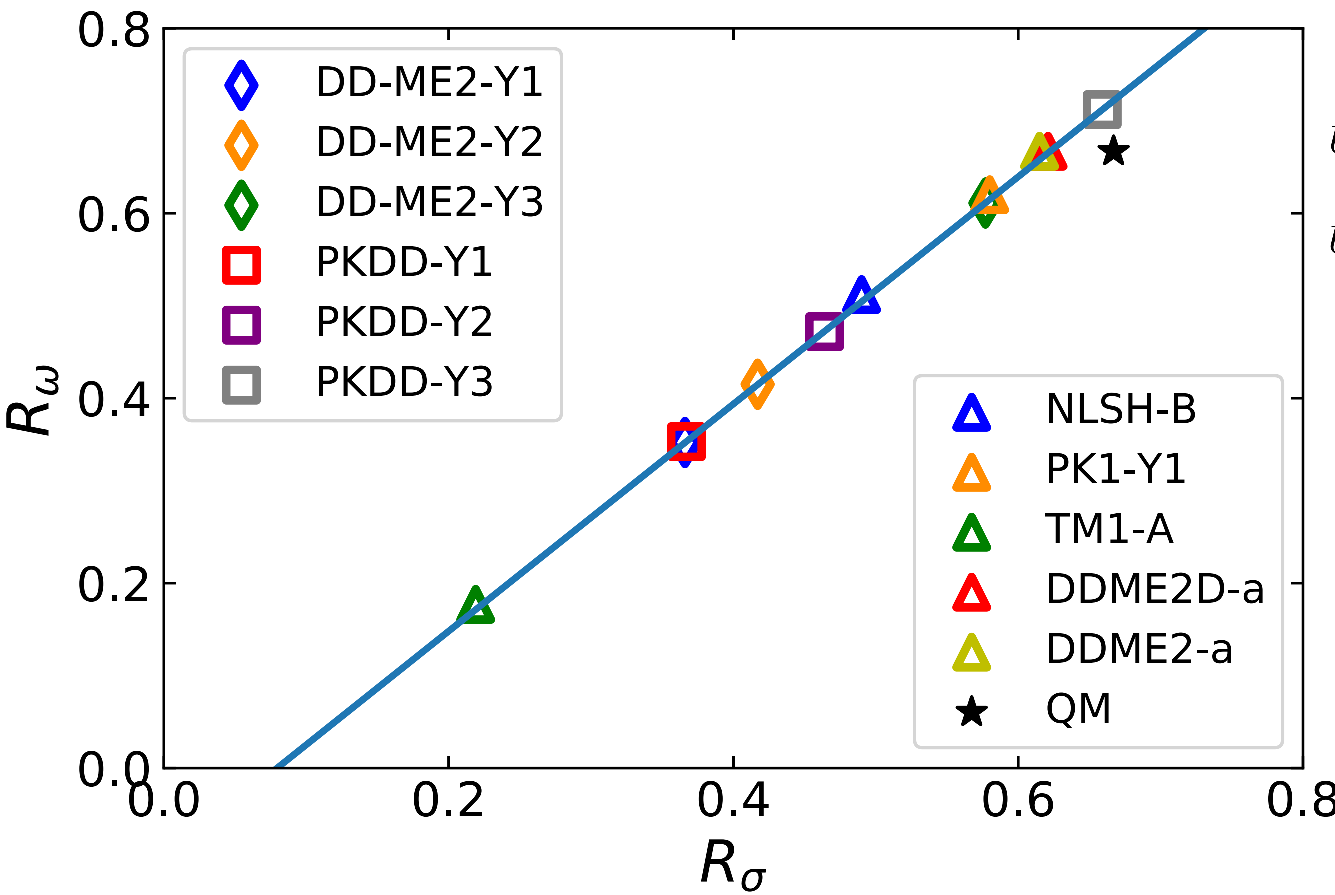

$U_\Lambda^N = -30$ MeV, $U_\Sigma^N = +30$ MeV

$U_\Xi^N = -14$ MeV,

$$R_{\omega\Lambda} = 1.24969 R_{\sigma\Lambda} - 0.10946,$$
$$R_{\omega\Sigma} = 1.24969 R_{\sigma\Sigma} + 0.10946,$$
$$R_{\omega\Xi} = 1.24969 R_{\sigma\Xi} - 0.05108.$$

Y. T. Rong, Z. H. Tu, S. G. Zhou, Phys. Rev. C 104(2021)054321

The EoSs with different the coupling strengths

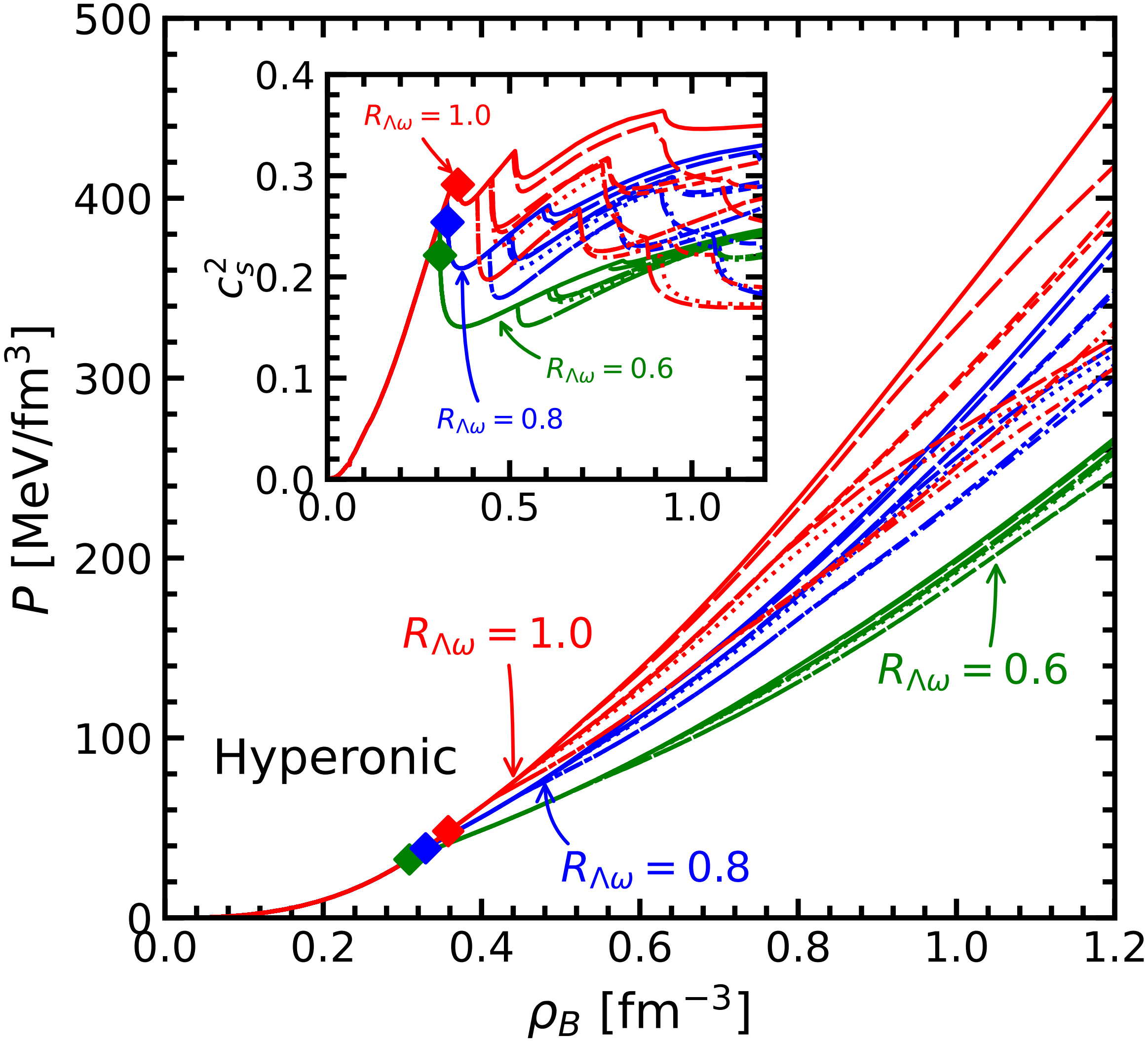

The Mass-radius relation with different the coupling strengths

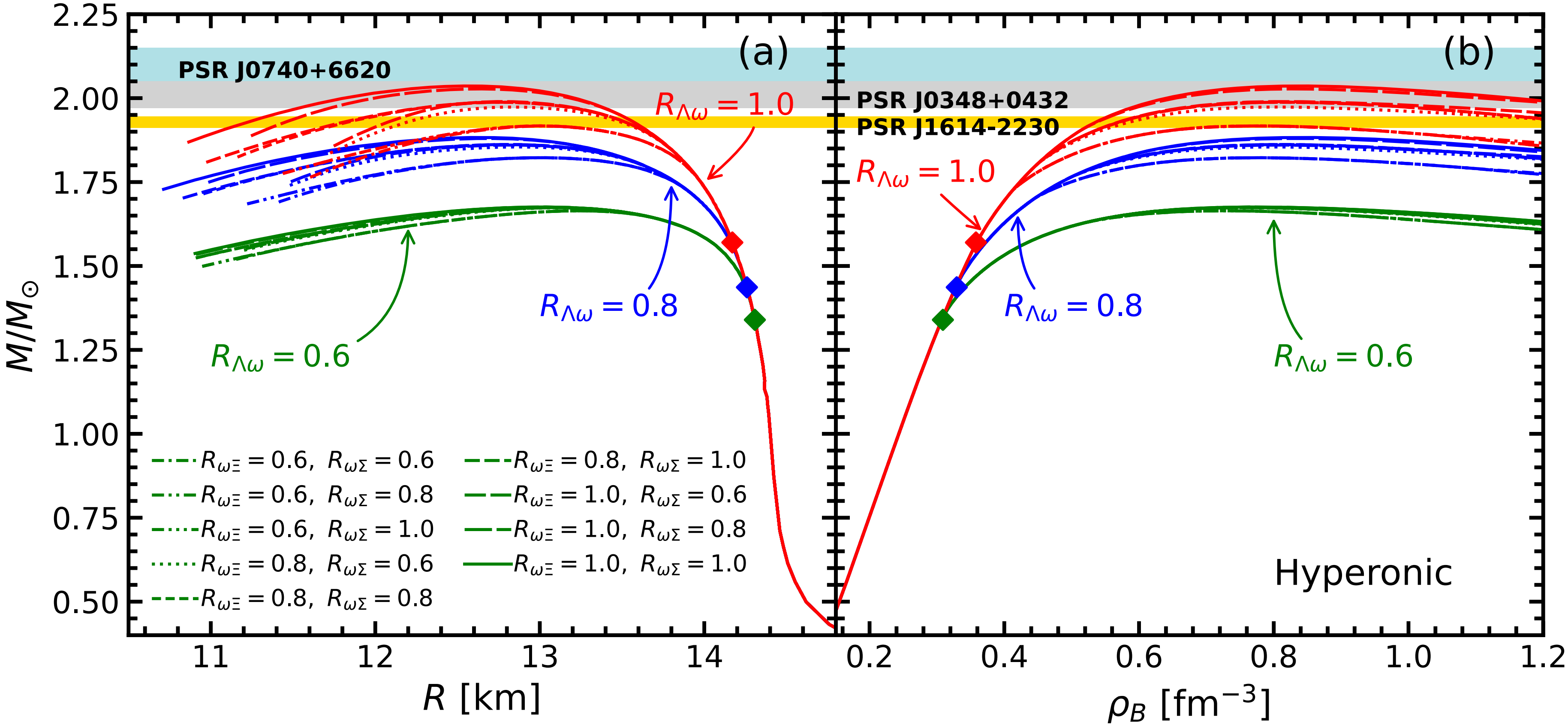

The properties of neutron star

$R_{\omega\Lambda}$	$R_{\omega\Xi}$	$R_{\omega\Sigma}$	Hyperon thresholds ([fm^{-3}])	$M_{\max}$	$R_{\max}$[km]	ρ_c[fm^{-3}]	$R_{1.4}$[km]	$\rho_{1.4}$[fm^{-3}]	$\Lambda_{1.4}$
0.6	0.6	0.6	$\mathbf{\Lambda(0.3089)}$, $\mathbf{\Xi^-(0.5245)}$, $\Sigma^-(0.9032)$, $\Xi^0(1.0710)$, $\Sigma^0(1.4447)$	1.6645	13.2465	0.7251	12.2770	0.3255	1055
0.6	0.6	0.8	$\mathbf{\Lambda(0.3089)}$, $\mathbf{\Xi^-(0.5245)}$, $\Xi^0(1.0759)$	1.6645	13.2465	0.7251	12.2770	0.3255	1055
0.6	0.6	1.0	$\mathbf{\Lambda(0.3089)}$, $\mathbf{\Xi^-(0.5245)}$, $\Xi^0(1.0759)$	1.6645	13.2465	0.7251	12.2770	0.3255	1055
0.6	0.8	0.6	$\mathbf{\Lambda(0.3089)}$, $\mathbf{\Sigma^-(0.6106)}$, $\mathbf{\Xi^-(0.6394)}$, $\Xi^0(1.3176)$, $\Sigma^0(1.3237)$	1.6733	13.1347	0.7456	12.2770	0.3255	1055
0.6	0.8	0.8	$\mathbf{\Lambda(0.3089)}$, $\mathbf{\Xi^-(0.6306)}$, $\Sigma^-(1.2072)$, $\Xi^0(1.3924)$, $\Sigma^0(1.8611)$	1.6742	13.1101	0.7456	12.2770	0.3255	1055
0.6	0.8	1.0	$\mathbf{\Lambda(0.3089)}$, $\mathbf{\Xi^-(0.6306)}$, $\Xi^0(1.3989)$	1.6742	13.1101	0.7456	12.2770	0.3255	1055
0.6	1.0	0.6	$\mathbf{\Lambda(0.3089)}$, $\mathbf{\Sigma^-(0.6106)}$, $\Sigma^0(1.2995)$, $\Sigma^+(1.4989)$	1.6736	13.1111	0.7514	12.2770	0.3255	1055
0.6	1.0	0.8	$\mathbf{\Lambda(0.3089)}$, $\Sigma^-(0.7830)$, $\Xi^-(0.8546)$, $\Sigma^0(1.7530)$, $\Xi^0(1.8356)$	1.6757	13.0391	0.7635	12.2770	0.3255	1055
0.6	1.0	1.0	$\mathbf{\Lambda(0.3089)}$, $\Xi^-(0.8237)$, $\Sigma^-(1.7052)$, $\Xi^0(1.8870)$	1.6757	13.0391	0.7635	12.2770	0.3255	1055
0.8	0.6	0.6	$\mathbf{\Lambda(0.3294)}$, $\mathbf{\Xi^-(0.4485)}$, $\mathbf{\Sigma^-(0.6979)}$, $\Xi^0(0.8050)$, $\Sigma^0(1.0959)$	1.8225	13.0424	0.7615	12.2775	0.3200	1050
0.8	0.6	0.8	$\mathbf{\Lambda(0.3294)}$, $\mathbf{\Xi^-(0.4485)}$, $\Xi^0(0.8087)$	1.8225	13.0423	0.7612	12.2775	0.3200	1050
0.8	0.6	1.0	$\mathbf{\Lambda(0.3294)}$, $\mathbf{\Xi^-(0.4485)}$, $\Xi^0(0.8087)$	1.8225	13.0423	0.7612	12.2775	0.3200	1050
0.8	0.8	0.6	$\mathbf{\Lambda(0.3294)}$, $\mathbf{\Sigma^-(0.5009)}$, $\mathbf{\Xi^-(0.5150)}$, $\Xi^0(0.9242)$, $\Sigma^0(0.9501)$	1.8547	12.8733	0.7972	12.2775	0.3200	1050
0.8	0.8	0.8	$\mathbf{\Lambda(0.3294)}$, $\mathbf{\Xi^-(0.5103)}$, $\Sigma^-(0.8429)$, $\Xi^0(0.9545)$, $\Sigma^0(1.3483)$	1.8619	12.7947	0.8135	12.2775	0.3200	1050
0.8	0.8	1.0	$\mathbf{\Lambda(0.3294)}$, $\mathbf{\Xi^-(0.5103)}$, $\Xi^0(0.9589)$	1.8619	12.7947	0.8135	12.2775	0.3200	1050
0.8	1.0	0.6	$\mathbf{\Lambda(0.3294)}$, $\mathbf{\Sigma^-(0.5009)}$, $\Sigma^0(0.9200)$, $\Sigma^+(1.0661)$, $\Xi^-(1.1906)$	1.8603	12.8329	0.8026	12.2775	0.3200	1050
0.8	1.0	0.8	$\mathbf{\Lambda(0.3294)}$, $\mathbf{\Sigma^-(0.5967)}$, $\mathbf{\Xi^-(0.6220)}$, $\Sigma^0(1.1906)$, $\Xi^0(1.2128)$	1.8799	12.6868	0.8316	12.2775	0.3200	1050
0.8	1.0	1.0	$\mathbf{\Lambda(0.3294)}$, $\mathbf{\Xi^-(0.6135)}$, $\Sigma^-(1.1163)$, $\Xi^0(1.2699)$, $\Sigma^0(1.8870)$	1.8828	12.6492	0.8371	12.2775	0.3200	1050
1.0	0.6	0.6	$\mathbf{\Lambda(0.3579)}$, $\mathbf{\Xi^-(0.4186)}$, $\mathbf{\Sigma^-(0.6050)}$, $\mathbf{\Xi^0(0.6947)}$, $\Sigma^0(0.9589)$	1.9170	13.0352	0.7661	12.2775	0.3200	1050
1.0	0.6	0.8	$\mathbf{\Lambda(0.3579)}$, $\mathbf{\Xi^-(0.4128)}$, $\mathbf{\Xi^0(0.6979)}$, $\Sigma^-(1.4852)$, $\Sigma^0(1.5409)$	1.9174	12.9932	0.7795	12.2775	0.3200	1050
1.0	0.6	1.0	$\mathbf{\Lambda(0.3579)}$, $\mathbf{\Xi^-(0.4128)}$, $\mathbf{\Xi^0(0.6979)}$	1.9174	12.9932	0.7795	12.2775	0.3200	1050
1.0	0.8	0.6	$\mathbf{\Lambda(0.3579)}$, $\mathbf{\Sigma^-(0.4506)}$, $\mathbf{\Xi^-(0.4590)}$, $\mathbf{\Xi^0(0.7617)}$, $\mathbf{\Sigma^0(0.8013)}$	1.9736	12.8272	0.8047	12.2775	0.3200	1050
1.0	0.8	0.8	$\mathbf{\Lambda(0.3579)}$, $\mathbf{\Xi^-(0.4548)}$, $\mathbf{\Sigma^-(0.6947)}$, $\mathbf{\Xi^0(0.7759)}$, $\Sigma^0(1.1061)$	1.9878	12.7682	0.8093	12.2775	0.3200	1050
1.0	0.8	1.0	$\mathbf{\Lambda(0.3579)}$, $\mathbf{\Xi^-(0.4548)}$, $\mathbf{\Xi^0(0.7759)}$	1.9879	12.7682	0.8093	12.2775	0.3200	1050
1.0	1.0	0.6	$\mathbf{\Lambda(0.3579)}$, $\mathbf{\Sigma^-(0.4506)}$, $\mathbf{\Xi^-(0.6726)}$, $\mathbf{\Sigma^0(0.7617)}$, $\Sigma^+(0.8826)$	1.9898	12.7706	0.8146	12.2775	0.3200	1050
1.0	1.0	0.8	$\mathbf{\Lambda(0.3579)}$, $\mathbf{\Sigma^-(0.5126)}$, $\mathbf{\Xi^-(0.5221)}$, $\Xi^0(0.9074)$, $\Sigma^0(0.9328)$	2.0275	12.6470	0.8254	12.2775	0.3200	1050
1.0	1.0	1.0	$\mathbf{\Lambda(0.3579)}$, $\mathbf{\Xi^-(0.5197)}$, $\Sigma^-(0.8546)$, $\Xi^0(0.9328)$, $\Sigma^0(1.4447)$	2.0363	12.5920	0.8327	12.2775	0.3200	1050

- Introduction
- The inner crust of neutron star
- The properties of neutron star
- The hyperons in neutron star
- Summary

Summary

南開大學

The neutron star is a natural laboratory to check the nuclear many-body methods

The pasta structure in the inner crust was investigated with the effects of symmetry energy, magnetic field and temperature.

Properties of neutron star were calculated within RMF model

The strangeness degree of freedom was discussed in neutrons star.

Summary

Inner Crust

S. S. Bao, J. N. Hu, Z. W. Zhang, H. Shen, Phys. Rev. C 90(2014)045802
S. S. Bao and H. Shen, Phys. Rev. C 91(2015)015807
S. S. Bao, J. N. Hu, H. Shen, Phys. Rev. C 103(2021)015804
F. Ji, J. N. Hu, H. Shen, Phys. Rev. C 103(2021)055802

Out core

J. N. Hu and H. Shen, Phys. Rev. C 95(2017)025804
Y. Zhang, J. N. Hu, and P. Liu, Int. J. Mod. Phys. E 28(2019)1950094
F. Ji, J. N. Hu, S. S. Bao, and H. Shen, Phys. Rev. C, 100 (2019)045801
J. N. Hu, et al., Prog. Theo. Exp. Phys., 2020 (2020) 043D01
C. Wang, J. N. Hu, Y. Zhang, and H. Shen, Astrophys. J. 897(2020)96
K. Huang, J. N. Hu, Y. Zhang, and H. Shen, Astrophys. J. 904(2020)39

Baryon degrees of freedom

Z. Y. Zhu, A. Li, J. N. Hu, and H. Sagawa, Phys. Rev. C, 94 (2016)045803
X. Y. Xing, J. N. Hu and H. Shen, Phys. Rev. C 95(2017)054310
Y. Zhang, J. N. Hu, and P. Liu, Phys. Rev. C 97(2018)015805
K. Huang, J. N. Hu, Y. Zhang, and H. Shen, arXiv: 2203.12357

Hadron-quark phase

M. Ju, X. Wu, F. Ji, J. N. Hu, and H. Shen, Phys. Rev. C, 103 (2021)025809
M. Ju, J. N. Hu, and H. Shen, Astrophys. J. 923(2021)250
K. Huang, J. N. Hu, Y. Zhang, and H. Shen, in preparation

EOS table

H. Shen, F. Ji, J. N. Hu, and K. Sumiyoshi, Astrophys. J 891(2019)148
H. Sumiyoshi, et al., Astrophys. J 887(2019)110
F. Ji, J. N. Hu, S. S. Bao, and H. Shen, Phys. Rev. C, 102 (2020)015806

Thank you very much!

My collaborators:

Mr. Chencan Wang	(Nankai Univ.)
Ms. Kaixuan Huang	(Nankai Univ.)
Ms. Min Ju	(Nankai Univ.)
Dr. Fan Ji	(Nankai Univ.)
Dr. Shishao Bao	(Shanxi Normal Univ.)
Dr. Ying Zhang	(Tianjin Univ.)
Prof. Ang Li	(Xiamen Univ.)
Prof. Hong Shen	(Nankai Univ.)

南開大學

Landau level

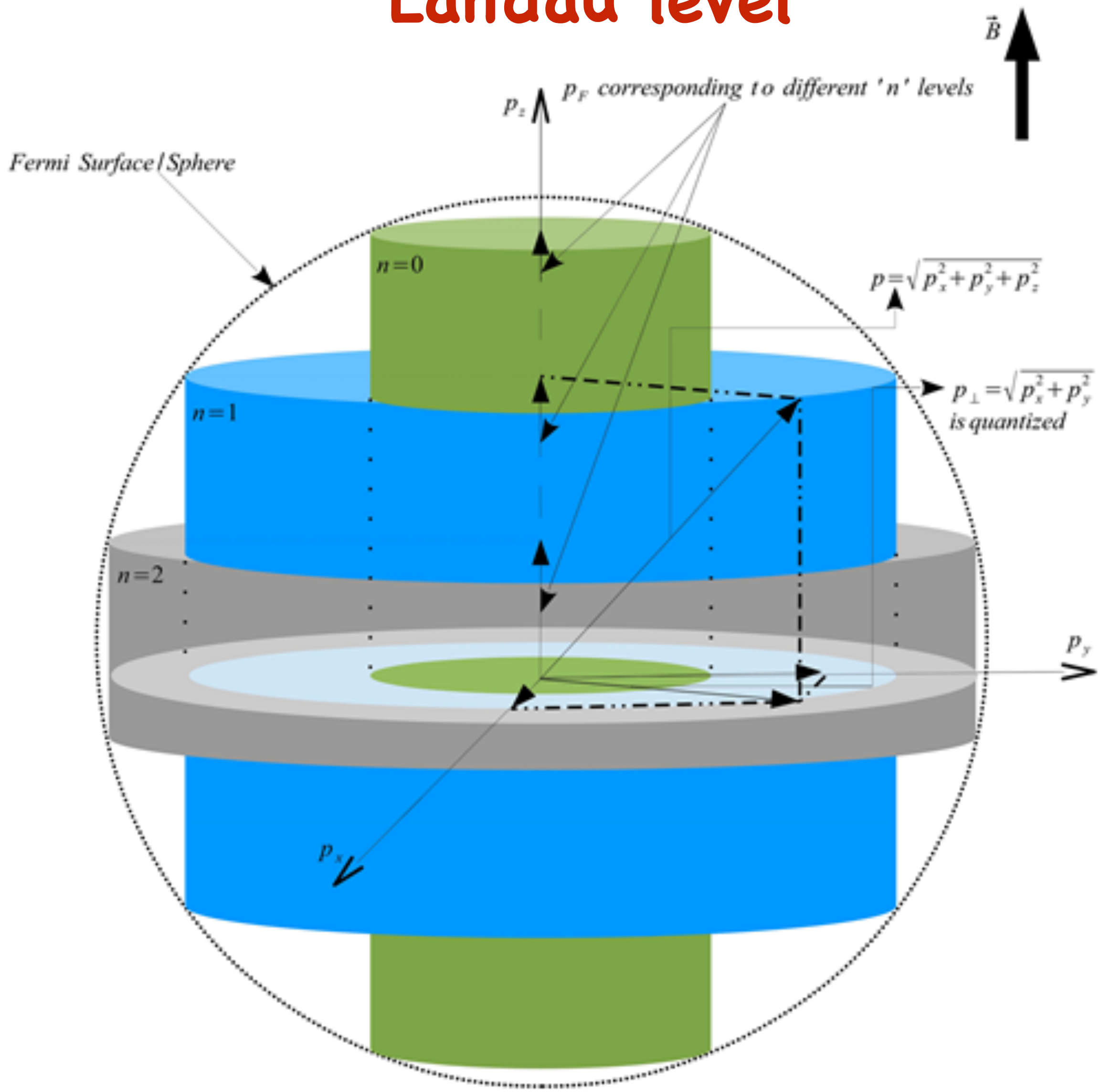

Proton scalar and vector densities

$$n_p^s = \frac{eBM^*}{2\pi^2} \sum_\nu \sum_s \left(\frac{\sqrt{M^{*2} + 2\nu eB} - s\kappa_p B}{\sqrt{M^{*2} + 2\nu eB}} \times \ln \left| \frac{k_{F,\nu,s}^p + E_F^p}{\sqrt{M^{*2} + 2\nu eB} - s\kappa_p B} \right| \right),$$

$$n_p = \frac{eB}{2\pi^2} \sum_\nu \sum_s k_{F,\nu,s}^p,$$

Proton energy densities

$$\varepsilon_p = \frac{eB}{4\pi^2} \sum_\nu \sum_s \left[k_{F,\nu,s}^p E_F^p + (\sqrt{M^{*2} + 2\nu eB} - s\kappa_p B)^2 \times \ln \left| \frac{k_{F,\nu,s}^p + E_F^p}{\sqrt{M^{*2} + 2\nu eB} - s\kappa_p B} \right| \right],$$

S. S. Bao, J. N. Hu, H. Shen, Phys. Rev. C 103(2021)015804

Fermi-Dirac distribution

$$f_{i\pm}^{k} = \{1 + \exp[(\sqrt{k^2 + M^{*2}} \mp \nu_i)/T]\}^{-1},$$

The number density of protons or neutrons

$$n_i = \frac{1}{\pi^2}\int_0^\infty dk\, k^2 (f_{i+}^{k} - f_{i-}^{k}).$$

The energy density

$$\begin{aligned}\epsilon = &\sum_{i=p,n} \frac{1}{\pi^2}\int_0^\infty dk\, k^2 \sqrt{k^2 + M^{*2}}(f_{i+}^{k} + f_{i-}^{k}) \\ &+ \frac{1}{2}m_\sigma^2\sigma^2 + \frac{1}{3}g_2\sigma^3 + \frac{1}{4}g_3\sigma^4 \\ &+ \frac{1}{2}m_\omega^2\omega^2 + \frac{3}{4}c_3\omega^4 + \frac{1}{2}m_\rho^2\rho^2 + 3\Lambda_{\rm v}(g_\omega^2\omega^2)(g_\rho^2\rho^2),\end{aligned}$$

New DDRMF parameterizations

南開大學

DD-MEX

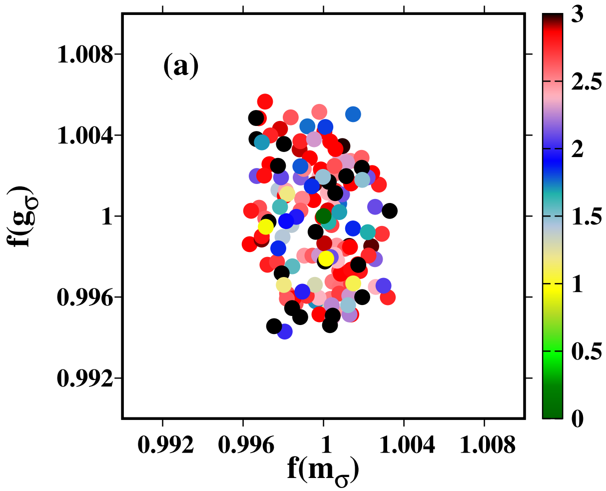

A. Taninah, et al. Phys. Lett. B 800,135065(2020)

DD-LZ1

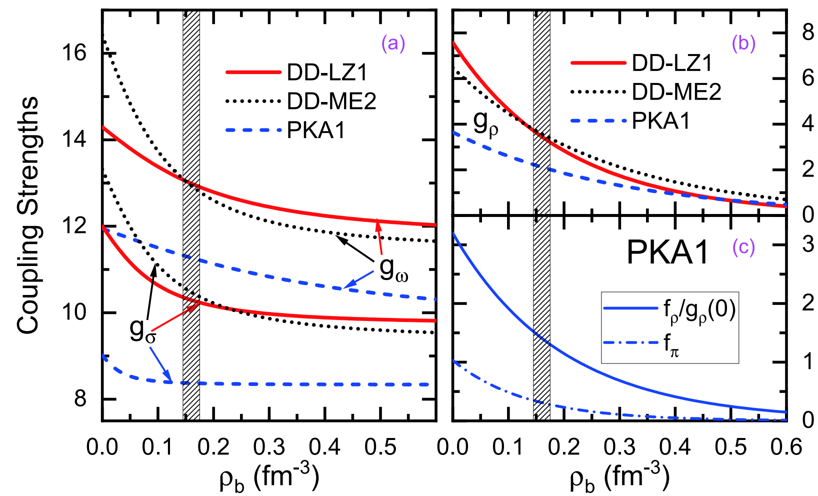

B. Wei, et al. Chin. Phys. C 44, 074107 (2020)

DDV, DDVT, DDVTD

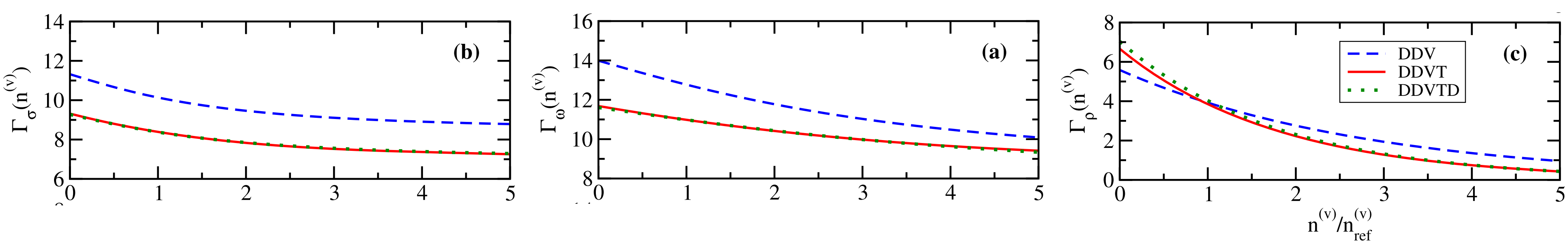

S. Typel and D. A. Terrero, Eur. Phys. J. A 56, 160 (2020)

南開大學 NANKAI UNIVERSITY 1919

The Lagrangian of DDRMF model

$$\mathcal{L}_{DD} = \sum_{i=p,\ n} \overline{\psi}_i \left[\gamma^\mu \left(i\partial_\mu - \Gamma_\omega(\rho_B)\omega_\mu - \frac{\Gamma_\rho(\rho_B)}{2}\gamma^\mu \vec{\rho}_\mu \vec{\tau} \right) - \left(M - \Gamma_\sigma(\rho_B)\sigma - \Gamma_\delta(\rho_B)\vec{\delta}\vec{\tau} \right) \right] \psi_i$$
$$+ \frac{1}{2}\left(\partial^\mu\sigma\partial_\mu\sigma - m_\sigma^2\sigma^2\right) + \frac{1}{2}\left(\partial^\mu\vec{\delta}\partial_\mu\vec{\delta} - m_\delta^2\vec{\delta}^2\right)$$
$$- \frac{1}{4}W^{\mu\nu}W_{\mu\nu} + \frac{1}{2}m_\omega^2\omega_\mu\omega^\mu - \frac{1}{4}\vec{R}^{\mu\nu}\vec{R}_{\mu\nu} + \frac{1}{2}m_\rho^2\vec{\rho}_\mu\vec{\rho}^\mu,$$

The density dependent coupling constants

for σ and ω mesons

$$\Gamma_i(\rho_B) = \Gamma_i(\rho_{B0})f_i(x), \quad \text{with} \quad f_i(x) = a_i\frac{1 + b_i(x + d_i)^2}{1 + c_i(x + d_i)^2}, \quad x = \rho_B/\rho_{B0},$$

for ρ and δ mesons

$$\Gamma_i(\rho_B) = \Gamma_i(\rho_{B0})\exp[-a_i(x - 1)].$$

K. Huang, J. N. Hu, Y. Zhang, and H. Shen, Astrophys. J. 904(2020)39

Density-dependent coupling constants

DD2

DD-ME1

DD-ME2

DD-MEX

DD-LZ1

DDV

DDVT

DDVTD

	DD-LZ1		DD2	DD-ME1	DD-ME2	DD-MEX	DDV	DDVT	DDVTD
m_n[MeV]	938.900000	m_n	939.56536	939.0000	939.0000	939.0000	939.565413	939.565413	939.565413
m_p[MeV]	938.900000	m_p	938.27203	939.0000	939.0000	939.0000	938.272081	938.272081	938.272081
m_σ[MeV]	538.619216	m_σ	546.212459	549.5255	550.1238	547.3327	537.600098	502.598602	502.619843
m_ω[MeV]	783.0000	m_ω	783.0000	783.0000	783.0000	783.0000	783.0000	783.0000	783.0000
m_ρ[MeV]	769.0000	m_ρ	763.0000	763.0000	763.0000	763.0000	763.0000	763.0000	763.0000
m_δ[MeV]	—	m_δ	—	—	—	—	—	—	980.0000
$\Gamma_\sigma(0)$	12.001429	$\Gamma_\sigma(\rho_{B0})$	10.686681	10.4434	10.5396	10.7067	10.136960	8.382863	8.379269
$\Gamma_\omega(0)$	14.292525	$\Gamma_\omega(\rho_{B0})$	13.342362	12.8939	13.0189	13.3388	12.770450	10.987106	10.980433
$\Gamma_\rho(0)$	15.150934	$\Gamma_\rho(\rho_{B0})$	7.25388	7.6106	7.3672	7.2380	7.84833	7.697112	8.06038
$\Gamma_\delta(0)$	—	$\Gamma_\delta(\rho_{B0})$	—	—	—	—	—	—	0.8487420
ρ_{B0}[fm^{-3}]	0.158100	ρ_{B0}	0.149	0.152	0.152	0.153	0.1511	0.1536	0.1536
a_σ	1.062748	a_σ	1.357630	1.3854	1.3881	1.3970	1.20993	1.20397	1.19643
b_σ	1.763627	b_σ	0.634442	0.9781	1.0943	1.3350	0.21286844	0.19210314	0.19171263
c_σ	2.308928	c_σ	1.005358	1.5342	1.7057	2.0671	0.30798197	0.27773566	0.27376859
d_σ	0.379957	d_σ	0.575810	0.4661	0.4421	0.4016	1.04034342	1.09552817	1.10343705
a_ω	1.059181	a_ω	1.369718	1.3879	1.3892	1.3936	1.23746	1.16084	1.16693
b_ω	0.418273	b_ω	0.496475	0.8525	0.9240	1.0191	0.03911422	0.04459850	0.02640016
c_ω	0.538663	c_ω	0.817753	1.3566	1.4620	1.6060	0.07239939	0.06721759	0.04233010
d_ω	0.786649	d_ω	0.638452	0.4957	0.4775	0.4556	2.14571442	2.22688558	2.80617483
a_ρ	0.776095	a_ρ	0.518903	0.5008	0.5647	0.6202	0.35265899	0.54870200	0.55795902
a_δ	—	a_δ	—	—	—	—	—	—	0.55795902